

https://dspace.org/

The propagation of a linear hydraulic fracture with tortuosity and uid leak-off at the uid-rock interface

Mabasa, Rishile

2018

https://hdl.handle.net/10539/26504

Mabasa, Rishile (2018) The propagation of a linear hydraulic fracture with tortuosity and fluid leak-off at the fluid-rock interface, University of the Witwatersrand, Johannesburg, https://hdl.handle.net/10539/26504

Downloaded from a DSpace repository. https://dspace.org/

SCHOOL OF
COMPUTER SCIENCE AND APPLIED MATHEMATICS



MASTER OF SCIENCE: DISSERTATION

The propagation of a linear hydraulic fracture with tortuosity and fluid leak-off at the fluid-rock interface

Author:
Rishile Mabasa
(536670)

Supervisor(s):
Dr M.R.R. Kgatle
Dr A.G. Fareo

A dissertation submitted the faculty of Science, University of the Witwatersrand, South Africa, in fulfillment of the degree Master of Science.

The financial assistance of the National Research Foundation (NRF) towards this research is hereby acknowledged. Opinions expressed and conclusions arrived at, are those of the author and are not necessarily to be attributed to the NRF (SFH160712177372)

Declaration

I, Rishile Mabasa, declare that this dissertation is my own unaided work. It is being submitted to the University of the Witwatersrand, Johannesburg, for the degree of Master of Science. It has not been submitted before for any degree or examination at any other university.

Signed: Rishile Mabasa



Date: 24 August 2018

Abstract

In this work, the propagation of a pre-existing hydraulic fracture in permeable rock is investigated. A partially open tortuous fracture with leak-off is replaced by a two-dimensional symmetric model fracture with a modified Reynolds' flow law to account for the effect of asperities on the fluid flow. The model is closed by considering a linear crack law, which considers the presence of touching asperities, and a Perkins-Kern and Nordgren (PKN) approximation, which relates the half-width of the model fracture to the normal stress at the fracture walls. The result is a nonlinear diffusion equation that accounts for leak-off at the fluid-rock interface as a result of the rock's permeability.

The leak-off velocity is not specified a priori and its functional form is determined by calculating Lie point symmetries of the governing non-linear diffusion equation for a model fracture which leads to a group invariant solution of the half-width of the fracture and the leak-off velocity respectively. We consider different forms of the Lie point symmetry of the governing equations by taking some of the constants in the generator to be zero. This leads to three cases of the group invariant solution, namely the general case, the traveling wave solution and the exponential solution.

Two exact analytical solutions are obtained as a result of association of a Lie point symmetry with a conserved vector. However, the constant volume working condition is not further investigated as the requirements for it to hold are not sufficient for the model considered. Other operating conditions at the fracture entry are also obtained by analysing the different properties of the partially open fracture. Numerical solutions of the half-width and the leak-off depth are computed. The propagation of a linear hydraulic fracture with tortuosity for three cases of the Lie point symmetry are fully analysed by numerically solving for the half-width and the length of the fracture.

The derivation and analysis of the width averaged fluid velocity leads to the derivation of an approximate analytical solution for the half-width of the model fracture which will then be compared to the numerical solution obtained. The approximate solution could prove useful when analytical solutions are unattainable or when numerical solutions are difficult to compute. The effects of leak-off and no leak-off in tortuous hydraulic fracture are compared to gain insight on the effect porosity has on the characteristics of the model fracture with tortuosity.

In loving memory

of

Mukhwanazi Khubani Geregere

1933-2016

Within these pages, your legacy will live forever.

Acknowledgments

Firstly, I would like to thank God Almighty for giving the courage to pursue this journey, and the strength to see it through.

To my amazing supervisors, Dr M.R.R. Kgatle-Maseko and Dr A.G. Fareo, your insights, guidance and dedication to this work has paid off. Thank you for giving me the opportunity to learn from you. You have gone far and beyond your call of duty in helping me reach for the stars. Without your help, I would not have been able to complete this work. I hope to employ the lessons learned throughout this journey wherever I go. I would also like to sincerely thank Prof D.P. Mason for sharing his knowledge with me. Na khensa swinene.

To my parents, thank you for your love and support throughout my schooling career. You have inspired me to pursue my dreams and to work extremely hard. A special thank you to my amazing siblings; especially Rixongile, I hope this will serve as inspiration for you going forward. To baby Malwandla, you have filled our hearts with so much joy, this is my gift to you. To the entire Mabasa clan I thank you.

I would like to acknowledge and thank my amazing colleagues and the staff from the School of Computer Science and Applied Mathematics, my sincerest gratitude for your assistance throughout this journey. You have encouraged and cheered me on even when I could not see the finish line.

Also, it would be unkind of me to forget my circle of friends; Elelwani Mafela, Lungile Ringani, Xirhandziwa Maswanganyi and those whose name I have failed to mention, thank you for always lifting me up in prayer. Your friendship has seen me through so many tough situations, I am extremely grateful.

Finally, I would like to acknowledge and express much gratitude to the National Research Foundation (NRF) and the Centre of Excellence in Mathematical and Statistical Sciences (CoE-MaSS) for the financial support during my postgraduate studies.

"An equation has no meaning to me ... unless it expresses a thought of God."

S. Ramanujan, The Man Who Knew Infinity

Contents

1 Introduction **11**
- 1.1 Introduction . . . 11
- 1.2 Background . . . 12
- 1.3 Literature review . . . 12
- 1.4 Outline of the dissertation . . . 14

2 Model Formulation **16**
- 2.1 Problem description . . . 16
- 2.2 Assumptions . . . 16
- 2.3 Governing equations . . . 18
  - 2.3.1 Mathematical model . . . 18
  - 2.3.2 Fluid leak-off at the fluid-rock interface . . . 19
  - 2.3.3 Nonlinear diffusion equation with leak-off . . . 20
  - 2.3.4 Mathematical model of fluid flow in a tortuous hydraulic fracture. . . . 20
  - 2.3.5 Model closure . . . 21
  - 2.3.6 Boundary conditions . . . 23
  - 2.3.7 Dimensionless equations . . . 25
  - 2.3.8 Form of leak-off velocity $v_\ell(t,x,z)$ . . . 26
- 2.4 Conclusions . . . 26

3 Methods of solution **27**
- 3.1 Introduction . . . 27
- 3.2 Lie point symmetry . . . 27
  - 3.2.1 Group invariant solution . . . 29
- 3.3 Conservation laws . . . 29
  - 3.3.1 Direct method . . . 30
  - 3.3.2 Multiplier method . . . 30
  - 3.3.3 Association of a Lie point symmetry with a conserved vector . . . 30
- 3.4 The shooting method for nonlinear problems . . . 31
- 3.5 Conclusions . . . 31

4 Conservation laws **32**
- 4.1 Introduction . . . 32
- 4.2 Direct method . . . 32
- 4.3 Multiplier method . . . 37
- 4.4 Relationship between Lie point symmetries and conservation laws . . . 40
- 4.5 Conclusions . . . 46

5 Case I: Group invariant solutions for $c_2 \neq 0$ and $c_4 \neq 0$ - General Solution **47**
5.1 Lie point symmetries . . . 47
5.2 Scaling transformation . . . 53
5.3 Leak-off velocity proportional to the half-width of the fracture . . . 54
5.4 Asymptotic solution at the fracture tip . . . 56
5.5 Working conditions at the fracture entry . . . 57
5.5.1 Uncategorized working conditions . . . 57
5.5.2 Constant pressure at the entry . . . 58
5.5.3 The speed of propagation of the fracture . . . 58
5.5.4 Constant volume . . . 58
5.5.5 Constant rate of fluid injection at the fracture entry . . . 58
5.5.6 Constant rate of leak-off at the fluid-rock interface . . . 58
5.6 Exact analytical solutions . . . 59
5.6.1 Exact solution when $\alpha = \frac{1}{2(n+1)}$ and $\gamma = 1$ . . . 59
5.6.2 Exact solution when $\alpha = \frac{1}{n+1}$ and $\gamma = 1$ . . . 60
5.7 Numerical solutions . . . 63
5.7.1 A boundary value problem transformed into an initial value problem 64
5.7.2 Graphical results . . . 67
5.7.3 Constant pressure $\left(\alpha = \frac{1}{2}\right)$ . . . 68
5.7.4 Constant speed of propagation $(\alpha = 1)$ . . . 70
5.7.5 Constant rate of fluid injection at the fracture entry $\left(\alpha = \frac{n+1}{n+2}\right)$ . . . 70
5.7.6 Constant rate of fluid leak-off at the fluid-rock interface $\left(\alpha = \frac{n+1}{2}\right)$ . . . 70
5.7.7 Length of the fracture . . . 70
5.8 Width-averaged fluid velocity . . . 73
5.9 Approximate analytical solutions . . . 74
5.10 Comparisons between leak-off and no leak-off . . . 78

6 Case II: Group invariant solution for $c_2 = c_4 = 0$ - Traveling Wave Solution **82**
6.1 Introduction . . . 82
6.2 Group invariant solution . . . 82
6.3 Leak-off velocity proportional to the half-width of the fracture . . . 85
6.4 Asymptotic Solution . . . 86
6.5 Numerical solutions . . . 87
6.6 Results . . . 88
6.6.1 The length of the fracture . . . 89
6.7 Width-averaged fluid velocity . . . 89

7 Case III: Group invariant solution for $c_2 = 0$, $c_4 \neq 0$ - Exponential solution **92**
7.1 Introduction . . . 92
7.2 Group Invariant solution . . . 92
7.3 Leak-off velocity proportional to the half-width of the fracture . . . 96
7.4 Asymptotic Solution . . . 97
7.5 Numerical Solutions . . . 98

8 CONCLUSIONS **101**

Appendices **103**

A Lie point symmetries 104

List of Figures

1.1 The hydraulic fracturing process in a oil/gas field is illustrated [1]. 13

2.1 A pre-existing two-dimensional linear hydraulic fracture propagating in a permeable rock. 17

5.1 The half-width, (5.119), of a partially open fracture with $\beta = 0.5$, $\gamma = 1$ and $\alpha = \frac{1}{2(n+1)}$ plotted against x for increasing values of $K_n t$ and for a) $n = 0.5$, b) $n = 1$ and c) $n = 3$. Analytical solution (—) and numerical solution (- - -) . . 61

5.2 The half-width, (5.130), of a partially open fracture with $\beta = 0.5$, $\gamma = 1$ and $\alpha = \frac{1}{(n+1)}$ plotted against x for increasing values of $K_n t$ and for a) $n = 0.5$, b) $n = 1$ and c) $n = 3$. Analytical solution (—) and numerical solution (- - -) . . 61

5.3 The numerical solution of the half-width, (5.172) and the leak-off depth, (5.171), of a partially open fracture ($\beta = 0.5$) and $\gamma = 0.2$ plotted against x for increasing values of the scaled time $K_n t$ for $\alpha = 1/2$ and for a) $n = 0.5$, b) $n = 1$ and c) $n = 3$. 69

5.4 The numerical solution of the half-width, (5.158) and the leak-off depth, (5.173), of a partially open fracture ($\beta = 0.5$) and $\gamma = 0.2$ plotted against x for increasing values of the scaled time $K_n t$ for $\alpha = 1$ and for a) $n = 0.5$, b) $n = 1$ and c) $n = 3$. 69

5.5 The numerical solution of the half-width, (5.158) and the leak-off depth, (5.173), of a partially open fracture ($\beta = 0.5$) and $\gamma = 0.2$ plotted against x for increasing values of the scaled time $K_n t$ for $\alpha = (n+1)/(n+2)$ and for a) $n = 0.5$, b) $n = 1$ and c) $n = 3$. 71

5.6 The numerical solution of the half-width, (5.158) and the leak-off depth, (5.173), of a partially open fracture ($\beta = 0.5$) and $\gamma = 0.2$ plotted against x for increasing values of the scaled time $K_n t$ for $\alpha = (n+1)/2$ and for a) $n = 0.5$, b) $n = 1$ and c) $n = 3$. 71

5.9 The straight line joining the points $(0, c)$ and $(1, 1)$ which approximates the fluid velocity ratio curves 74

5.7 The length, (5.161), of a partially open fracture ($\beta = 0.5$) and $\gamma = 0.2$ is plotted against the scaled time $K_n t$ for the working conditions i) $\alpha = \frac{1}{2(n+1)}$, ii) $\alpha = \frac{1}{n+1}$, iii) $\alpha = \frac{1}{2}$, iv) $\alpha = 1$, v) $\alpha = \frac{n+1}{n+2}$, vi) $\alpha = \frac{n+1}{2}$ and vii) $\alpha = \frac{1}{n+2}$ and for a) $n = 0.5$, b) $n = 1$ and c) $n = 3$. 75

5.8 The velocity ratios, $\frac{\tilde{v}_x}{(dL/dt)}$, of a partially open fracture ($\beta = 0.5$) and with $\gamma = 0.2$ plotted against u with parameter values for the working conditions i) $\alpha = \frac{1}{2(n+1)}$, ii) $\alpha = \frac{1}{n+1}$, iii) $\alpha = \frac{1}{2}$, iv) $\alpha = 1$, v) $\alpha = \frac{n+1}{n+2}$, vi) $\alpha = \frac{n+1}{2}$ and vii) $\alpha = \frac{1}{n+2}$ and for a) $n = 0.5$, b) $n = 1$ and c) $n = 3$. 75

5.10 A comparison of the approximate analytical solution and the numerical solution of the half-width of the fracture for a partially open fracture ($\beta = 0.5$) and $\gamma = 0.2$ for the constant pressure working condition $\alpha = 1/2$ and for a) $n = 0.5$, b) $n = 1$, and c) $n = 3$. Analytical solution (—) and numerical solution (- - -) 77
5.11 The volume, (5.189), without leak-off ($\gamma = 0$) and with leak-off ($\gamma > 0$) of a partially open fracture ($\beta = 0.5$) is plotted against $K_n t$ and $n = 0.5$ for the working conditions a) $\alpha = 1/2$, b) $\alpha = 1$ and c) $\alpha = (n+1)/(n+2)$. 79
5.12 The length, (5.161), without leak-off ($\gamma = 0$) and with leak-off ($\gamma > 0$) of a partially open fracture ($\beta = 0.5$) is plotted against $K_n t$ for $n = 0.5$ for the working conditions a) $\alpha = 1/2$, b) $\alpha = 1$ and c) $\alpha = (n+1)/(n+2)$. 79
5.13 The ratio of volumes, (**??**), of a partially open fracture ($\beta = 0.5$) with leak-off ($\gamma > 0$) and without leak-off ($\gamma = 0$) is plotted against the scaled time $K_n t$ for for $n = 0.5$ using the working conditions a) $\alpha = 1/2$, b) $\alpha = 1$, and c) $\alpha = \frac{n+1}{n+2}$. 81
5.14 The ratio of volumes, (**??**), of a partially open fracture ($\beta = 0.5$) with leak-off ($\gamma > 0$) and without leak-off ($\gamma = 0$) is plotted against the scaled time $K_n t$ for for $n = 3$ using the working conditions a) $\alpha = 1/2$, b) $\alpha = 1$, and c) $\alpha = \frac{n+1}{n+2}$. . 81

6.1 The half-width, 6.34 , is plotted against x for different values of time t for $\beta = 0.75$, $\gamma = 0.2$ and $K_n = 1/3$ for values of $\frac{c_3}{c_1}$ given in Table 6.1 for a) $n = 0.5$, b) $n = 1$ and c) $n = 3$. 90
6.2 The length, 6.36 , is plotted against time t, for $\beta = 0.75$, $\gamma = 0.2$ and $K_n = 1/3$ for values of $\frac{c_3}{c_1}$ given in Table 6.1 for a) n=0.5, b) n=1 and c) n=3 90
6.3 The fluid velocity ratio for a traveling wave solution is plotted against ξ at time $t = 0$ with parameter values $\beta = 0.75$, $\gamma = 0.2$ and $K_n = 1/3$, for values of the ratio $\frac{c_3}{c_1}$ given in Table 6.1 and for a) $n = 0.5$, b) $n = 1$ and c) $n = 3$. 91

7.1 The half-width of the fracture, 7.10, is plotted against x with parameter values $\beta = 0.75$, $\gamma = 0.2$ and for a) $K_n = 1/3$ and $n = 0.5$ and b) $K_n = 2/3$ and $n = 1$. 100

List of Tables

5.1 A summary of the physical significance of the working conditions at the fracture entry and the corresponding value of the parameter α. 59

6.1 Parameter values $\frac{c_3}{c_1}$ for various values of n and $\beta = 0.75$ in the traveling wave solution. 88

Chapter 1

Introduction

1.1 Introduction

Fractures are cracks that divide a medium into parts. In this work, we shall assume the medium to be a rock with elastic properties. Fractures are commonly formed as a result of stress exceeding the rock strength, causing the rock to lose cohesion along its weakest plane. When a rock is subjected to some tensile stress, it creates cracks. This deformation can result in propagation of fractures into previously unfractured rock.

Fracking, a layman's term for hydraulic fracturing of rocks, is the process of creating cracks, and further inducing existing ones by injecting fluid at ultra high pressure into rocks. The purpose of hydraulic fracturing in the petroleum industry is to increase the permeability of the rock formation by using the injected water with some additives to open up existing fractures and create new ones to enhance the extraction of gas and oil reserves. A proppant, typically sand, keeps the fractures open [2]. The analysis of fluid-driven fractures has many applications in the engineering field [3].

In this work we will investigate the propagation of a tortuous hydraulic fracture in permeable rock. Tortuosity refers to the complicated fracture geometry resulting from the surface roughness at the fracture walls caused by the presence of asperities at the fluid-rock interface. Fractures can either be open or partially open depending on the stresses acting along the fracture. For the former, fluid pressure is sufficient to support the compressive normal stresses at the fluid-rock interface. While for partially open fractures, the fluid pressure is insufficient to support the normal elastic stress at the fracture walls resulting in contact regions [4]. This work will focus primarily on partially open fractures.

Since the rock being fractured is assumed to be permeable, fluid leak-off at the fluid-rock interface and into the surrounding formation must be accounted for [5, 6]. A model to account for leak-off velocity at the fluid rock interface will be investigated. Darcy's law for porous media can be used to account for fluid leak-off [7]. In this work fluid leak-off velocity is not specified a priori, its functional form has to satisfy a partial differential equation in order for the governing equation to admit a Lie point symmetry generator [6].

A two-dimensional symmetric model will be used to replace a pre-existing tortuous hydraulic fracture in permeable rock in the modelling process, while the linear crack law will be used to account for the presence of contact regions, formed by touching asperities, within the fracture.

1.2 Background

Hydraulic fractures can either be natural or man-made. Naturally, intrusive dykes and sills form as a result of magma flow propagating through cracks in the earth's crust during volcanic eruptions. Man-made fractures are commonly used in the energy industry, created by injecting a viscous fluid from a bore hole into the earth's subsurface rock [3, 8, 9, 10]. Water is pumped at ultra-high pressures to open and enlarge fissures in order to enhance fluid flow in geothermal energy reservoirs [4]. In the petroleum industry man-made fractures are mostly created for the extraction of oil and gas from shale. Man-made hydraulic fracture experiments were first conducted in 1947. In 1950, its application became commercially successful in the extraction of gas from shale.

Hydraulic fracturing has been used in areas that were known to be rich in natural gas that had been locked tightly in the shale rock over 2000 metres beneath the subsurface for years, as it was both economically and technologically not feasible to produce [5]. The technique has been proven to be very useful as it has enabled the extraction of oil and natural gases from shale [6]. Fracturing is designed to maximize permeability, increasing the accessibility and production of oil and/or gas [2, 5].

The procedure of creating man-made hydraulic fractures for the extraction of oil and/or gas from shale is illustrated in Figure 1.1. The method used in the petroleum industry may be outlined as follows: a fluid-driven crack is created by drilling a vertical well-bore through the earth's layers and rocks until a shale layer is reached. Once the shale layer is reached the drill changes direction and begins to drill horizontally. A steel casting secured by cement is fed into the entire length of the well-bore. A fracturing fluid made from water, sand and some chemical additives is pumped into the well-bore which widens existing cracks, while inducing new ones and further propagating all cracks. The fractures will remain open because of the proppants in the fracturing fluid. The fluid is pumped at a rate that increases the pressure within the crack such that the fluid pressure exceeds the minimum principal stress in the rock resulting in fractures that propagate [2, 10].

The aim of the research is to investigate a tortuous hydraulic fracture in permeable rock.This work seeks to give insight into how fluid leak-off in permeable rocks affects the fracture propagation of tortuous hydraulic fractures.

1.3 Literature review

Since the first experiment was conducted on hydraulic fracturing, numerous contributions have been made to the analysis of fluid-driven fractures. There is extensive literature for laminar hydraulic fracturing in both permeable and impermeable rock [2, 3, 4, 6, 11]. Authors have designed significant models and proposed laws that have contributed tremendously to the advancement of this technique, both in permeable and impermeable rocks. One such law is the cubic flow law. which applies well to fractures with little or no asperities at the fluid-rock interface and no contact regions [4, 12].

Fitt et. al [4] investigated the propagation of a one-dimensional fluid-driven crack in a hot dry rock geothermal energy reservoirs (HDRGERs), assumed to consist of linearly elastic rock, from one borehole to another. They focused on the mathematical models that can arise for a one-dimensional crack. Lubrication approximation was used given that the crack length is much longer than the crack height. Generally in literature, open fractures without contact regions are considered where the fluid pressure sufficiently sup-

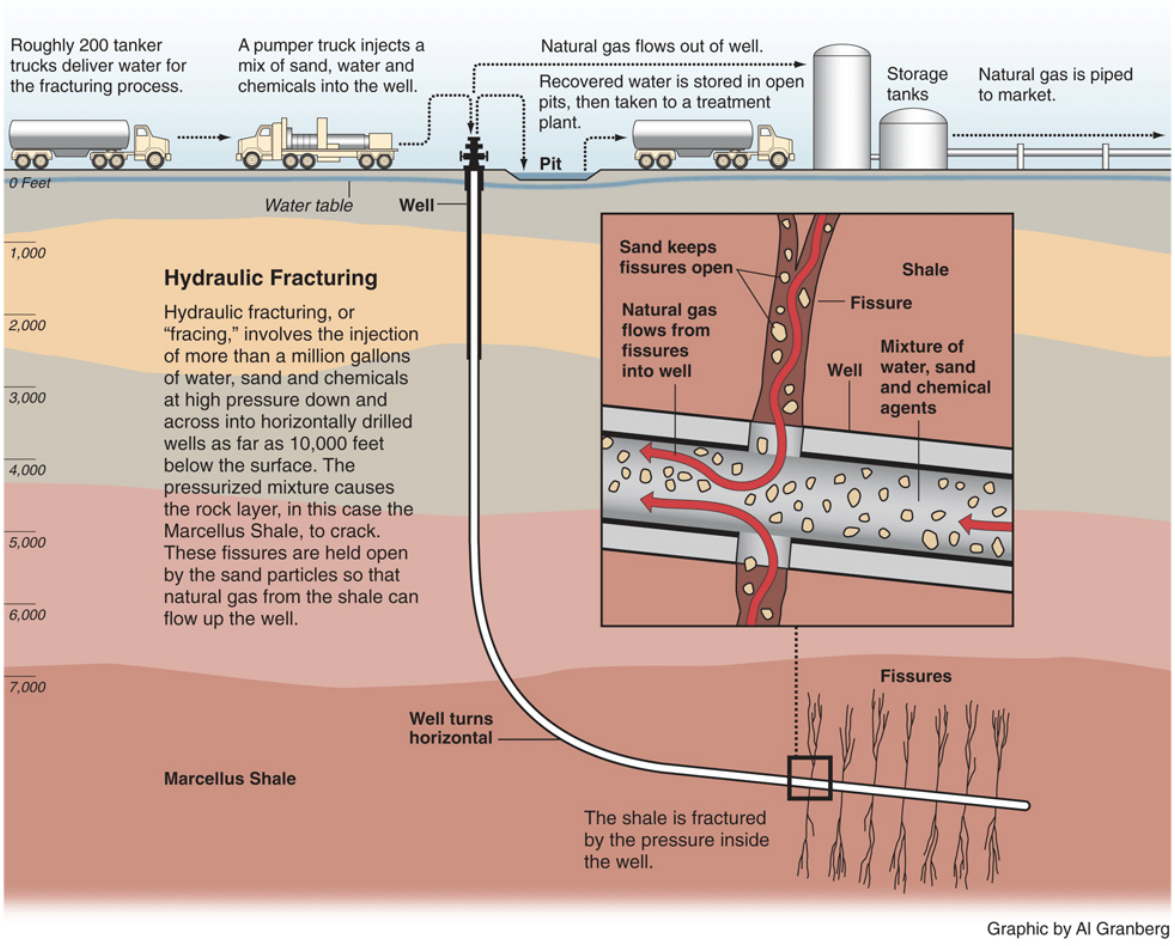


Figure 1.1: The hydraulic fracturing process in a oil/gas field is illustrated [1].

ports the compressive normal stress at the fluid-rock interface. However, cracks in HDRGERs are partially open and possess many contact regions, touching asperities, where the fluid pressure needs the aid of contact regions to sufficiently support the compressive normal stress at the fracture walls. Several authors have investigated and found that the cubic flow law fails when the asperities in the fracture in question are well-defined, making it not advisable to use in modelling highly tortuous fractures [12, 13, 14]. Due to the limitations of the cubic flow law, various other authors have proposed alternative models to account for well-defined asperities in very tortuous fractures. One such model is the modified Reynolds' flow law, which we shall refer to as the general flow law, that accounts for the presence of asperities at the fluid-rock interface. Fitt et. al [4] used this law to describe the nature of the fluid-flow resulting from a tortuous hydraulic fracture with contact regions as a result of touching asperities. In this work, we will consider a tortuous hydraulic fracture with contact regions and fluid leak-off at the fluid-rock interface.

Fluid injection in a tortuous fracture propagating in impermeable rock with contact regions being modelled by a linear crack law was investigated by Kgatle and Mason [11]. In this article, the lubrication approximation is applied due to the excessively narrow and long nature of the fracture. In both [4] and [11] a linear crack law was incorporated in the modelling process, in which the half-width of the fracture is related to the effective stress by a piece-wise linear function, in order to account for the presence of touching asperities in the fracture. The Perkins-Kern-Nordgren (PKN) approximation relating the half-width of the fracture to the normal stresses at the fluid-rock interface was used to close the model [15, 16].

Propagation of a fracture in permeable rock results in fluid leak-off at the fluid-rock interface. In the propagation of a hydraulic fracture in permeable media, leak-off velocity plays an essential part, and as such it must be accounted for. Fareo and Mason [6] have considered investigating the propagation of a hydraulic fracture with no tortuosity in permeable rock, a case where leak-off velocity is not described a priori. Lie group analysis is performed in order to derive the functional form of the leak-off velocity. With the aid of lubrication theory and the PKN approximation, a partial differential equation relating the half-width to the leak-off velocity was derived.

Although there is extensive literature on porous media and some literature on tortuosity, these two concepts have not been richly investigated together in one problem. There is room for further exploration towards the modelling of a linear hydraulic fracture propagating in permeable rock. In this work we will extend on the work done on tortuous hydraulic fractures [11] by considering the case where the rock being fractured is permeable [6]. The linear crack law will be used to account for contact regions in partially open fractures [17].

1.4 Outline of the dissertation

The propagation of a linear hydraulic fracture with tortuosity in permeable rock is investigated in this dissertation. The structure of this dissertation is as follows:

- In Chapter 2, a detailed derivation of the mathematical formulation of the governing equation describing a linear hydraulic fracture with tortuosity and fluid leak-off at the fluid-rock interface is done. The assumptions underlying the derivation are also outlined. The effect of tortuosity is introduced using the modified Reynolds'

flow law while the porosity of the rock is considered by using the appropriate interface conditions resulting in a nonlinear diffusion equation.

- Methods of solutions that are to be employed in solving the derived nonlinear diffusion equation will be discussed in Chapter 3. Here, a brief introduction and theory related to obtaining group invariant solutions and conservation laws will be presented.

- In Chapter 4, we derive the conservation laws of the governing equation. By Sjöberg's double reduction theorem [18], association of a conserved vector and a Lie point symmetry may lead to the derivation of analytical solutions.

- Chapter 5 will show the derivation of the group invariant solution of the half-width and leak-off velocity of the fracture. We then investigate various operating conditions at the fracture entry. Exact analytical solutions are investigated. Numerical solutions will be investigated in Section 5.7. We also investigate an approximate analytical solution of the problem by anaylsing the width-averaged fluid velocity of the fracture. A comparison of a tortuous hydraulic fracture with and without leak-off will conclude this chapter.

- In Chapters 6 and 7, we present other forms of the group invariant solution derived from different forms of the Lie point symmetry generator. These solutions, the traveling wave solution and the exponential solution, are obtained by taking a linear combination of some of the symmetries.

Chapter 2

Model Formulation

In this chapter, we consider a mathematical derivation of a model fracture for a pre-existing tortuous hydraulic fracture propagating in a permeable rock. The permeability of the rock mass results in fluid leaking off into the surrounding rock mass encasing the fracture. We will confine our study to partially open fractures although the model considered can be applicable to open fractures as well. The partially open fracture is driven by an incompressible fluid.

A detailed description of the problem will be provided. We will then state important assumptions on which the model depends. The mathematical model governing the fluid-driven fracture is then formulated.

2.1 Problem description

A pre-existing tortuous fracture propagating in permeable rock is replaced by the pre-existing symmetric two-dimensional model fracture in permeable rock illustrated in Figure 2.1. A modified Reynolds' flow law is used to account for the effect of asperities in the tortuous fracture on the fluid flow. The fluid injected into the fracture at the fracture entry propagates the fracture further in the positive x-direction while some of the fluid is lost to the surrounding permeable rock formed by cracked rock segments. The boundary of the fracture is $z = \pm h(t,x)$ across the fracture with $0 \leq x \leq L(t)$ along the fracture length, $L(t)$, where $h(t,x)$ is half-width of the fracture. An important assumption made in the derivation of the model is that the fluid that is being injected at the entry of the fracture is Newtonian. The fracture entry is at $x = 0$ and all quantities related to the fracture are independent of y.

The components of the fluid velocity vector are

$$v_x = v_x(t,x,z), \qquad v_y = 0, \qquad v_z = v_z(t,x,z),$$

and the pressure is

$$p = p(t,x,z).$$

2.2 Assumptions

To build a mathematical model that describes the process of hydraulic fracturing, it is necessary to consider the following assumptions:

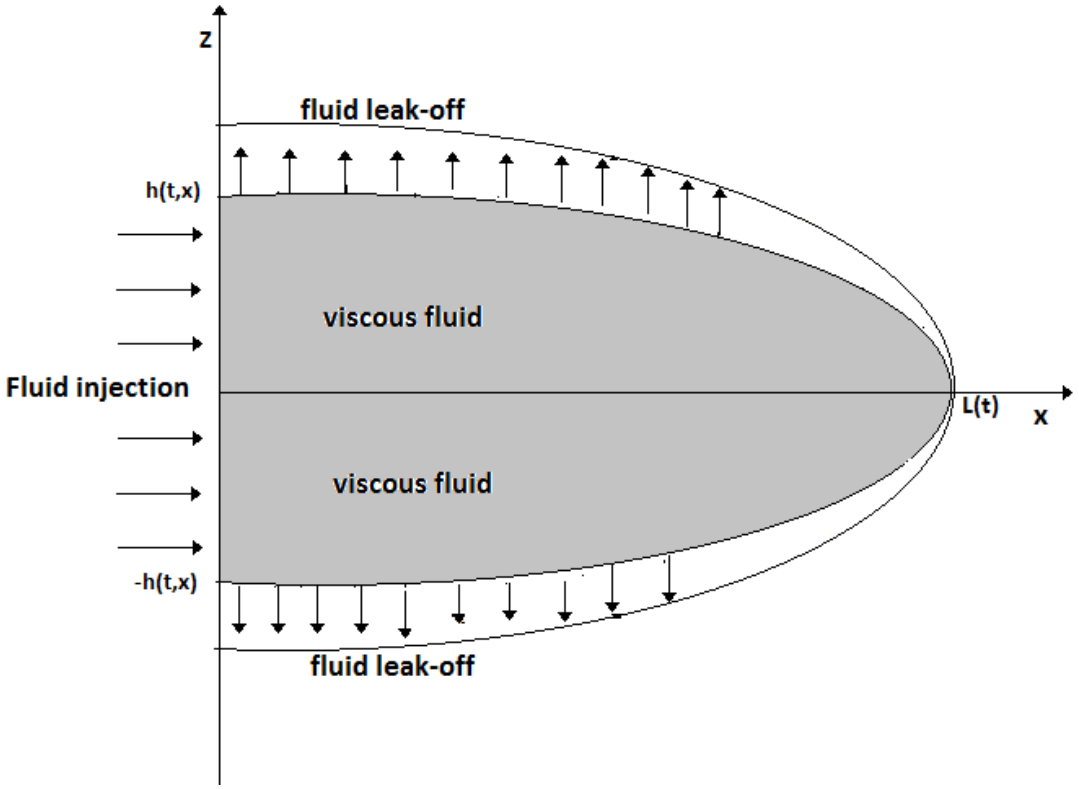


Figure 2.1: A pre-existing two-dimensional linear hydraulic fracture propagating in a permeable rock.

- The fracture is two-dimensional;
- The fracture propagates along the positive x-direction;
- The fracture is completely filled with a Newtonian fluid;
- The flow of fluid in the fracture is laminar;
- The fracture is symmetrical about the x-axis;
- The fracture is pre-existing, the initial length is non-zero $L(0)$;
- Lubrication theory is applied to the problem as the length of the fracture is considerably less than the magnitude of the half-width of the fracture;
- The rock mass encasing the fracture is linearly elastic;
- The rock mass encasing the fracture is permeable and fluid leaks off into the surrounding cracked rock segments [6];
- Tortuosity is modelled using a modified Reynolds' flow law [4, 11].

2.3 Governing equations

2.3.1 Mathematical model

We first consider a model for a fracture with little to no asperities at the fluid-rock interface [4, 11]. The fluid flow in such a fracture satisfies the Navier-Stokes equation for an incompressible fluid with zero body force,

$$\frac{\partial \underline{v}}{\partial t} + (\underline{v} \cdot \underline{\nabla})\underline{v} = -\frac{1}{\rho}\nabla p + \nu \nabla^2 \underline{v}, \tag{2.1}$$

and the conservation of mass equation,

$$\underline{\nabla} \cdot \underline{v} = 0, \tag{2.2}$$

where $\underline{v} = (v_x(t,x,z), 0, v_z(t,x,z))$ is the fluid velocity , t is the time, $p(t,x)$ is the fluid pressure, ρ is the fluid density and $\nu = \mu/\rho$ is the kinematic viscosity of the fluid with μ, the dynamic viscosity. From (2.1) it can be shown that the x and z components of the Navier-Stokes equation are

$$\rho\Big[\frac{\partial v_x}{\partial t} + v_x\frac{\partial v_x}{\partial x} + v_z\frac{\partial v_x}{\partial z}\Big] = -\frac{\partial p}{\partial x} + \mu\Big[\frac{\partial^2 v_x}{\partial x^2} + \frac{\partial^2 v_x}{\partial z^2}\Big], \tag{2.3}$$

$$\rho\Big[\frac{\partial v_z}{\partial t} + v_x\frac{\partial v_z}{\partial x} + v_z\frac{\partial v_z}{\partial z}\Big] = -\frac{\partial p}{\partial z} + \mu\Big[\frac{\partial^2 v_z}{\partial x^2} + \frac{\partial^2 v_z}{\partial z^2}\Big]. \tag{2.4}$$

The following dimensionless variables are defined

$$x^* = \frac{x}{L},\ z^* = \frac{z}{H},\ v_x^* = \frac{v_x}{U},\ v_z^* = \frac{v_z L}{UH},\ p^* = \frac{p}{P},\ t^* = \frac{Ut}{L}, \tag{2.5}$$

where

the characteristic fracture length in the x-direction = L;

the characteristic fracture half-width in the z-direction = H;

the characteristic fluid velocity in the x-direction = U;

the characteristic fluid velocity in the z-direction V = $\frac{HU}{L}$;

the characteristic fluid pressure for the lubrication approximation
$P = \frac{\mu UL}{H^2}$

and the characteristic time T = $\frac{L}{U}$.

In dimensionless form, equations (2.3) and (2.4), using the dimensionless variables (2.5), reduces to:

$$Re\Big(\frac{H}{L}\Big)^2\Big[\frac{\partial v_x^*}{\partial t^*} + v_x^*\frac{\partial v_x^*}{\partial x^*} + v_z^*\frac{\partial v_x^*}{\partial z^*}\Big] = -\frac{\partial p^*}{\partial x^*} + \Big(\frac{H}{L}\Big)^2\frac{\partial^2 v_x^*}{\partial x^{*2}} + \frac{\partial^2 v_x^*}{\partial z^{*2}}, \tag{2.6}$$

$$Re\Big(\frac{H}{L}\Big)^4\Big[\frac{\partial v_z^*}{\partial t^*} + v_x^*\frac{\partial v_z^*}{\partial x^*} + v_z^*\frac{\partial v_z^*}{\partial z^*}\Big] = -\frac{\partial p^*}{\partial z^*} + \Big(\frac{H}{L}\Big)^4\frac{\partial^2 v_z^*}{\partial x^{*2}} + \Big(\frac{H}{L}\Big)^2\frac{\partial^2 v_z^*}{\partial z^{*2}}, \tag{2.7}$$

while equation (2.2) remains invariant under the scaling transformation (2.5). We apply the lubrication approximation:

$$Re\left(\frac{H}{L}\right)^2 << 1, \qquad \frac{H}{L} << 1, \tag{2.8}$$

where Re is the Reynolds number,

$$Re = \frac{UL}{\nu}, \tag{2.9}$$

since the half-width of the fracture is much less in magnitude than the length of the fracture. With the aid of (2.5), it follows that the continuity equation (2.2) and the x and z components of the Navier-Stokes equations, (2.6) and (2.7), in dimensional form are

$$\frac{\partial p}{\partial x} = \mu \frac{\partial^2 v_x}{\partial z^2}, \tag{2.10}$$

$$\frac{\partial p}{\partial z} = 0, \tag{2.11}$$

$$\frac{\partial v_x}{\partial x} + \frac{\partial v_z}{\partial z} = 0. \tag{2.12}$$

The system of equations (2.10) to (2.12) can be solved subject to appropriate boundary conditions which will be discussed next.

2.3.2 Fluid leak-off at the fluid-rock interface

The concept of fluid leak-off at the fluid-rock interface in the modelling process is considered by investigating the boundary conditions at the fluid-rock interface $z = \pm h(t,x)$.

The first boundary condition is the no-slip condition for a viscous fluid at the fluid rock interface which satisfies the following equations:

$$z = h(t,x): \quad v_x(t,x,h) = 0, \tag{2.13}$$

$$z = -h(t,x): \quad v_x(t,x,-h) = 0. \tag{2.14}$$

The no-slip boundary condition is satisfied when fluid does not slip but sticks to the fracture walls.

The second boundary condition is the fluid leak-off condition at the fluid-rock interface which satisfies the following equations:

$$z = h(t,x): \quad v_z(t,x,h) = \frac{\partial h}{\partial t} + v_\ell(t,x), \tag{2.15}$$

$$z = -h(t,x): \quad v_z(t,x,-h) = -\frac{\partial h}{\partial t} - v_\ell(t,x), \tag{2.16}$$

where the leak-off velocity relative to the moving interface is denoted by $v_\ell(t,x)$. The z-component of the fluid velocity in the fracture is a linear combination of the rate at which the half-width of the fracture is evolving and the leak-off velocity.

Since the fracture considered is pre-existing, the following initial conditions are imposed on the model:
The fracture has an initial half-width profile given by

$$h(0,x) = h_0(x), \tag{2.17}$$

and the initial length is given by

$$L(0) = L_0 \tag{2.18}$$

At the fracture tip, the half-width of the fracture vanishes

$$h(t, L(t)) = 0. \tag{2.19}$$

2.3.3 Nonlinear diffusion equation with leak-off

The governing nonlinear diffusion equation for the half-width of the fracture will be derived. From equation (2.11), it is clear that the fluid pressure in the fracture is only dependent on the spatial variable x and time t, i.e. $p = p(t,x)$. It follows that integrating (2.10) twice with respect to z subject to the no-slip boundary conditions (2.13) and (2.14) gives

$$v_x(t,x,z) = -\frac{1}{2\mu}\left(h^2(t,x) - z^2\right)\frac{\partial p}{\partial x}(t,x). \tag{2.20}$$

Integrating the continuity equation, (2.12), with respect to z across the fracture from $-h(t,x)$ to $h(t,x)$ gives

$$\int_{-h(t,x)}^{h(t,x)} \frac{\partial v_x}{\partial x} dz + v_z(t,x,z)\Big|_{-h(t,x)}^{h(t,x)} = 0, \tag{2.21}$$

which clearly, with the aid of the leak-off boundary conditions (2.15) and (2.16), simplifies to

$$2\frac{\partial h}{\partial t} + 2v_\ell(t,x) + \int_{-h(t,x)}^{h(t,x)} \frac{\partial v_x}{\partial x} dz = 0. \tag{2.22}$$

Applying Leibniz rule for differentiation under the integral sign [19] to equation (2.22) and the no-slip boundary conditions, (2.13) and (2.14), to the result gives the conservation equation:

$$\frac{\partial h}{\partial t} + \frac{1}{2}\frac{\partial Q}{\partial x} = -v_\ell(t,x), \tag{2.23}$$

where

$$Q(t,x) = \int_{-h(t,x)}^{h(t,x)} v_x(t,x,z) dz, \tag{2.24}$$

is the volume flux per unit breadth across the fracture. With the aid of equation (2.20) it can be shown that equation (2.24) reduces to

$$Q(t,x) = \frac{-2}{3\mu} h^3 \frac{\partial p}{\partial x}. \tag{2.25}$$

2.3.4 Mathematical model of fluid flow in a tortuous hydraulic fracture.

The validity of applying a cubic flow law in tortuous fractures was investigated for open fractures encased by impermeable rock by Oron and Berkowitz [13] and Witherspoon et. al [14]. It has been found that the cubic flow law fails when the asperities in the fracture

are well-defined. Therefore it is not recommended to make use of this cubic law when modeling a very tortuous fracture. In order to account for the effects of tortuosity due to the asperities at the fluid-rock interface on the fluid flow in a fracture, we consider a modified Reynolds' flow law in which the cubed half-width h^3 is replaced by $a_n h^n$ where a_n and n are constants that can be determined from experiments [4]. Equation (2.25) becomes

$$Q(t,x) = \frac{-2a_n}{3\mu} h^n \frac{\partial p}{\partial x}. \tag{2.26}$$

Finally, substituting (2.26) into (2.23) gives the nonlinear partial differential equation

$$\frac{\partial h}{\partial t} = \frac{a_n}{3\mu} \frac{\partial}{\partial x}\left(h^n \frac{\partial p}{\partial x}\right) - v_\ell(t,x). \tag{2.27}$$

The width-averaged fluid velocity, $\bar{v}_x(t,x)$ is

$$\bar{v}_x(t,x) = \frac{1}{2h(t,x)} \int_{-h(t,x)}^{h(t,x)} v_x(t,x,z)\,dz, \tag{2.28}$$

which by (2.24) can be expressed as

$$\bar{v}_x(t,x) = \frac{Q(t,x)}{2h(t,x)}. \tag{2.29}$$

From (2.26), equation (2.29) reduces to

$$\bar{v}_x(t,x) = -\frac{a_n}{3\mu} h^{n-1} \frac{\partial p}{\partial x}. \tag{2.30}$$

2.3.5 Model closure

The type of stresses that occur in the rock mass encasing the fracture tell us about the nature of fracture that propagates; depending on the type of stresses acting at the fluid rock-interface, the fracture can either be open or a partially open. When asperities in the fracture are sufficiently large, they touch to form contact regions. Open fractures do not possess contact regions in most of the area in the fracture until one approaches the fracture tip, where contact regions are inevitable. Partially open fractures have contact regions in most of the area in the fracture [4, 11]. The presence of contact regions in the fracture is determined by whether or not the fluid pressure, $p(t,x)$, is adequate to reinforce the compressive normal stress, $-\sigma_{zz}(t,x)$, at the fluid-rock interface.

An open fracture occurs when the fluid pressure is sufficient to support the normal stress along the fluid-rock interface:

$$p(t,x) = -\sigma_{zz}(t,x), \tag{2.31}$$

where $\sigma_{zz}(t,x) < 0$. It follows that the zero effective stress condition,

$$p(t,x) + \sigma_{zz}(t,x) = 0, \tag{2.32}$$

must be satisfied in order to affirm that a fracture is open.

If the fluid pressure is insufficient to support the normal stress at the fluid-rock interface then

$$p(t,x) < -\sigma_{zz}(t,x), \tag{2.33}$$

where $\sigma_{zz}(t,x) < 0$. It follows that the negative effective stress condition must be satisfied [20]:

$$p(t,x) + \sigma_{zz}(t,x) < 0. \tag{2.34}$$

Although both open and partially open fractures can be considered [11], we will confine our study to partially open fractures.

The linear crack law

This was proposed by Pine and Cundall [17], and it satisfies the negative effective stress condition (2.34). The linear crack law gives a linear relationship between the fracture half-width, $h(t,x)$, and the effective stress, $\sigma_{zz}(t,x) + p(t,x)$:

$$h(t,x) = \begin{cases} h_{max} - \left(\frac{\sigma_{zz}(t,x)+p(t,x)}{\sigma_R}\right)(h_{max} - h_{min}), & \text{if} \quad \sigma_R < \sigma_{zz}(t,x) + p(t,x) < 0, \\ h_{min}, & \text{if} \quad \sigma_{zz}(t,x) + p(t,x) \leq \sigma_R, \end{cases} \tag{2.35}$$

where $\sigma_R < 0$ is the least effective stress, also known as the reference stress, h_{max} is the maximum height of the fracture and h_{min} is the minimum height of the fracture. We assume that the minimum half-width of the fracture is much less than the maximum half-width of the fracture, $h_{min} << h_{max}$, we can make an approximation that $h_{min} = 0$ [11]. The linear crack law reduces to

$$h(t,x) = \begin{cases} h_{max}\left(1 - \frac{\sigma_{zz}(t,x)+p(t,x)}{\sigma_R}\right), & 0 < \frac{\sigma_{zz}(t,x)+p(t,x)}{\sigma_R} < 1, \\ 0, & \frac{\sigma_{zz}(t,x)+p(t,x)}{\sigma_R} \geq 1, \end{cases} \tag{2.36}$$

which defines the half-width, $h(t,x)$, of the symmetric model fracture in the domain $0 \leq h(t,x) < h_{max}$.

The Perkins-Kern and Nordgren (PKN) approximation

The PKN approximation is used in order to relate the normal stress, $\sigma_{zz}(t,x)$, to the half-width of the fracture, $h(t,x)$ [16, 15]. The theory of plane strain can be applied to the surrounding rock mass encasing the fracture in order to express the normal stress, $\sigma_{zz}(t,x)$, as a Cauchy principal value integral. Spence and Sharp gave a relation between the normal surface stress and the half-width of the fracture as [21]

$$\sigma_{zz}(t,x) = \sigma_{zz}^{(\infty)} + \frac{G}{2\pi(1-\nu)} \fint_{-\infty}^{\infty} \frac{\partial h}{\partial s}(t,x) \frac{ds}{(s-x)}, \tag{2.37}$$

where the barred integral sign represents the Cauchy principal value which was used by Fitt et al [4] in the study of crack propagation models in geothermal reservoirs. The parameters in equation (2.37) are defined as follows:

G is the elastic shear modulus,

$\frac{G}{2\pi(1-\nu)}$ is the measure of resistance of a rock to deformation,

ν is the Poisson ratio of the rock mass and

σ^{∞}_{zz} is the far field normal stress within the rock.

An alternative to using the Cauchy principal value is needed as it results in a boundary value problem that is difficult to solve [4, 21]. In this work, instead of using (2.37) for the normal stress $\sigma_{zz}(t,x)$ we will use the PKN approximation given as [15, 16]

$$\sigma_{zz}(t,x) = \sigma^{\infty}_{zz} - \Lambda h(t,x), \tag{2.38}$$

where

$$\Lambda = \frac{E}{(1-\nu^2)B}, \tag{2.39}$$

E is the Young's modulus and B is the breadth of the fracture, which is used widely in the gas and oil industry to design fracture treatments [22].

We use (2.38) to express the normal stress, $\sigma_{zz}(t,x)$, in terms of the half-width of the fracture $h(t,x)$ and the linear crack law to close the model. Using the linear crack law (2.36) and the PKN approximation (2.38) we obtain the equation for fluid pressure :

$$p(t,x) = -\sigma^{\infty}_{zz} + \Lambda h(t,x) + \left(1 - \frac{h(t,x)}{h_{max}}\right)\sigma_R. \tag{2.40}$$

Differentiating (2.40) with respect to x gives an expression for the pressure gradient

$$\frac{\partial p}{\partial x}(t,x) = \Lambda\left(1 - \frac{\sigma_R}{\Lambda h_{max}}\right)\frac{\partial h}{\partial x}(t,x). \tag{2.41}$$

Therefore, using (2.41), the governing non-linear diffusion equation (2.27) is

$$\frac{\partial h}{\partial t} = \frac{\Lambda a_n}{3\mu}\left(1 - \frac{\sigma_R}{\Lambda h_{max}}\right)\frac{\partial}{\partial x}\left(h^n \frac{\partial h}{\partial x}\right) - v_\ell(t,x), \tag{2.42}$$

and the volume flux of fluid and the width-averaged fluid velocity given by (2.26) and (2.30) respectively are

$$Q(t,x) = \frac{-2\Lambda a_n}{3\mu}\left(1 - \frac{\sigma_R}{\Lambda h_{max}}\right)h^n \frac{\partial h}{\partial x} \tag{2.43}$$

and

$$\bar{v}_x(t,x) = \frac{-\Lambda a_n}{3\mu}\left(1 - \frac{\sigma_R}{\Lambda h_{max}}\right)h^{n-1}\frac{\partial h}{\partial x}. \tag{2.44}$$

2.3.6 Boundary conditions

The following boundary conditions for the nonlinear diffusion equation (2.42) are considered:
At the fracture tip, the half-width of the fracture vanishes

$$h(t, L(t)) = 0, \qquad t \geq 0. \tag{2.45}$$

The volume flux of fluid at the fracture tip, $Q(t,L(t))$, will later be investigated.

The boundary condition (2.45) is a moving boundary condition, given that as the fracture propagates, the length, $L(t)$, of the fracture is also increasing [23].

We also consider a boundary condition at the fracture entry,

$$Q(t,0) = S(t), \tag{2.46}$$

where the form of $S(t)$ will be determined from the group invariant solution of the problem. This boundary condition will be obtained from the fluid flux at the fracture entry related to a power-law or an exponential function of time specified at the fracture entry [24].

Integrating equation (2.23) with respect to x from 0 to $L(t)$ with the aid of Leibniz rule of differentiation under the integral sign gives

$$\int_0^{L(t)} \frac{\partial h}{\partial t} dx + \frac{1}{2}\int_0^{L(t)} \frac{\partial Q}{\partial x} dx + \int_0^{L(t)} v_\ell(t,x) dx = 0. \tag{2.47}$$

From Leibniz:

$$\frac{d}{dt}\int_0^{L(t)} h(t,x) = h(t,L(t)\frac{dL}{dt} - h(t,0)\frac{d}{dt}(0) + \int_0^{L(t)} \frac{\partial h}{\partial t} dx. \tag{2.48}$$

Therefore, using (2.48), (2.47) becomes

$$\begin{aligned}&\frac{d}{dt}\int_0^{L(t)} h(t,x)dx - h(t,L(t))\frac{dL}{dt} + h(t,0)\frac{d}{dt}(0) + \frac{1}{2}\Big[Q(t,L(t)) - Q(t,0)\Big] \\ &+ \int_0^{L(t)} v_\ell(t,x)dx = 0.\end{aligned} \tag{2.49}$$

Let $V(t)$ denote the total volume of the fracture per unit length, given by

$$V(t) = 2\int_0^{L(t)} h(t,x)dx, \tag{2.50}$$

and the flux of fluid leaving the fracture due to fluid leak-off at the fluid-rock interface is

$$q(t) = 2\int_0^{L(t)} v_\ell(t,x)dx. \tag{2.51}$$

It follows that, with the aid of the boundary condition at the fracture tip (2.45), that equation (2.49) becomes

$$\frac{1}{2}\frac{dV}{dt} + \frac{1}{2}\Big[Q(t,L(t)) - Q(t,0)\Big] + \frac{1}{2}q(t) = 0. \tag{2.52}$$

As a result,

$$\frac{dV}{dt} = Q(t,0) - q(t) - Q\left(t,L(t)\right), \tag{2.53}$$

where $Q(t,0)$ and $Q\left(t,L(t)\right)$ can be deduced from (2.43). Using (2.43) and (2.51), equation (2.53) becomes

$$\begin{aligned}\frac{dV}{dt} =& -\frac{2\Lambda a_n}{3\mu}\left(1 - \frac{\sigma_R}{\Lambda h_{max}}\right)h^n(t,0)\frac{\partial h}{\partial x}(t,0) - 2\int_0^{L(t)} v_\ell(t,x)dx \\ &+ \frac{2\Lambda a_n}{3\mu}\left(1 - \frac{\sigma_R}{\Lambda h_{max}}\right)h^n(t,L(t))\frac{\partial h}{\partial x}(t,L(t)),\end{aligned} \tag{2.54}$$

which is the consistency condition that is satisfied everywhere along the fracture.

2.3.7 Dimensionless equations

The characteristic length of the fracture is chosen to be the initial length of the pre-existing fracture

$$L(t) = L(0) = L_0. \tag{2.55}$$

The characteristic half-width of the fracture is chosen to be the maximum half-width of the fracture,

$$H = h_{max}. \tag{2.56}$$

The characteristic velocity in the x-direction, U, is determined by balancing the expression for the characteristic fluid pressure given by the lubrication approximation (2.10) with the characteristic pressure deduced from (2.40),

$$p = -\sigma_{zz}^{(\infty)} + \Lambda h_{max}. \tag{2.57}$$

It follows that the characteristic velocity is

$$U = \frac{\Lambda h_{max}^3}{\mu L_0}\left(1 - \frac{\sigma_{zz}^{\infty}}{\Lambda h_{max}}\right). \tag{2.58}$$

In addition to the dimensionless variables introduced in (2.5), the following dimensionless variables are introduced

$$h^* = \frac{h}{h_{max}}, \quad L^* = \frac{L}{L_0}, \quad Q^* = \frac{Q}{h_{max}U}, \quad v_\ell = \frac{L_0 v_\ell}{UH}, \quad q^* = \frac{q}{h_{max}U}, \quad S^* = \frac{S}{h_{max}U}. \tag{2.59}$$

In terms of the dimensionless variables in (2.5) and (2.59), with the aid of specified characteristic quantities (2.55) to (2.58), the nonlinear diffusion equation (2.42), in dimensionless form becomes

$$\frac{\partial h}{\partial t} = K_n \frac{\partial}{\partial x}\left(h^n \frac{\partial h}{\partial x}\right) - v_\ell(t,x), \tag{2.60}$$

where

$$K_n = \frac{a_n h_{max}^{n-3}}{3}\left(\frac{1 - \frac{\sigma_R}{\Lambda h_{max}}}{1 - \frac{\sigma_{zz}^{\infty}}{\Lambda h_{max}}}\right) \tag{2.61}$$

is the diffusion constant. Since equation (2.60) has two dependent variables, an equation for $v_\ell(t,x)$ has to be provided or a form of $v_\ell(t,x)$ determined. Once a form of $v_\ell(t,x)$ is known, equation (2.60) can then be solved subject to the boundary conditions

$$h(t, L(t)) = 0, \tag{2.62}$$

$$Q(t,0) = S(t). \tag{2.63}$$

The solution obtained from (2.60) to (2.63) satisfies the consistency condition:

$$\frac{dV}{dt} = -2K_n h^n(t,0)\frac{\partial h}{\partial x}(t,0) - 2\int_0^{L(t)} v_\ell(t,x)\,dx + 2K_n h^n(t,L(t))\frac{\partial h}{\partial x}(t,L(t)). \tag{2.64}$$

The total volume flux of fluid, the width-averaged fluid velocity and the fluid pressure respectively are:

$$Q(t,x) = -2K_n h^n \frac{\partial h}{\partial x} \tag{2.65}$$

$$q(t) = 2\int_0^{L(t)} v_\ell(t,x)\,dx, \tag{2.66}$$

$$\bar{v}_x(t,x) = -K_n h^{n-1} \frac{\partial h}{\partial x}, \tag{2.67}$$

$$p(t,x) = \left(\frac{1-\frac{\sigma_R}{\Lambda h_{max}}}{1-\frac{\sigma_{zz}^\infty}{\Lambda h_{max}}}\right) h(t,x) + \left(\frac{\sigma_R - \sigma_{zz}^\infty}{\Lambda h_{max} - \sigma_{zz}^\infty}\right). \tag{2.68}$$

The effect that tortuosity has on the specified model is described by the diffusion constant, K_n, and the factor h^n. The form of the leak-off velocity, $v_\ell(t,x)$, contained in the nonlinear diffusion equation (2.60) is yet to be obtained.

2.3.8 Form of leak-off velocity $v_\ell(t,x,z)$

The fluid leak-off velocity, $v_\ell(t,x)$, is not described a priori. Its functional form has to satisfy a partial differential equation obtained from the derivation of the Lie point symmetry generator of the governing nonlinear diffusion equation.

2.4 Conclusions

In this chapter the mathematical model for a partially open fracture was formulated. The concept of fluid leak-off at the fluid-rock interface was considered by investigating the boundary conditions at the fluid-rock interface $z = \pm h(t,x)$. A model with the modified Reynolds' flow law to account for the effect of asperities on the fluid flow. The model is closed by the linear crack law to account for the presence of contact regions in the fracture and the PKN approximation which relates the normal stress at the fracture walls and the half-width of the fracture. The dimensionless form of the model was obtained and will thus be used in the subsequent chapters. The resulting model accounts for fluid leak-off where the form of leak-off, $v_\ell(t,x)$, is not described a priori.

Chapter 3

Methods of solution

3.1 Introduction

In Chapter 2, a rigorous derivation of the governing nonlinear diffusion equation for a linear hydraulic fracture with tortuosity and fluid-leak-off at the fluid-rock interface was presented. It is necessary to investigate methods of solution that will enable us to obtain some analytical and/or numerical solutions to the governing nonlinear diffusion equation. Obtaining analytical solutions will enable us to investigate the relationships between variables and to understand the effect of parameters on the derived equations.

In this chapter, we review the various methods of solutions that can be used to solve the governing equation obtained in Chapter 2. Firstly, we investigate the Lie group analysis of the nonlinear diffusion equation for a linear pre-existing model fracture with the effects of tortuosity and fluid leak-off at the fluid-rock interface considered. This leads to group invariant solutions for the half-width of the fracture and the leak-off velocity which satisfies a partial differential equation determined in the calculation of Lie point symmetries [3, 6, 11].

In this section, we also outline different methods of deriving conservation laws. Association will lead to a reduction of a PDE to an ODE which may at times be completely integrable to give analytical solutions to the problem based on Sjöberg's double reduction theorem [18].

3.2 Lie point symmetry

Mathematically, symmetry is a change, a transformation that leaves an object unchanged. Symmetry analysis of differential equations was developed and applied by Sophus Lie (1842-1899) during the period 1872–1899. This theory enables us to derive exact analytical solutions of differential equations in a completely algorithmic manner or to reduce a partial differential equation to an ordinary differential equation [25].

A Lie point symmetry, adapted for a second order PDE, is defined in [26] as follows: *Consider a second order partial differential equation (PDE) in the dependent variable u and 2 independent variables, t and x:*

$$F(t, x, u, u_{(1)}, u_{(2)}) = 0, \tag{3.1}$$

where $u_{(1)}, u_{(2)}$, are partial derivatives of u with respect to the independent variables, t and x:

$$u_{x^1} = \frac{\partial u}{\partial x^i},\ u_{x^i x^j} = \frac{\partial^2 u}{\partial x^i \partial x^j},$$

with $1 \le i, j \le 2$.
Then

$$X = \xi^1(t,x,u)\frac{\partial}{\partial t} + \xi^2(t,x,u)\frac{\partial}{\partial x} + \eta(t,x,u)\frac{\partial}{\partial u}, \tag{3.2}$$

is the Lie point symmetry of the PDE (3.1) provided

$$X^{[2]}(F)\Big|_{F=0} = 0, \tag{3.3}$$

where

$$X^{[2]} = X + \sum_{i=1}^{2} \zeta_{x^i}\frac{\partial}{\partial u_{x^i}} + \sum_{i=1}^{2}\sum_{j=1}^{2} \zeta_{x^i x^j}\frac{\partial}{\partial u_{x^i x^j}}, \qquad x^1 \equiv t,\ x^2 \equiv x, \tag{3.4}$$

for $i \le j$, is the second order prolongation of the generator X with

$$\begin{aligned} \zeta_{x^i} &= D_{x^i}(\eta) - \sum_{l=1}^{n} u_{x^l} D_{x^i}(\xi^l), \qquad l = 1,2, \\ \zeta_{x^i x^j} &= D_{x^j}(\zeta_{x^i}) - \sum_{l=1}^{n} u_{x^i x^l} D_{x^j}(\xi^l). \end{aligned} \tag{3.5}$$

The total derivatives with respect to the independent variable x^i in (3.5) is

$$D_i = D_{x^i} = \frac{\partial}{\partial x^i} + u_{x^i}\frac{\partial}{\partial u} + \sum_{l=1}^{n} u_{x^i x^l}\frac{\partial}{\partial u_{x^l}} + \cdots \tag{3.6}$$

The unknown functions $\xi^1(t,x,u), \xi^2(t,x,u)$ and $\eta(t,x,u)$ do not depend on the derivatives of u. The determining equation can thus be solved by separating by powers and products of the partial derivatives of the dependent variable u.

The symmetries admitted by equation (3.1) are of the form

$$X = \xi_i^1\frac{\partial}{\partial x^1} + \xi_i^2\frac{\partial}{\partial x^2} + \eta_i\frac{\partial}{\partial u}, \tag{3.7}$$

for $i = 1,2.\cdots m$, where m is the total number of admitted Lie point symmetries for the partial differential equation. A linear combination of Lie point symmetries denoted as

$$X_T = c_1 X_1 + c_2 X_2 + \cdots + c_m X_m, \tag{3.8}$$

where all c_i's are constants, is also a Lie point symmetry of the differential equation.

3.2.1 Group invariant solution

The group invariant solution $u = \psi(t,x)$ of the partial differential equation generated by the Lie point symmetry, X, of the PDE (3.1) may then be constructed by solving the equation

$$X\Big(u-\psi(t,x)\Big)\Big|_{u=\psi(t,x)} = 0. \tag{3.9}$$

Substituting the resulting group invariant solution into the original partial differential equation will reduce the PDE (3.1) into an ordinary differential equation. The group invariant solutions obtained via Lie's approach may provide insight into the physical characteristics of the model [27]. A group invariant solution which depends on an unknown function, called a similarity variable, is obtained. The nonlinear diffusion equation and boundary conditions are then expressed in terms of the group invariant solution which transforms the PDE into an ODE. The unknown function can be determined by solving the ODE subject to the corresponding boundary conditions.

3.3 Conservation laws

Another method that has been used in the literature to find solutions to differential equations is that of conservation laws. The idea of conservation laws plays a vital role in the study of partial differential equations. The mathematical idea of conservation laws comes from the formulation of familiar physical laws such as that of mass, energy and momentum [28]. Conservation laws can also be used to investigate other solutions of the governing equations. Conserved quantities may be of physical significance if they relate to conditions which may be physically attainable. This is useful in the analysis of differential equations. There are many different methods for the systematic construction of conservation laws as described in literature such as in Kara and Mahomed [29], Bluman et al [30], Naz [31] and Naz et al [32]. The most elementary method that does not rely on the knowledge of the Lagrangian function is the direct method. A comprehensive review of methods used to obtain conservation laws with applicative examples are outlined by Naz et al [32]. By the double reduction theorem of Sjöberg [18], association of a Lie point symmetry and a conserved vector, defined by Kara and Mahomed [29, 33], may lead to the derivation of an invariant analytical solution. This was illustrated by examples given by Sjöberg [18].

An outline of the basic theory of the methods that will be required to calculate the conservation laws for the nonlinear diffusion equation is given below:

Consider a second order system of differential equations of 2 *independent and n dependent variables:*

$$F(x,u,u_{(1)},u_{(2)}) = 0, \tag{3.10}$$

which is assumed to be of maximal rank and locally solvable. A conserved vector of (3.10) is a 2-tuple $\boldsymbol{T} = (T^1, T^2)$, $T^i \in \mathcal{A}, i = 1,2$ *such that:*

$$D_1 T^1 + D_2 T^2 = 0 \tag{3.11}$$

holds for all solutions of (3.10), then equation (3.11) is called a local conservation law [28, 29].

3.3.1 Direct method

The direct method is an elementary method of deriving conservation laws. This method was first introduced by Laplace. The method has been successfully applied to obtain conservation laws for several well-known differential equations [28].
Firstly, an assumption is made on the variables that the conserved vector **T** depends. Then a substitution of **T** into the conservation law (3.11), is made to give

$$D_1 T^1 + D_2 T^2\big|_{F=0} = 0, \tag{3.12}$$

for each T^i. The result if then evaluated on the governing partial differential equation. Upon doing this, an over-determined system of equations is obtained. The conservation law is then separated by powers and products of the partial derivatives of variables which **T** does not depend on. Then exact forms of **T** can be obtained [29, 30, 32]. This approach gives all the local conservation laws for the partial differential equation. Illustrative examples of this method being applied are given in [28, 29, 31, 32]. The conservation laws of a linear hydraulic fracture with tortuosity were also calculated by Kgatle and Mason [34].

3.3.2 Multiplier method

The multiplier method has been used in the literature by various authors to obtain conservation laws for partial differential equations [28, 31, 32]. A characteristic function $\Lambda = \Lambda(\underline{x}, u, u_{(1)}, u_{(2)})$ and conserved vector $\mathbf{T} = (T^1, T^2)$ are defined. A multiplier of the PDE (3.10) has the property that

$$\Lambda(F) = D_1 T^1 + D_2 T^2, \tag{3.13}$$

for all functions.

The Euler operator

$$E_h = \frac{\partial}{\partial h} - D_t \frac{\partial}{\partial h_t} - D_x \frac{\partial}{\partial h_x} + D_t^2 \frac{\partial}{\partial h_{tt}} + D_x D_t \frac{\partial}{\partial h_{tx}} + D_x^2 \frac{\partial}{\partial h_{xx}} - \cdots, \tag{3.14}$$

which annihilates divergence expressions, is applied on (3.13) to give

$$E_h\big[\Lambda(F)\big] = 0, \tag{3.15}$$

which is the determining equation for Λ. Since (3.15) is satisfied for all functions, it can be separated by powers and products of the partial derivatives of the variables which Λ does not depend on. Upon solving for $\Lambda = \Lambda(\underline{x}, u, u_{(1)}, u_{(2)})$, it is then substituted back into equation (3.13) to solve for **T** [31, 32]. Examples of application of this method can be found in [31, 32].

3.3.3 Association of a Lie point symmetry with a conserved vector

Kara and Mahomed [33] introduced a method of generating conserved vectors from known conserved vectors. If the Lie point symmetry generator of a PDE is

$$X = \xi^1(t,x,h)\frac{\partial}{\partial t} + \xi^2(t,x,h)\frac{\partial}{\partial x} + \eta(t,x,h)\frac{\partial}{\partial h}, \tag{3.16}$$

then Kara and Mahomed have shown that the Lie point symmetry generator (3.16) is associated with a conserved vector **T** provided

$$T^i_* = X(T^i) + T^i D_k(\xi^k) - T^k D_k(\xi^i) = 0, \qquad i = 1,2. \tag{3.17}$$

By the double reduction theorem of Sjöberg [18] association leads to the reduction of PDEs to ODEs and the integration of the ODEs once. In some cases the result is completely integrable leading to an exact analytical solution. This method allows investigation of the existence of analytical solutions corresponding to the derived conserved vectors.

3.4 The shooting method for nonlinear problems

Consider a nonlinear second-order boundary value problem [35]

$$y'' = f(x, y, y'), \qquad x \in [a, b] \tag{3.18}$$

where

$$y(a) = \alpha \quad \text{and} \quad y(b) = \beta. \tag{3.19}$$

The shooting method for nonlinear BVP for an ordinary differential equation involves finding an approximate solution to (3.18) by solving the IVP

$$y'' = f(x, y, y'), \qquad a \le x \le b, \qquad y(a) = \alpha, \qquad y'(a) = t, \tag{3.20}$$

with varying values of the parameter t, thereby generating a sequence of end points $y(b, t_k)$ for $k = 0, 1, 2, 3, \cdots$ until the condition

$$|y(\beta, t_k) - y_\beta| < \epsilon, \quad k = 0, 1, 2, 3, ... \tag{3.21}$$

where $\epsilon << 1$ is the tolerance is satisfied.

We start with an initial guess t, say t_0, then solve the IVP (3.20). If equation (3.21) is not satisfied, we adjust the value of t_k using the route finding method until a point such that (3.21) is satisfied. This technique is called a “shooting method". There are various route finding methods to find t_k. In this work we will use the bisection method.

3.5 Conclusions

In this section we briefly outlined the various methods of solutions that will be applied to solve the partial differential equation. The method of deriving the Lie point symmetries that lead to the solution of the group invariant solution were described. This method allows us to express the PDE and its related boundary conditions in terms of the group invariant solution. It also gives a solution of the fracture half-width provided the leak-off velocity satisfies a partial differential equation.

Two methods of deriving the conservation laws that will be used were outlined. Association of a Lie point symmetry with a conserved vector will be used to investigate the existence of analytical solutions. The method of transforming a boundary value problem (BVP) into an initial value problem (IVP) will be used to obtain numerical solutions using the shooting method which works by identifying a target and shooting or iterating until a shot that hits the fixed target is achieved hence giving a solution that satisfies boundary value problem.

Chapter 4

Conservation laws

4.1 Introduction

In this chapter, we investigate the existence of conservations laws for a fluid-driven fracture propagating in permeable rock. In Chapter (2), we derived the nonlinear diffusion equation that describes a linear hydraulic fracture with tortuosity and fluid leak-off at the fluid-rock interface:

$$\frac{\partial h}{\partial t} = K_n \frac{\partial}{\partial x}\left(h^n \frac{\partial h}{\partial x}\right) - v_\ell(t,x). \tag{4.1}$$

As outlined in Chapter 3, the two methods used to investigate the conservation laws will be the direct and the multiplier method. Firstly we consider the direct method.

4.2 Direct method

Consider the partial differential equation (4.1), which can be expressed as

$$F(t,x,h,h_x,h_t,h_{xx}) = h_t - K_n n h^{n-1} h_x^2 - K_n h^n h_{xx} + v_\ell(t,x) = 0, \tag{4.2}$$

where subscripts denote partial differentiation and $t, x, h, h_x, h_t, h_{xx}, \ldots$ and all partial derivatives of h are treated as independent variables. We seek to investigate a conserved vector of the form $\mathbf{T} = (T^1, T^2)$ or $\mathbf{R} = (R^1, R^2)$ of the partial differential equation (4.2) which satisfies the conservation law

$$D_t T^1 + D_x T^2 \Big|_{(4.2)} = 0, \tag{4.3}$$

where D_t and D_x are total derivatives:

$$D_t = \frac{\partial}{\partial t} + h_t \frac{\partial}{\partial h} + h_{tt} \frac{\partial}{\partial h_t} + h_{tx} \frac{\partial}{\partial h_x} + \ldots, \tag{4.4}$$

$$D_x = \frac{\partial}{\partial x} + h_x \frac{\partial}{\partial h} + h_{xx} \frac{\partial}{\partial h_x} + h_{tx} \frac{\partial}{\partial h_t} + \ldots. \tag{4.5}$$

Consider conserved vectors of the form

$$T^1 = T^1(t,x,h,h_x), \qquad T^2 = T^2(t,x,h,h_x). \tag{4.6}$$

It follows that expanding equation (4.3) gives

$$\left(\frac{\partial T^1}{\partial t}+\frac{\partial T^1}{\partial h}h_t+\frac{\partial T^1}{\partial h_x}h_{tx}+\frac{\partial T^2}{\partial x}+\frac{\partial T^2}{\partial h}h_x+\frac{\partial T^2}{\partial h_x}h_{xx}\right)\Bigg|_{(4.2)}=0, \tag{4.7}$$

which when evaluated at the nonlinear diffusion equation (4.2) becomes

$$\begin{aligned}0=&\frac{\partial T^1}{\partial t}+\frac{\partial T^1}{\partial h}(K_n n h^{n-1}h_x^2)+\frac{\partial T^1}{\partial h}(K_n h^n h_{xx})-v_\ell(t,x)\frac{\partial T^1}{\partial h}\\&+\frac{\partial T^1}{\partial h_x}h_{tx}+\frac{\partial T^2}{\partial x}+\frac{\partial T^2}{\partial h}h_x+\frac{\partial T^2}{\partial h_x}h_{xx}.\end{aligned} \tag{4.8}$$

Separating equation (4.8) according to the derivatives of h which the components of the conserved vector $\mathbf{T}=(T^1,T^2)$ does not depend on gives

$$h_{xx}: \qquad \frac{\partial T^2}{\partial h_x}+K_n h^n\frac{\partial T^1}{\partial h}=0, \tag{4.9}$$

and

$$h_{tx}: \qquad \frac{\partial T^1}{\partial h_x}=0. \tag{4.10}$$

Equation (4.10) implies that

$$T^1=T^1(t,x,h). \tag{4.11}$$

Integrating (4.9) with respect to h_x gives

$$T^2=-K_n h^n\frac{\partial T^1}{\partial h}h_x+A(t,x,h), \tag{4.12}$$

where $A(t,x,h)$ is a function still to be determined. The remainder from (4.8) is

$$\frac{\partial T^1}{\partial t}+\frac{\partial T^1}{\partial h}(K_n n h^{n-1}h_x^2)-v_\ell(t,x)\frac{\partial T^1}{\partial h}+\frac{\partial T^2}{\partial x}+\frac{\partial T^2}{\partial h}h_x=0. \tag{4.13}$$

Substituting (4.12) into (4.13) gives

$$\begin{aligned}&\frac{\partial T^1}{\partial t}+\frac{\partial A}{\partial x}+\frac{\partial T^1}{\partial h}\left(K_n n h^{n-1}h_x^2\right)+\left(\frac{\partial A}{\partial h}-K_n h^n\frac{\partial^2 T^1}{\partial x\partial h}\right)h_x-v_\ell(t,x)\frac{\partial T^1}{\partial h}\\&+\left(-K_n n h^{n-1}\frac{\partial T^1}{\partial h}-K_n h^n\frac{\partial^2 T^1}{\partial h^2}\right)h_x^2=0,\end{aligned} \tag{4.14}$$

which can be separated in powers of h_x to give

$$h_x^2: \qquad \frac{\partial^2 T^1}{\partial h^2}=0 \tag{4.15}$$

$$h_x: \qquad \frac{\partial A}{\partial h}-K_n h^n\frac{\partial^2 T^1}{\partial x\partial h}=0. \tag{4.16}$$

Integrating (4.15) twice with respect to h where the form of T^2 is given by (4.12) gives

$$T^1(t,x,h)=B(t,x)h+C(t,x). \tag{4.17}$$

Applying equation (4.17) to equation (4.16) and integrating the result with respect to h gives

$$A(t,x,h) = K_n \frac{h^{n+1}}{(n+1)} \frac{\partial B}{\partial x}(t,x) + D(t,x). \tag{4.18}$$

The remaining terms from (4.14) are

$$\frac{\partial T^1}{\partial t} + \frac{\partial A}{\partial x} - v_\ell(t,x) \frac{\partial T^1}{\partial h} = 0. \tag{4.19}$$

Substituting (4.17) for T^1 and (4.18) for $A(t,x,h)$ into (4.19) gives

$$\begin{aligned} &\frac{\partial}{\partial t}\Big(B(t,x)h + C(t,x)\Big) + \frac{\partial}{\partial x}\left(K_n \frac{h^{n+1}}{(n+1)} \frac{\partial B}{\partial x}(t,x) + D(t,x)\right) \\ &- v_\ell(t,x) \frac{\partial}{\partial h}\Big(B(t,x)h + C(t,x)\Big) = 0, \end{aligned} \tag{4.20}$$

which can be separated in powers of h to give

$$h: \qquad \frac{\partial B}{\partial t}(t,x) = 0, \tag{4.21}$$

$$h^{n+1}: \qquad \frac{\partial^2 B}{\partial x^2}(t,x) = 0. \tag{4.22}$$

Integrating (4.21) gives

$$B = B(x). \tag{4.23}$$

Integrating (4.22) twice and using (4.23) gives

$$B(x) = ax + b, \tag{4.24}$$

where a and b are constants. The remaining terms from (4.20) are

$$\frac{\partial C}{\partial t}(t,x) + \frac{\partial D}{\partial x}(t,x) - (ax+b)\, v_\ell(t,x) = 0. \tag{4.25}$$

Using (4.12) for T^2, (4.17) for T^1 and (4.18) and (4.23) for $A(t,x,h)$ and $B(x)$ respectively gives the conserved vector

$$\mathbf{T} = \left((ax+b)h + C(t,x), \quad -K_n h^n (ax+b) h_x + K_n \frac{h^{n+1}}{(n+1)} a + D(t,x)\right), \tag{4.26}$$

where the components of the conserved vector are

$$T^1 = (ax+b)h + C(t,x), \tag{4.27}$$

and

$$T^2 = -K_n h^n (ax+b) h_x + K_n \frac{h^{n+1}}{(n+1)} a + D(t,x). \tag{4.28}$$

We can now use (4.25) to replace $C(t,x)$ or $D(t,x)$ in the conserved vector (4.26). We first consider replacing $D(t,x)$ in (4.26) by integrating the remainder, (4.25), with respect to χ from 0 to x:

$$D(t,x) = D(t,0) - \frac{\partial E}{\partial t}(t,x) + a\int_0^x \chi v_\ell(t,\chi)d\chi + b\int_0^x v_\ell(t,\chi)d\chi \tag{4.29}$$

where

$$E(t,x) = \int_0^x C(t,\chi)d\chi \tag{4.30}$$

and

$$\frac{\partial E}{\partial x} = C(t,x). \tag{4.31}$$

The components of the conserved vectors (4.27) and (4.28) become

$$T^1 = (ax+b)h + T^1_{\circledast}, \tag{4.32}$$

and

$$T^2 = -K_n h^n (ax+b)h_x + K_n \frac{h^{n+1}}{(n+1)}a + a\int_0^x \chi v_\ell(t,\chi)d\chi + b\int_0^x v_\ell(t,\chi)d\chi + T^1_{\circledast}, \tag{4.33}$$

where

$$T^1_{\circledast} = C(t,x), \tag{4.34}$$

$$T^2_{\circledast} = D(t,0) - \frac{\partial E}{\partial t}(t,x). \tag{4.35}$$

The conservation law

$$D_t T^1_{\circledast} + D_x T^2_{\circledast} = 0, \tag{4.36}$$

is identically satisfied without imposing the partial differential (4.2). It is therefore a trivial conservation law and we set

$$T^1_{\circledast} = 0, \quad T^2_{\circledast} = 0. \tag{4.37}$$

Therefore, by the direct method the elementary conserved vectors of the first kind is

$$\mathbf{T}_{(1)} = \left[h, -K_n h^n h_x + \int_0^x v_\ell(t,\chi)d\chi\right], \tag{4.38}$$

and the second conserved vector of the first kind is

$$\mathbf{T}_{(2)} = \left[xh, -K_n h^n x h_x + K_n \frac{h^{n+1}}{(n+1)} + \int_0^x \chi v_\ell(t,\chi)d\chi\right]. \tag{4.39}$$

We now replace $C(t,x)$ by integrating the remainder, (4.25), with respect to τ from 0 to t which gives

$$C(t,x) = C(0,x) - \frac{\partial F}{\partial t}(t,x) + (ax+b)\int_0^t v_\ell(\tau,x)d\tau, \tag{4.40}$$

where

$$F(t,x) = \int_0^t D(\tau,x)d\tau, \tag{4.41}$$

and

$$\frac{\partial F}{\partial t} = D(t,x). \tag{4.42}$$

The components of the conserved vector (4.26) become

$$R^1 = (ax+b)h + (ax+b)\int_0^t v_\ell(\tau,x)d\tau + R^1_{\circledast}, \tag{4.43}$$

and

$$R^2 = -(ax+b)K_n h^n h_x + K_n \frac{h^{n+1}}{n+1}a + R^2_{\circledast}, \tag{4.44}$$

where

$$R^1_{\circledast} = C(0,x) - \frac{\partial F}{\partial x}(t,x), \tag{4.45}$$

$$R^2_{\circledast} = D(t,x). \tag{4.46}$$

The conservation law

$$D_t R^1_{\circledast} + D_x R^2_{\circledast} = 0, \tag{4.47}$$

is also identically satisfied without imposing the partial differential equation (4.2) and is therefore a trivial conservation law. We set

$$R^1_{\circledast} = 0, \quad R^2_{\circledast} = 0. \tag{4.48}$$

Therefore, by the direct method the elementary conserved vectors of the second kind is

$$\mathbf{R}_{(1)} = \left[h + \int_0^t v_\ell(\tau,x)d\tau, -K_n h^n h_x\right], \tag{4.49}$$

and the second conserved vector of the second kind is

$$\mathbf{R}_{(2)} = \left[xh + x\int_0^t v_\ell(\tau,x)d\tau, -K_n h^n x h_x + K_n \frac{h^{n+1}}{(n+1)}\right]. \tag{4.50}$$

We will now investigate the multiplier method of obtaining conserved vectors.

4.3 Multiplier method

Consider a multiplier of the form $\Lambda = \Lambda(t,x,h)$ and the conserved vector

$$\mathbf{T} = T^i(t,x,h,h_t,h_x), \quad i = 1,2. \tag{4.51}$$

We are interested in finding the components of the conserved vectors T^1 and T^2 and a multiplier Λ which has the property

$$\Lambda F(t,x,h,h_t,h_x,h_{xx}) = D_t T^1 + D_x T^2, \tag{4.52}$$

for all functions $h(t,x)$ and $v_\ell(t,x)$ and where D_t and D_x are total derivatives given by equations (4.4) and (4.5). Since (4.52) is a function of $h(t,x)$ it can be separated later according to the partial derivatives of $h(t,x)$.When $h(t,x)$ and $v_\ell(t,x)$ satisfy the PDE (4.2), then (4.52) is a conservation law of the PDE. We apply the Euler operator

$$E_h = \frac{\partial}{\partial h} - D_t\frac{\partial}{\partial h_t} - D_x\frac{\partial}{\partial h_x} + D_t^2\frac{\partial}{\partial h_{tt}} + D_xD_t\frac{\partial}{\partial h_{tx}} + D_x^2\frac{\partial}{\partial h_{xx}} + \cdots, \tag{4.53}$$

which annihilates divergence expressions, to the left hand side of (4.52) and equate the result to zero:

$$E_h\Big[\Lambda(t,x,h)\Big(h_t - K_n n h^{n-1}h_x^2 - K_n h^n h_{xx} + v_\ell(t,x)\Big)\Big] = 0. \tag{4.54}$$

Expanding (4.54) gives

$$\begin{aligned}&\frac{\partial\Lambda}{\partial h}\Big(h_t - K_n n h^{n-1}h_x^2 - K_n h^n h_{xx} + v_\ell(t,x)\Big) + \Lambda\Big(-K_n n(n-1)h^{n-2}h_x^2 - K_n n h^{n-1}h_{xx}\Big)\\ &- D_t(\Lambda) - D_x\Lambda\Big(-2K_n n h^{n-1}h_x\Big) + D_x^2(-\Lambda K_n h^n) = 0,\end{aligned} \tag{4.55}$$

which simplifies to

$$\begin{aligned}&-2K_n h^n\frac{\partial\Lambda}{\partial h}h_{xx} + v_\ell(t,x)\frac{\partial\Lambda}{\partial h} - \frac{\partial\Lambda}{\partial t} - K_n h^n\frac{\partial^2\Lambda}{\partial x^2} - 2K_n h^n\frac{\partial^2\Lambda}{\partial x\partial h}h_x\\ &- K_n h^n\frac{\partial^2\Lambda}{\partial h^2}h_x^2 - K_n n h^{n-1}\frac{\partial\Lambda}{\partial h}h_x^2 = 0.\end{aligned} \tag{4.56}$$

Now $\Lambda = \Lambda(t,x,h)$. Since (4.56) is satisfied for all functions of $h(t,x)$ and $v_\ell(t,x)$, it can be separated by equating the coefficients of the partial derivatives of h.

$$h_{xx}: \qquad \frac{\partial\Lambda}{\partial h} = 0, \tag{4.57}$$

$$h_x^2: \qquad h\frac{\partial^2\Lambda}{\partial h^2} + n\frac{\partial\Lambda}{\partial h} = 0, \tag{4.58}$$

$$h_x: \qquad \frac{\partial^2\Lambda}{\partial x\partial h} = 0, \tag{4.59}$$

which implies that $\Lambda = \Lambda(t,x)$. Equations (4.58) and (4.59) are identically satisfied. The remaining terms from (4.56) are

$$-K_n h^n\frac{\partial^2\Lambda}{\partial x^2} - \frac{\partial\Lambda}{\partial t} = 0. \tag{4.60}$$

Equation (4.60) can now be separated in powers of h

$$h^0: \qquad \frac{\partial \Lambda}{\partial t} = 0, \tag{4.61}$$

which implies that

$$\Lambda = \Lambda(x), \tag{4.62}$$

and

$$h^n: \qquad \frac{\partial^2 \Lambda}{\partial x^2} = 0, \tag{4.63}$$

which can be integrated with respect to x to give

$$\Lambda = ax + b, \tag{4.64}$$

where a and b are constants. The multiplier Λ is found to be independent of the leak-off velocity. Using (4.64) and (4.52) we find that

$$(ax+b)\Big[h_t - K_n n h^{n-1} h_x^2 - K_n h^n h_{xx} + v_\ell(t,x)\Big] = D_t T^1 + D_x T^2. \tag{4.65}$$

By elementary manipulation

$$\begin{aligned}(ax+b)\Big(h_t - K_n n h^{n-1} h_x^2 - K_n h^n h_{xx} + v_\ell\Big) & \qquad (4.66)\\ = D_t(axh+bh) + D_x\Big(b\Big[-K_n h^n h_x + \int_0^x v_\ell(t,x)d\chi\Big] & \\ + a\Big[-K_n x h^n h_x + K_n \frac{h^{n+1}}{(n+1)} + \int_0^x \chi v_\ell(t,x)d\chi\Big]\Big), & \qquad (4.67)\end{aligned}$$

for arbitrary functions $h(t,x)$ and $v_\ell(t,x)$. When $h(t,x)$ and $v_\ell(t,x)$ satisfy (4.2) then

$$\begin{aligned}&D_t(axh+bh) + D_x\Big(b\Big[-K_n h^n h_x + \int_0^x v_\ell(t,x)d\chi\Big] + a\Big[-K_n x h^n h_x + K_n \frac{h^{n+1}}{(n+1)}\\ &+ \int_0^x \chi v_\ell(t,x)d\chi\Big]\Big) = 0. \end{aligned} \tag{4.68}$$

Thus setting the constants a and b from (4.67) equal to zero in alternative turns, we obtain that

$$\mathbf{T}_{(1)} = \Big[h, \quad -K_n h^n h_x + \int_0^x v_\ell(t,x)d\chi\Big] \tag{4.69}$$

$$\mathbf{T}_{(2)} = \Big[xh, \quad -K_n x h^n h_x + K_n \frac{h^{n+1}}{(n+1)} + \int_0^x \chi v_\ell(t,x)d\chi\Big], \tag{4.70}$$

which are the conserved vectors of the first kind. We observe that these conserved vectors are the same as the those obtained in (4.38) and (4.39).

Equation (4.52) using (4.64), can be written as

$$
\begin{aligned}
(ax+b)\Big(h_t - K_n n h^{n-1} h_x^2 - K_n h^n h_{xx} + v_\ell\Big) = \\
D_t\left[ax\left(h+\int_0^t v_\ell(\tau,x)d\tau\right)+b\left(h+\int_0^t v_\ell(\tau,x)d\tau\right)\right] \\
+ D_x\left[-axK_n h^n h_x + K_n\frac{h^{n+1}}{(n+1)} + b\big(-K_n h^n h_x\big)\right],
\end{aligned} \tag{4.71}
$$

for arbitrary functions $h(t,x)$ and $v_\ell(t,x)$. When $h(t,x)$ and $v_\ell(t,x)$ satisfy (4.2) the left hand side of (4.71) is zero.
Thus after setting the constants $a=0$, $b=1$ and $a=1$, $b=0$ in alternating turns, we obtain for the conserved vectors of the second kind

$$
\mathbf{R}_{(1)} = \left[h+\int_0^t v_\ell(\tau,x)d\tau, \quad -K_n h^n h_x\right], \tag{4.72}
$$

and

$$
\mathbf{R}_{(2)} = \left[xh + x\int_0^t v_\ell(\tau,x)d\tau, \quad -K_n h^n x h_x + K_n\frac{h^{n+1}}{(n+1)}\right], \tag{4.73}
$$

which are the same as those obtained from using the direct method (4.49) and (4.50).

We now investigate if other conserved vectors exists by considering a multiplier of the form

$$
\Lambda = \Lambda(t,x,h,h_t,h_x), \tag{4.74}
$$

which has the property

$$
\Lambda(t,x,h,h_t,h_x)(h_t - k_n n h^{n-1} h_x^2 - K_n h^n h_{xx} + v_\ell(t,x)) = D_t T^1 + D_x T^2 \tag{4.75}
$$

for arbitrary functions $h(t,x)$ and $v_\ell(t,x)$.
Applying the Euler operator (4.3) which annihilates the divergence expressions to the left hand side of (4.75), we obtain

$$
E_h\left[\Lambda(t,x,h,h_t,h_x)\Big(h_t - K_n n h^{n-1} h_x^2 - K_n h^n h_{xx} + v_\ell\Big)\right] = 0. \tag{4.76}
$$

Expanding (4.76) gives:

$$
\begin{aligned}
&\frac{\partial\Lambda}{\partial h}\Big(h_t - k_n n h^{n-1} h_x^2 - K_n h^n h_{xx} + v_\ell\Big) \\
&+\Lambda\Big(-K_n n(n-1)h^{n-2}h_x^2 - K_n h^{n-1} h_{xx}\Big) \\
&- D_t(\Lambda) - D_x\Big(-2\Lambda K_n n h^{n-1} h_x\Big) + D_x^2\Big(-\Lambda K_n h^n\Big) \\
&- D_x\left(\frac{\partial\Lambda}{\partial h_x}h_t - K_n n h^{n-1}\frac{\partial\Lambda}{\partial h_x}h_x^2 - k_n h^n\frac{\partial\Lambda}{\partial h_x}h_{xx} + \frac{\partial\Lambda}{\partial h_x}v_\ell\right) \\
&- D_t\left(\frac{\partial\Lambda}{\partial h_t}h_t - K_n n h^{n-1}\frac{\partial\Lambda}{\partial h_t}h_x^2 - k_n h^n\frac{\partial\Lambda}{\partial h_t}h_{xx} + \frac{\partial\Lambda}{\partial h_t}v_\ell\right) = 0.
\end{aligned} \tag{4.77}
$$

The fifth term in (4.77) gives

$$+D_x^2\left(-\Lambda K_n h^n\right) = -K_n h^n\left(\frac{\partial \Lambda}{\partial h_x}h_{xxx} + \frac{\partial \Lambda}{\partial h_t}h_{xxt}\right) + \textit{terms independent of third order derivatives,} \tag{4.78}$$

the sixth term gives

$$-D_x\left(\frac{\partial \Lambda}{\partial h_x}h_t - K_n n h^{n-1}\frac{\partial \Lambda}{\partial h_x}h_x^2 - K_n h^n \frac{\partial \Lambda}{\partial h_x}h_{xx} + \frac{\partial \Lambda}{\partial h_x}v_\ell\right) = K_n h^n \frac{\partial \Lambda}{\partial h_x}h_{xxx} + \textit{terms independent of third order derivatives,} \tag{4.79}$$

and the seventh term gives

$$-D_t\left(\frac{\partial \Lambda}{\partial h_t}h_t - K_n n h^{n-1}\frac{\partial \Lambda}{\partial h_t}h_x^2 - K_n h^n \frac{\partial \Lambda}{\partial h_t}h_{xx} + \frac{\partial \Lambda}{\partial h_t}v_\ell\right) = K_n h^n \frac{\partial \Lambda}{\partial h_t}h_{xxt} + \textit{terms independent of third order derivatives.} \tag{4.80}$$

The third order partial derivatives do not give any useful information as they are equal to zero. Analysing the results gives that the multiplier Λ is independent of any partial derivatives of h, which results in a multiplier of the form

$$\Lambda = \Lambda(t, x, h). \tag{4.81}$$

No new conserved vectors could be obtained from the multiplier method as we obtained the same conserved vectors as previously obtained using the direct method.

4.4 Relationship between Lie point symmetries and conservation laws

In this section we investigate the relationship between Lie point symmetries of the governing partial differential equation (4.1) and the derived conservation laws for the partial differential equation. This investigation is motivated by Sjöberg's double reduction theorem. If a Lie point symmetry generator is associated with a conserved vector, it may lead to the derivation of some analytical solutions.

Firstly, we state a theorem due to Kara and Mahomed [33] specifically for partial differential equations.

Theorem 1. *If X is a Lie point point symmetry of the partial differential equation (2.60) and $T = (T^1, T^2)$ is a conserved vector for the PDE, then*

$$T^i_* = X(T^i) + T^i D_k(\xi^k) - T^k D_k(\xi^i), \qquad i = 1,2 \tag{4.82}$$

are the components of a conserved vector for the PDE (2.60), that is

$$D_1 T^1_* + D_2 T^2_*\Big|_{PDE} = 0. \tag{4.83}$$

X is prolongated as many orders as required whenever T depends on the derivatives of h.

This theorem provides a way of obtaining new conserved vectors for the partial differential equation (4.1) from the Lie point symmetries of (4.1) and the existing conserved vectors obtained above. If $\mathbf{T}^*$ is a linear combination of known conserved vectors then the generated conserved vector is trivial.

Suppose that

$$X = \xi^1(t,x,h)\frac{\partial}{\partial t} + \xi^2(t,x,h)\frac{\partial}{\partial x} + \eta(t,x,h)\frac{\partial}{\partial h}, \tag{4.84}$$

is a Lie point symmetry generator of (4.1) and $\mathbf{T} = (T^1, T^2)$ are the components of a conserved vectors of (4.1), then according to Kara and Mahomed

$$T^i_* = X(T^i) + T^i D_j(\xi^j) - T^j D_j(\xi^i), \qquad i = 1,2, \tag{4.85}$$

constitutes the components of a conserved vector of (4.1). Expanding equation (4.85) gives

$$T^1_* = X(T^1) + T^1 D_2(\xi^2) - T^2 D_2(\xi^1) \tag{4.86}$$

and

$$T^2_* = X(T^2) + T^2 D_1(\xi^1) - T^1 D_1(\xi^2). \tag{4.87}$$

The Lie point symmetry generator of (4.1) which is derived in detail in Appendix A is

$$X = (c_1 + c_2 t)\frac{\partial}{\partial t} + (c_3 + c_4 x)\frac{\partial}{\partial x} + \frac{1}{n}(2c_4 - c_2)h\frac{\partial}{\partial h}, \tag{4.88}$$

provided the leak-off velocity satisfies the partial differential equation

$$(c_1 + c_2 t)\frac{\partial v_\ell}{\partial t} + (c_3 + c_4 x)\frac{\partial v_\ell}{\partial x} = \frac{1}{n}(2c_4 - (n+1)c_2)v_\ell(t,x). \tag{4.89}$$

The first prolongation of X is

$$\begin{aligned} X^{[1]} = {} & (c_1 + c_2 t)\frac{\partial}{\partial t} + (c_3 + c_4 x)\frac{\partial}{\partial x} + \frac{h}{n}(2c_4 - c_2)\frac{\partial}{\partial h} \\ & + \frac{1}{n}((2-n)c_4 - c_2)h_x\frac{\partial}{\partial h_x}. \end{aligned} \tag{4.90}$$

Consider the first elementary conserved vector of the first kind

$$T^1 = h, \qquad T^2 = -K_n h^n h_x + \int_0^x v_\ell(t,\chi)d\chi. \tag{4.91}$$

It can be verified that using (4.86) and (4.87) we obtain

$$T^1_* = \frac{1}{n}[(n+2)c_4 - c_2]T^1 \tag{4.92}$$

and

$$\begin{aligned} T^2_* = {} & (c_1 + c_2 t)\int_0^x \frac{\partial v_\ell}{\partial t}(t,x)d\chi + (c_3 + c_4 x)v_\ell(t,x) \\ & + \frac{1}{n}[(n+2)c_4 - c_2](-K_n h^n h_x) + c_2\int_0^x v_\ell(t,x))d\chi. \end{aligned} \tag{4.93}$$

Integrating (4.89) with respect to χ from $\chi = 0$ to $\chi = x$ gives

$$(c_1 + c_2 t)\int_0^x \frac{\partial v_\ell}{\partial t}(t,x)d\chi + (c_3 + c_4 x)v_\ell(t,x) \\ = c_3 v_\ell(t,0) + \frac{1}{n}[(n+2)c_4 - (n+1)c_2]\int_0^x v_\ell(t,\chi)d\chi, \tag{4.94}$$

which when substituted into (4.93) gives

$$T_*^2 = \frac{1}{n}[(n+2)c_4 - c_2]T^2 + c_3 v_\ell(t,0). \tag{4.95}$$

Expressing equations (4.92) and (4.95) in vector form gives

$$\mathbf{T}^*_{(1)} = \frac{1}{n}[(n+2)c_4 - c_2]\mathbf{T}_{(1)} + c_3\mathbf{P}_{(0)}, \tag{4.96}$$

where

$$\mathbf{T}_{(1)} = [h, -K_n h^n h_x + \int_0^x v_\ell(t,x)d\chi], \tag{4.97}$$

and

$$\mathbf{P}_{(0)} = [0, v_\ell(t,0)]. \tag{4.98}$$

The vector $\mathbf{T}^*_{(1)}$ is not a new conserved vector since the vector $\mathbf{P}_{(0)}$ is a trivial vector

$$D_1 P^1_{(0)} + D_2 P^2_{(0)} \equiv 0. \tag{4.99}$$

The condition that (4.96) is associated with (4.88) is obtained by setting (4.96) to zero to find that

$$\frac{c_4}{c_2} = \frac{1}{n+2}, \qquad c_3 = 0. \tag{4.100}$$

The Lie point symmetry associated with the conserved vector $\mathbf{T}_{(1)}$ of the first kind is obtained by substituting (4.100) into (4.88):

$$X = \Big(\frac{c_1}{c_2} + t\Big)\frac{\partial}{\partial t} + \Big(\frac{1}{n+2}\Big)x\frac{\partial}{\partial x} - \Big(\frac{1}{n+2}\Big)h\frac{\partial}{\partial h}. \tag{4.101}$$

Considering the components of the elementary conserved vector of the second kind

$$R^1 = h + \int_0^t v_\ell(\tau,x)d\tau, \qquad R^2 = -K_n h^n h_x. \tag{4.102}$$

Now, using (4.102), it can be verified that the first component of another conserved vector derived from (4.102) is

$$R^1_* = (c_1 + c_2 t)v_\ell(t,x) + (c_3 + c_4 x)\int_0^t \frac{\partial v_\ell}{\partial x}(\tau,x)d\tau + \frac{1}{n}[2c_4 - c_2]h \\ + c_4[h + \int_0^t v_\ell(\tau,x)d\tau]. \tag{4.103}$$

Integrating (4.89) with respect to τ from $\tau = 0$ to $\tau = t$ gives

$$(c_1 + c_2 t)v_\ell(t,x) + (c_3 + c_4 x)\int_0^t \frac{\partial v_\ell}{\partial x}(\tau,x)d\tau = c_1 v_\ell(0,x) + \frac{1}{n}[2c_4 - (n+1)c_2]\int_0^t v_\ell(\tau,x)d\tau, \tag{4.104}$$

which when substituted into (4.103) gives

$$R^1_* = \frac{1}{n}[(n+2)c_4 - c_2]R^1 + c_1 v_\ell(0,x). \tag{4.105}$$

Also, it can be shown that using (4.87)

$$R^2_* = \frac{1}{n}[(n+2)c_4 - c_2]R^2. \tag{4.106}$$

Expressing (4.105) and (4.106) in vector form gives

$$\mathbf{R}^*_{(1)} = \frac{1}{n}[(n+2)c_4 - c_2]\,\mathbf{R}_{(1)} + c_1\mathbf{Q}_{(0)}, \tag{4.107}$$

where

$$\mathbf{R}_{(1)} = [h + \int_0^t v_\ell(\tau,x)d\tau, -K_n h^n h_x], \tag{4.108}$$

$$\mathbf{Q}_{(0)} = [v_\ell(0,x), 0]. \tag{4.109}$$

The vector $\mathbf{R}^*_{(1)}$ is not a new conserved vector since the vector $\mathbf{Q}_{(0)}$ is trivial. The condition that (4.107) is associated with (4.88) is obtained by setting (4.107) to zero to find that

$$c_1 = 0, \qquad \frac{c_4}{c_2} = \frac{1}{n+2}. \tag{4.110}$$

Therefore the Lie point symmetry associated with the elementary conserved vector of the second kind $\mathbf{R}_{(1)}$ is

$$X = t\frac{\partial}{\partial t} + \left(\frac{c_3}{c_2} + \frac{1}{n+2}x\right)\frac{\partial}{\partial x} - \frac{1}{(n+2)}h\frac{\partial}{\partial h}. \tag{4.111}$$

The elementary conserved vectors of the first and second kind are both associated with Lie point symmetries which generate a solution for a fracture with constant volume. This working condition only corresponds to the constant volume when there is no flux at the entry and no leak-off i.e. $\gamma = 0$, as previously obtained in [11]. For $\gamma > 0$, this solution means that the flux of fluid into the fracture equals the rate of leak-off at the fluid-rock interface resulting in a non-propagating fracture.

Consider now the second conserved vectors of the first and second kind. The components of the second conserved vector of the first kind are given by

$$T^1 = xh, \qquad T^2 = -K_n x h^n h_x + K_n\frac{h^{n+1}}{(n+1)} + \int_0^x \chi v_\ell(t,\chi)d\chi. \tag{4.112}$$

It can be verified that using (4.86) and (4.87) gives

$$T_*^1 = c_3 T_{(1)}^1 + \frac{1}{n}[2(n+1)c_4 - c_2]\, T_{(2)}^1 \tag{4.113}$$

and

$$\begin{aligned} T_*^2 = {} & (c_1 + c_2 t)\frac{\partial}{\partial t}\int_0^x \chi \frac{\partial v_\ell}{\partial t}(t,\chi)d\chi + (c_3 + c_4 x)x v_\ell(t,x) + c_3(-K_n h^n h_x) \\ & + \frac{1}{n}[2(n+1)c_4 - c_2](-K_n x h^n h_x) + \frac{1}{n}[2(n+1)c_4 - c_2]K_n \frac{h^{n+1}}{(n+1)} \\ & + c_2 \int_0^x \chi v_\ell(t,\chi)d\chi. \end{aligned} \tag{4.114}$$

Multiplying (4.89) by χ and integrating the result with respect to χ from $\chi = 0$ to $\chi = x$ gives

$$\begin{aligned} & (c_1 + c_2 t)\frac{\partial}{\partial t}\int_0^x \chi \frac{\partial v_\ell}{\partial t}(t,\chi)d\chi + (c_3 + c_4 x)x v_\ell(t,x) \\ & \quad = c_3 \int_0^x v_\ell(t,\chi)d\chi + \frac{1}{n}[2(n+1)c_4 - (n+1)c_2]\int_0^x \chi v_\ell(t,\chi)d\chi, \end{aligned} \tag{4.115}$$

which when substituted into (4.114) gives

$$\begin{aligned} T_*^2 = {} & c_3[-K_n h^n h_x + \int_0^x v_\ell(t,\chi)d\chi] \\ & + \frac{1}{n}[2(n+1)c_4 - c_2]\left[-K_n x h^n h_x + K_n \frac{h^{n+1}}{(n+1)} + \int_0^x \chi v_\ell(t,\chi)d\chi\right]. \end{aligned} \tag{4.116}$$

Thus

$$\mathbf{T}_{(2)}^* = c_3 T_{(1)} + \frac{1}{n}[2(n+1)c_4 - c_2]\, T_{(2)} \tag{4.117}$$

where

$$\mathbf{T}_{(1)} = \left[h, \quad -K_n h^n h_x + \int_0^x v_\ell(t,\chi)d\chi\right] \tag{4.118}$$

and

$$\mathbf{T}_{(2)} = \left[xh, \quad -K_n x h^n h_x + K_n \frac{h^{n+1}}{(n+1)} + \int_0^x \chi v_\ell(t,\chi)d\chi\right]. \tag{4.119}$$

Thus $\mathbf{T}_{(2)}^*$ is not a new conserved vector as it is a linear combination of the conserved vector of the first kind, $\mathbf{T}_{(1)}$ and $\mathbf{T}_{(2)}$. The condition that (4.117) and (**??**) is associated with the Lie point symmetry generator (4.88) is obtained by setting (4.117) to zero to find that

$$c_3 = 0, \qquad \frac{c_4}{c_2} = \frac{1}{2(n+1)}. \tag{4.120}$$

Therefore the Lie point symmetry associated with the conserved vector of the second kind is

$$X = \left(\frac{c_1}{c_2} + t\right)\frac{\partial}{\partial t} + \left(\frac{1}{2(n+1)}x\right)\frac{\partial}{\partial x} - \left(\frac{1}{(n+1)}\right)h\frac{\partial}{\partial h}. \tag{4.121}$$

Finally, we consider the components of second conserved vector of the second kind,

$$R^1 = xh + x\int_0^t v_\ell(\tau,x)d\tau, \qquad R^2 = -K_n x h^n h_x + K_n \frac{h^{n+1}}{(n+1)}. \tag{4.122}$$

Now, using (4.86), it can be verified that

$$R^1_* = (c_1 + c_2 t)x v_\ell(t,x) + (c_3 + c_4 x)x\int_0^t \frac{\partial v_\ell}{\partial x}(\tau,x)d\tau + c_3(h + \int_0^t v_\ell(\tau,x)d\tau)$$
$$\frac{1}{n}[2(n+1)c_4 - c_2]xh + 2c_4 x\int_0^t v_\ell(\tau,x)d\tau. \tag{4.123}$$

Multiplying (4.89) by x and integrating the result with respect to τ from $\tau = 0$ to $\tau = x$ gives

$$(c_1 + c_2 t)x v_\ell(t,x) + (c_3 + c_4 x)x\int_0^t \frac{\partial v_\ell}{\partial x}(\tau,x)d\tau = c_1 x v_\ell(0,x)$$
$$+ \frac{1}{n}[2c_4 - c_2]x\int_0^t v_\ell(\tau,x)d\tau. \tag{4.124}$$

Substituting (4.124) into (4.123) gives

$$R^1_* = c_1 x v_\ell(0,x) + c_3[h + \int_0^t v_\ell(\tau,x)d\tau]$$
$$+ \frac{1}{n}[2(n+1)c_4 - c_2]\left[xh + x\int_0^t v_\ell(\tau,x)d\tau\right] \tag{4.125}$$

Also, it can be readily shown that

$$R^2_* = c_3(-K_n h^n h_x) + \frac{1}{n}[2(n+1)c_4 - c_2]\left[K_n\frac{h^{n+1}}{(n+1)} - K_n x h^n h_x\right]. \tag{4.126}$$

Equations (4.125) and (4.126) can be expressed in vector form as

$$\mathbf{R}^*_{(2)} = c_3 R_{(1)} + \frac{1}{n}[2(n+1)c_4 - c_2]\mathbf{R}_{(2)} + c_1\mathbf{S}_{(0)} \tag{4.127}$$

where

$$\mathbf{R}_{(1)} = [h + \int_0^t v_\ell(\tau,x)d\tau, -K_n h^n h_x], \tag{4.128}$$

$$\mathbf{R}_{(2)} = [xh + x\int_0^t v_\ell(\tau,x)d\tau, -K_n x h^n h_x + K_n\frac{h^{n+1}}{n+1}], \tag{4.129}$$

and

$$\mathbf{S}_{(0)} = [x v_\ell(0,x), 0]. \tag{4.130}$$

The vector $\mathbf{R}_{(2)}$ is not a new conserved vector since $\mathbf{S}_{(0)}$ is a trivial conserved vector. The condition that (4.126) is associated with (4.88) is obtained by setting (4.126) to zero to find that

$$c_1 = 0, \qquad c_3 = 0, \qquad \frac{c_4}{c_2} = \frac{1}{2(n+1)}. \tag{4.131}$$

The Lie point symmetry associated with the second conserved vector of the second kind is

$$X = t\frac{\partial}{\partial t} + \frac{1}{2(n+1)}x\frac{\partial}{\partial x} - \frac{1}{n+1}h\frac{\partial}{\partial h}. \tag{4.132}$$

The solution $\alpha = 1/(2(n+1))$ was obtained to be a limiting solution for fluid extraction for the case of a fracture with tortuosity and no leak-off i.e. $\gamma = 0$ in [11]. For the case $\gamma > 0$, we are yet to determine the physical interpretation of this working condition.

4.5 Conclusions

In this chapter, we employed the direct and multiplier method to investigate the conserved vectors of the partial differential equation given by equation (4.1). It was found that the PDE admits conservation laws of the first and second kind as a results of the leak-off velocity term in the PDE. The multiplier method was considered to investigate other conserved vectors by introducing a multiplier of the form $\Lambda = \Lambda(t, x, h, h_x, h_t)$. A theorem due to Kara and Mahomed was used to investigate a relationship between a Lie point symmetry generator and the obtained conservation laws. No new conserved vectors were generated from the known conserved vectors as the calculation resulted in a linear combination of the known conserved vectors of the first and the second kind. However, the association of a Lie point symmetry with a conservation laws led to two working conditions, $\alpha = 1/(2(n+1))$ and $\alpha = 1/(n+2)$, which can be used to investigate analytical solutions.

Chapter 5

Case I: Group invariant solutions for $c_2 \neq 0$ and $c_4 \neq 0$ - General Solution

In this chapter, we consider a two-dimensional fluid driven model fracture with the effect of tortuosity included and in permeable rock. Due to permeability, the fluid injected at the fracture entry leaks off from the fracture into the rock mass encasing the fracture. We will analyse the partial differential equations that models the fracture. We will derive the group invariant solution of the model. The parameter c_3, first observed in the Lie point symmetry of the governing PDE in Appendix A, will later be set to zero in the process of expressing the remaining equations in the model in terms of the group invariant solution. The various general properties of the fracture will be investigated.

The governing nonlinear diffusion equation is given by

$$\frac{\partial h}{\partial t} = K_n \frac{\partial}{\partial x}\left(h^n \frac{\partial h}{\partial x}\right) - v_\ell(t,x), \tag{5.1}$$

where the fluid leak-off velocity is not described a priori. Its functional form has to satisfy a partial differential equation in order for the governing non-linear diffusion equation to admit a symmetry generator.

5.1 Lie point symmetries

In order to derive the group invariant solutions of the governing partial differential equation (5.1) we first consider the Lie point symmetry of the PDE, the calculation of which is outlined in detail in Appendix A. The Lie point symmetry generator of (5.1) is

$$X = (c_1 + c_2 t)\frac{\partial}{\partial t} + (c_3 + c_4 x)\frac{\partial}{\partial x} + \frac{1}{n}(2c_4 - c_2)h\frac{\partial}{\partial h}, \tag{5.2}$$

which can be expressed as

$$X = c_1 X_1 + c_2 X_2 + c_3 X_3 + c_4 X_4, \tag{5.3}$$

where c_1, c_2, c_3 and c_4 are unknown constants and

$$X_1 = \frac{\partial}{\partial t}, \tag{5.4}$$

$$X_2 = t\frac{\partial}{\partial t} - \frac{h}{n}\frac{\partial}{\partial h}, \tag{5.5}$$

$$X_3 = \frac{\partial}{\partial x}, \tag{5.6}$$

$$X_4 = x\frac{\partial}{\partial x} + \frac{2h}{n}\frac{\partial}{\partial h}, \tag{5.7}$$

provided that the leak-off velocity, $v_\ell(t,x)$, satisfies the first order linear partial differential equation

$$(c_1 + c_2 t)\frac{\partial v_\ell}{\partial t} + (c_3 + c_4 x)\frac{\partial v_\ell}{\partial x} = \frac{2}{n}\Big(c_4 - \frac{n+1}{2}c_2\Big)v_\ell. \tag{5.8}$$

Now, $h = \phi(t,x)$ is a group invariant solution of (5.1) provided

$$X\Big(h - \phi(t,x)\Big)\Big|_{h=\phi} = 0, \tag{5.9}$$

that is, provided

$$(c_1 + c_2 t)\frac{\partial \phi}{\partial t} + (c_3 + c_4 x)\frac{\partial \phi}{\partial x} = \frac{1}{n}(2c_4 - c_2)\phi. \tag{5.10}$$

The characteristic equations corresponding to the first order PDE (5.10) are

$$\frac{dt}{c_1 + c_2 t} = \frac{dx}{c_3 + c_4 x} = \frac{d\phi}{\big[\frac{1}{n}(2c_4 - c_2)\phi\big]}, \tag{5.11}$$

provided $2c_4 - c_2 \neq 0$, which can be equivalently written as

$$\frac{dt}{c_1 + c_2 t} = \frac{dx}{c_3 + c_4 x}, \quad \frac{dt}{c_1 + c_2 t} = \frac{d\phi}{\big[\frac{1}{n}(2c_4 - c_2)\phi\big]}. \tag{5.12}$$

Solving the differential equations in (5.12) gives, provided $c_2 \neq 0$ and $c_4 \neq 0$,

$$a_1 = \frac{c_3 + c_4 x}{(c_1 + c_2 t)^{\frac{c_4}{c_2}}}, \quad a_2 = \frac{\phi}{(c_1 + c_2 t)^{\frac{2}{n}\left(\frac{c_4}{c_2} - \frac{1}{2}\right)}}, \tag{5.13}$$

where a_1 and a_2 are constants. The first order PDE (5.10) has a general solution of the form

$$a_2 = F(a_1), \tag{5.14}$$

where F is an arbitrary function. Since $h(t,x) = \phi(t,x)$, it follows that the group invariant solution of the half-width of the fracture is

$$h(t,x) = (c_1 + c_2 t)^{\frac{2}{n}\left(\frac{c_4}{c_2} - \frac{1}{2}\right)} F(\xi), \tag{5.15}$$

where ξ is the similarity variable,

$$\xi = \frac{c_3 + c_4 x}{(c_1 + c_2 t)^{\alpha}}, \tag{5.16}$$

and

$$\alpha = \frac{c_4}{c_2}. \tag{5.17}$$

It is readily verified that when $2c_4 - c_2 = 0$, the solution (5.15) is again obtained. The existence of a group invariant solution (5.15) requires that the fluid leak-off velocity, $v_\ell(t,x)$, satisfies equation (5.8). The characteristic equations corresponding to the first order PDE (5.8) are

$$\frac{dt}{c_1 + c_2 t} = \frac{dx}{c_3 + c_4 x} = \frac{dv_\ell}{\frac{2}{n}\left(c_4 - \frac{n+1}{2}c_2\right) v_\ell}, \tag{5.18}$$

provided $c_4 \neq \frac{n+1}{2}c_2$, which can be equivalently written as

$$\frac{dt}{c_1 + c_2 t} = \frac{dx}{c_3 + c_4 x}, \quad \frac{dt}{c_1 + c_2 t} = \frac{dv_\ell}{\frac{2}{n}\left(c_4 - \frac{n+1}{2}c_2\right) v_\ell}. \tag{5.19}$$

Integrating the two differential equations in (5.19) gives

$$a_3 = \frac{c_3 + c_4 x}{(c_1 + c_2 t)^{\alpha}}, \quad a_4 = \frac{v_\ell}{(c_1 + c_2 t)^{\frac{2}{n}\left(\alpha - \frac{n+1}{2}\right)}}, \tag{5.20}$$

where a_3 and a_4 are constants. The general form of the solution of (5.19) is

$$a_4 = G(a_3), \tag{5.21}$$

where G is an arbitrary function. Hence

$$v_\ell(t,x) = (c_1 + c_2 t)^{\frac{2}{n}\left(\alpha - \frac{n+1}{2}\right)} G(\xi), \tag{5.22}$$

where the similarity variable ξ and the constant α are given by (5.16) and (5.17) respectively. It is readily verified that when $c_4 = \frac{n+1}{2}c_2$, the solution (5.22) is again obtained.

Now that the general form of the group invariant solution for the half-width of the fracture, $h(t,x)$, and the leak-off velocity of the fluid, $v_\ell(t,x)$ are obtained, it is necessary to express the problem in terms of the similarity variable, ξ, and the functions $F(\xi)$ and $G(\xi)$. Thus we must express the nonlinear diffusion equation (5.1), the corresponding boundary conditions and all related properties of the fracture in terms of the group invariant solution (5.15) and (5.22).

The partial derivatives of the similarity variable (5.16),

$$\frac{\partial \xi}{\partial t} = \frac{-c_4 \xi}{(c_1 + c_2 t)} \quad \text{and} \quad \frac{\partial \xi}{\partial x} = \frac{c_4}{(c_1 + c_2 t)^{\alpha}}, \tag{5.23}$$

will be useful in the process of expressing that problem in terms of the group invariant solutions (5.15) and (5.22).

Firstly, we consider the non-linear diffusion equation (5.1). Substituting (5.15) and (5.22),

with the aid of (5.23), into (5.1) transforms the partial differential equation into a second order non-linear ordinary differential equation

$$c_4 K_n \frac{d}{d\xi}\left(F^n \frac{dF}{d\xi}\right) + \frac{d}{d\xi}\left(\xi F\right) + \frac{1}{n}\left[\frac{1}{\alpha} - (n+2)\right]F - \frac{1}{c_4}G = 0. \tag{5.24}$$

It is clear that Equation (5.24) does not depend on the constant c_3. We choose $c_3 = 0$ in (5.16) such that when $x = 0$, $\xi = 0$.

We then consider boundary conditions of the non-linear diffusion equation (5.1). The boundary condition at the fracture tip, $x = L(t)$, is

$$h(t, L(t)) = 0, \tag{5.25}$$

which implies that

$$F(B(t)) = 0 \tag{5.26}$$

where

$$B(t) = \frac{c_4 L(t)}{(c_1 + c_2 t)^\alpha}. \tag{5.27}$$

Differentiating (5.27) with respect to t gives

$$\frac{dF}{dB}\frac{dB(t)}{dt} = 0. \tag{5.28}$$

Since $\frac{dF}{dB} \neq 0$, it follows that $\frac{dB(t)}{dt} = 0$. This implies that

$$B(t) = k = \frac{c_4 L(t)}{(c_1 + c_2 t)^\alpha}, \tag{5.29}$$

where k is a constant. Therefore the length of the fracture is

$$L(t) = \frac{k c_1^\alpha}{c_4}\left(1 + \frac{c_2}{c_1} t\right)^\alpha, \tag{5.30}$$

provided $c_1 \neq 0$. The characteristic length, L, is chosen to be the initial length of the fracture, $L(0)$, therefore the dimensionless fracture length is

$$L^*(t) = \frac{L(t)}{L(0)} = \frac{L(t)}{L_0}. \tag{5.31}$$

Where $L(t)$ in (5.30) is already dimensionless (although the stars * have been dropped for convenience), we apply (5.31) to it and find that

$$L(0) = 1. \tag{5.32}$$

Using (5.31), the combination of parameter values in (5.30) becomes

$$\frac{k c_1^\alpha}{c_4} = 1. \tag{5.33}$$

Therefore the length of the fracture is

$$L(t) = \left(1 + \frac{c_2}{c_1} t\right)^{\alpha} \tag{5.34}$$

and the boundary condition at the fracture tip is

$$F\left(\frac{c_4}{c_1^{\alpha}}\right) = 0. \tag{5.35}$$

In order to express the remaining boundary conditions in terms of the group invariant solutions, it is necessary to first express the volume flux of fluid per unit breadth in terms of the group invariant solution.

The volume flux of fluid per unit breadth in the fracture, from (2.65),

$$Q(t,x) = -2K_n h^n \frac{\partial h}{\partial x}, \tag{5.36}$$

$$\tag{5.37}$$

when expressed in terms of the group invariant solution (5.15) becomes

$$Q(t,x) = -2K_n c_4 c_1^{\frac{n+2}{n}\left[\alpha - \frac{n+1}{n+2}\right]} \left(1 + \frac{c_2}{c_1} t\right)^{\frac{n+2}{n}\left[\alpha - \frac{n+1}{n+2}\right]} F^n(\xi) \frac{dF}{d\xi}. \tag{5.38}$$

The volume flux of fluid into the fracture (5.38) evaluated at the fracture entry, $x = 0$, is

$$Q(t,0) = -2K_n c_4 c_1^{\frac{n+2}{n}\left[\alpha - \frac{n+1}{n+2}\right]} \left(1 + \frac{c_2}{c_1} t\right)^{\frac{n+2}{n}\left[\alpha - \frac{n+1}{n+2}\right]} F^n(0) \frac{dF}{d\xi}(0). \tag{5.39}$$

Therefore, using (2.63), we can deduce that $S(t)$ is of the form $A(1+Bt)^m$ where

$$A = -2K_n c_4 c_1^{\frac{n+2}{n}\left[\alpha - \frac{n+1}{n+2}\right]} F^n(0) \frac{dF}{d\xi}(0), \tag{5.40}$$

$$B = \frac{c_2}{c_1}, \tag{5.41}$$

$$m = \frac{n+2}{n}\left[\alpha - \frac{n+1}{n+2}\right]. \tag{5.42}$$

Equation (5.40) can be written as

$$F^n(0) \frac{dF}{d\xi}(0) = -\frac{A}{2K_n c_4 c_1^{\frac{n+2}{n}\left[\alpha - \frac{n+1}{n+2}\right]}}. \tag{5.43}$$

We now express the consistency condition in (2.53):

$$\frac{dV}{dt} = Q(t,0) - q(t) - Q(t, L(t)), \tag{5.44}$$

in terms of the group invariant solution. It is clear from (5.44) that the volume of the fracture is required in the calculation. In terms of the group invariant solution, the volume of the fracture

$$V(t) = 2\int_0^{L(t)} h(t,x)\,dx, \tag{5.45}$$

becomes

$$V(t) = V_0\left(1+\frac{c_2}{c_1}t\right)^{\frac{n+2}{n}\left[\alpha-\frac{1}{n+2}\right]}, \tag{5.46}$$

where

$$V_0 = \frac{2}{c_4}c_1^{\frac{n+2}{n}\left[\alpha-\frac{1}{n+2}\right]}\int_0^{\frac{c_4}{c_1^\alpha}} F(\xi)\,d\xi. \tag{5.47}$$

Using (5.15) and (5.22) with the aid of (5.46), it follows that in terms of the group invariant solution, the consistency condition (5.44) is

$$\begin{aligned} c_4K_nF^n(0)\frac{dF}{d\xi}(0) = \frac{1}{n}\left[\frac{1}{\alpha}-(n+2)\right]\int_0^{\frac{c_4}{c_1^\alpha}} F(\xi)\,d\xi - \frac{1}{c_4}\int_0^{\frac{c_4}{c_1^\alpha}} G(\xi)\,d\xi \\ + c_4K_nF^n\left(\frac{c_4}{c_1^\alpha}\right)\frac{dF}{d\xi}\left(\frac{c_4}{c_1^\alpha}\right), \end{aligned} \tag{5.48}$$

and is identically satisfied. Using (5.48) the value of A in (5.43) is given as:

$$A = -2c_1^{\frac{n+2}{n}\left[\alpha-\frac{n+1}{n+2}\right]}\left[\frac{1}{n}\left(\frac{1}{\alpha}-(n+2)\right)\int_0^{\frac{c_4}{c_1^\alpha}} F(\xi)\,d\xi - \frac{1}{c_4}\int_0^{\frac{c_4}{c_1^\alpha}} G(\xi)\,d\xi + c_4K_nF^n\left(\frac{c_4}{c_1^\alpha}\right)\frac{dF}{d\xi}\left(\frac{c_4}{c_1^\alpha}\right)\right]. \tag{5.49}$$

Therefore in terms of the group invariant solution, the problem is to solve

$$c_4K_n\frac{d}{d\xi}\left(F^n\frac{dF}{d\xi}\right)+\frac{d}{d\xi}\left(\xi F\right)+\frac{1}{n}\left[\frac{1}{\alpha}-(n+2)\right]F(\xi)-\frac{1}{c_4}G(\xi)=0, \tag{5.50}$$

subject to the boundary conditions,

$$F\left(\frac{c_4}{c_1^\alpha}\right)=0, \tag{5.51}$$

$$F^n(0)\frac{dF}{d\xi}(0) = -\frac{A}{2K_nc_4c_1^{\frac{n+2}{n}\left[\alpha-\frac{n+1}{n+2}\right]}}, \tag{5.52}$$

where the identically satisfied consistency condition gives

$$A = -2c_1^{\frac{n+2}{n}\left[\alpha-\frac{n+1}{n+2}\right]}\left[\frac{1}{n}\left(\frac{1}{\alpha}-(n+2)\right)\int_0^{\frac{c_4}{c_1^\alpha}} F(\xi)\,d\xi - \frac{1}{c_4}\int_0^{\frac{c_4}{c_1^\alpha}} G(\xi)\,d\xi + c_4K_nF^n\left(\frac{c_4}{c_1^\alpha}\right)\frac{dF}{d\xi}\left(\frac{c_4}{c_1^\alpha}\right)\right] \tag{5.53}$$

and the properties of the fracture and the fluid flow in the fracture are

$$h(t,x) = (c_1 + c_2 t)^{\frac{2}{n}\left(\alpha - \frac{1}{2}\right)} F(\xi), \tag{5.54}$$

$$v_\ell(t,x) = (c_1 + c_2 t)^{\frac{2}{n}\left(\alpha - \frac{n+1}{2}\right)} G(\xi), \tag{5.55}$$

$$\xi = \frac{c_4 x}{(c_1 + c_2 t)^\alpha}, \qquad \alpha = \frac{c_4}{c_2}, \tag{5.56}$$

$$L(t) = \left(1 + \frac{c_2}{c_1} t\right)^\alpha, \tag{5.57}$$

$$Q(t,x) = -2K_n c_4 c_1^{\frac{n+2}{n}\left[\alpha - \frac{n+1}{n+2}\right]} \left(1 + \frac{c_2}{c_1} t\right)^{\frac{n+2}{n}\left[\alpha - \frac{n+1}{n+2}\right]} F^n(\xi) \frac{dF}{d\xi}, \tag{5.58}$$

$$V(t) = V_0 \left(1 + \frac{c_2}{c_1} t\right)^{\frac{n+2}{n}\left[\alpha - \frac{1}{n+2}\right]}, \tag{5.59}$$

where

$$V_0 = \frac{2}{c_4} c_1^{\frac{n+2}{n}\left[\alpha - \frac{1}{n+2}\right]} \int_0^{\frac{c_4}{c_1^\alpha}} F(\xi) d\xi, \tag{5.60}$$

$$\bar{v}_x(t,x) = -c_4 K_n (c_1 + c_2 t)^{\alpha - 1} F^{n-1}(\xi) \frac{dF}{d\xi}. \tag{5.61}$$

5.2 Scaling transformation

The formulation can be simplified by introducing a scaling transformation

$$G(\xi) = \left(\frac{c_4^{n+1}}{K_n c_1^{2\alpha}}\right)^{1/n} g(u), \quad F(\xi) = \left(\frac{c_4}{K_n c_1^{2\alpha}}\right)^{1/n} f(u),$$
$$u = \frac{x}{L(t)}, \quad \xi = \frac{c_4}{c_1^\alpha} u. \tag{5.62}$$

The transformation is chosen such that the problem is defined in the domain $0 < u < 1$ instead of the domain $0 \le \xi \le \frac{c_4}{c_1^\alpha}$. It can be verified that equations (5.50) to (5.61) transform to give

$$\frac{d}{du}\left(f^n \frac{df}{du}\right) + \frac{d}{du}\left(uf\right) + \frac{1}{n}\left(\frac{1}{\alpha} - (n+2)\right) f - g = 0 \tag{5.63}$$

subject to

$$f(1) = 0, \tag{5.64}$$

$$f^n(0) \frac{df}{du}(0) = -\frac{A}{2}\left(K_n \left(\frac{c_1}{c_4}\right)^{n+1}\right)^{\frac{1}{n}} \tag{5.65}$$

where A satisfies the consistency condition

$$A = -2\left(\frac{1}{K_n}\left(\frac{c_4}{c_1}\right)^{n+1}\right)^{\frac{1}{n}} \left[\frac{1}{n}\left(\frac{1}{\alpha} - (n+1)\right)\int_0^1 f(u)du - \int_0^1 g(u)du + f^n(1)\frac{df}{du}(1)\right], \tag{5.66}$$

and

$$h(t,u)=\left(\frac{c_4}{K_n c_1}\right)^{\frac{1}{n}}\left(1+\frac{c_2}{c_1}t\right)^{\frac{2}{n}\left(\alpha-\frac{1}{2}\right)} f(u), \tag{5.67}$$

$$v_\ell(t,u)=\left(\frac{1}{K_n}\left(\frac{c_4}{c_1}\right)^{n+1}\right)^{\frac{1}{n}}\left(1+\frac{c_2}{c_1}t\right)^{\frac{2}{n}\left(\alpha-\frac{n+1}{2}\right)} g(u), \tag{5.68}$$

$$L(t)=\left(1+\frac{c_2}{c_1}t\right)^{\alpha}, \tag{5.69}$$

$$Q(t,u)=-2\left(\frac{1}{K_n}\left(\frac{c_4}{c_1}\right)^{n+1}\right)^{\frac{1}{n}}\left(1+\frac{c_2}{c_1}t\right)^{\frac{n+2}{n}\left(\alpha-\frac{n+1}{n+2}\right)} f^n(u)\frac{df}{du}, \tag{5.70}$$

$$V(t)=V_0\left(1+\frac{c_2}{c_1}t\right)^{\frac{n+2}{2}\left(\alpha-\frac{1}{n+2}\right)}, \tag{5.71}$$

where

$$V_0=2\left(\frac{c_4}{K_n c_1}\right)^{\frac{1}{n}}\int_0^1 f(u)\,du, \tag{5.72}$$

$$\bar{v}_x(t,u)=-\left(\frac{c_4}{c_1}\right)\left(1+\frac{c_2}{c_1}t\right)^{\alpha-1} f^{n-1}(u)\frac{df}{du}. \tag{5.73}$$

We will now investigate the relationship between the leak-off velocity, $v_\ell(t,x)$ and the half-width of the fracture, $h(t,x)$.

5.3 Leak-off velocity proportional to the half-width of the fracture

Suppose that $g(u)$ is proportional to $f(u)$:

$$g(u)=\gamma f(u), \tag{5.74}$$

where γ is the proportionality constant which indicates the strength of leak-off. It follows from (5.15) and (5.22) that

$$v_\ell(t,x)=\gamma\frac{h(t,x)}{(c_1+c_4 t)}. \tag{5.75}$$

There are three cases for the coefficient γ. Case one, $\gamma>0$ describes fluid leak-off into the surrounding rock mass since $v_\ell(t,x)>0$. The second case $\gamma<0$, describes fluid in-flow from the surrounding rock mass into the fracture at the fluid-rock interface. The third case, $\gamma=0$, when $v_l(t,x)=0$ results when the surrounding rock is impermeable since there is no fluid leak-off into or in-flow from the rock mass. In this work, we shall consider the case $\gamma>0$.

The boundary value problem (5.63)-(5.66) becomes

$$\frac{d}{du}\left(f^n\frac{df}{du}\right)+\frac{d}{du}(uf)+\frac{1}{n}\left(\frac{1}{\alpha}-\left[n(1+\gamma)+2\right]\right)f(u), \tag{5.76}$$

$$f(1)=0, \tag{5.77}$$

$$f^n(0)\frac{df}{du}(0)=-\frac{A}{2}\left(K_n\left(\frac{c_1}{c_4}\right)^{n+1}\right)^{\frac{1}{n}} \tag{5.78}$$

and the leak-off velocity, (5.68), becomes

$$v_\ell(t,u) = \gamma\left(\frac{1}{K_n}\left(\frac{c_4}{c_1}\right)^{n+1}\right)^{\frac{1}{n}}\left(1+\frac{c_2}{c_1}t\right)^{\frac{2}{n}\left(\alpha-\frac{(n+1)}{2}\right)} f(u). \tag{5.79}$$

The characteristic half-width of the fracture is chosen as the maximum half-width of the fracture such that in dimensionless form the half-width of the fracture at u_{max} at $t=0$ satisfies

$$h^*(0,u_{max}) = \beta, \tag{5.80}$$

where u_{max} is the length along the fracture at which the maximum half-width of the fracture, h_{max}, is attained. Since we consider a partially open fracture which occurs only when

$$0 \le h(t,u) < h_{max}, \tag{5.81}$$

it follows that

$$0 < \beta < 1. \tag{5.82}$$

Imposing condition (5.80) on the dimensionless half-width of the fracture, (5.67), gives

$$\frac{c_4}{c_1} = K_n\left(\frac{\beta}{f_{max}}\right)^n, \qquad B = \frac{c_2}{c_1} = \frac{c_2}{c_4}\frac{c_4}{c_1} = \frac{K_n}{\alpha}\left(\frac{\beta}{f_{max}}\right)^n, \tag{5.83}$$

where $f_{max} = f(u_{max})$. Substituting the ratios c_4/c_1 and c_2/c_1 into equations (5.67) to (5.73) and (5.79) gives

$$\frac{d}{du}\left(f^n\frac{df}{du}\right) + \frac{d}{du}(uf) + \frac{1}{n}\left(\frac{1}{\alpha} - \left[n(1+\gamma)+2\right]\right) f(u), \tag{5.84}$$

$$f(1) = 0, \tag{5.85}$$

$$f^n(0)\frac{df}{du}(0) = -\frac{A}{2}\left(K_n\left(\frac{c_1}{c_4}\right)^{n+1}\right)^{\frac{1}{n}}, \tag{5.86}$$

where

$$A = -2\left(\frac{1}{K_n}\left(\frac{c_4}{c_1}\right)^{n+1}\right)^{\frac{1}{n}}\left[\frac{1}{n}\left(\frac{1}{\alpha} - \left[n(1+\gamma)+2\right]\right)\int_0^1 f(u)\,du + f^n(1)\frac{df}{du}(1)\right], \tag{5.87}$$

and

$$h(t,u) = \frac{\beta}{f_{max}}\left(1+\frac{1}{\alpha}\left(\frac{\beta}{f_{max}}\right)^n K_n t\right)^{\frac{2}{n}\left(\alpha-\frac{1}{2}\right)} f(u), \tag{5.88}$$

$$v_\ell(t,u) = \gamma K_n\left(\frac{\beta}{f_{max}}\right)^{(n+1)}\left(1+\frac{1}{\alpha}\left(\frac{\beta}{f_{max}}\right)^n K_n t\right)^{\frac{2}{n}\left(\alpha-\frac{(n+1)}{2}\right)} f(u), \tag{5.89}$$

$$L(t) = \left(1+\frac{1}{\alpha}\left(\frac{\beta}{f_{max}}\right)^n K_n t\right)^{\alpha}, \tag{5.90}$$

$$Q(t,u) = -2K_n\left(\frac{\beta}{f_{max}}\right)^{(n+1)}\left(1+\frac{1}{\alpha}\left(\frac{\beta}{f_{max}}\right)^n K_n t\right)^{\frac{n+2}{n}\left(\alpha-\frac{n+1}{n+2}\right)} f^n(u)\frac{df}{du}, \tag{5.91}$$

$$\bar{v}_x(t,u) = -K_n\left(\frac{\beta}{f_{max}}\right)^n\left(1+\frac{1}{\alpha}\left(\frac{\beta}{f_{max}}\right)^n K_n t\right)^{\alpha-1} f^{n-1}(u)\frac{df}{du}, \tag{5.92}$$

$$V(t) = V_0\left(1+\frac{1}{\alpha}\left(\frac{\beta}{f_{max}}\right)^n K_n t\right)^{\frac{n+2}{n}\left(\alpha-\frac{1}{n+2}\right)}, \tag{5.93}$$

where

$$V_0 = \left(2\frac{\beta}{f_{max}}\right)\int_0^1 f(u)du. \tag{5.94}$$

We have obtained the various properties of the fracture such as the length, the half-width, the volume and the width-averaged fluid velocity of the fracture. The parameter K_n given by (2.61) can be obtained from experiments. Small values of n satisfying $n > 0$ will be considered. Since this work investigates partially open fractures, $0 < \beta < 1$. All parameter values are known except for α which leads us to the next section.

In the next section, we will investigate the various operating conditions α that can be applied at the fracture entry.

5.4 Asymptotic solution at the fracture tip

We can find the approximate behaviour of $f(u)$ as $u \to 1$ by investigating an asymptotic solution at the fracture tip that will hold for both analytical and numerical solutions in the epsilon neighbourhood of the fracture tip where $\epsilon \ll 1$. The asymptotic solution is of the form

$$f(u) \sim k(1-u)^p, \qquad u \to 1, \tag{5.95}$$

where k and p are constants to be determined. This form of solution is required to satisfy the boundary conditions at the fracture tip but is not required to satisfy the boundary condition at the fracture entry. Substituting (5.95) into (5.84) gives

$$\begin{aligned} &k^{n+1}p[(n+1)p-1](1-u)^{p(n+1)-2} - kp(1-u)^{p-1} \\ &+ k\left[p+1+\frac{1}{n}\left(\frac{1}{\alpha}-[n(1+\gamma)+2]\right)\right](1-u)^p = 0, \quad \text{as} \quad u \to 1. \end{aligned} \tag{5.96}$$

Balancing the dominant terms in (5.96) gives

$$p = \frac{1}{n}, \tag{5.97}$$

and

$$k = n^{\frac{1}{n}}, \tag{5.98}$$

provided the third term tends to zero as $u \to 1$. Using (5.127) and (5.98), the asymptotic solution (5.96) becomes

$$f(u) \sim n^{\frac{1}{n}}(1-u)^{\frac{1}{n}}, \quad \text{as} \quad u \to 1, \tag{5.99}$$

and the derivative of the asymptotic solution is

$$\frac{d}{du}f(u) \sim -n^{\frac{1-n}{n}}(1-u)^{\frac{1-n}{n}}, \quad \text{as} \quad u \to 1. \tag{5.100}$$

The asymptotic solution holds for all values of the working conditions α and for all values of γ. The asymptotic solution gives

$$f^n(u)\frac{d}{du}f(u) \sim -n^{\frac{1}{n}}(1-u)^{\frac{1}{n}} \quad \text{as} \quad u \to 1 \tag{5.101}$$

and therefore

$$f^n(1)\frac{df}{du}(1) = 0. \tag{5.102}$$

The fluid flux at the fracture tip is therefore zero. Using (5.99) and (5.88), the half-width of the fracture becomes

$$h(t,x) \sim \frac{\beta}{f_{max}}L(t)^{\frac{2}{n}\left(1-\frac{1}{2\alpha}\right)}n^{\frac{1}{n}}\left(1-\frac{x}{L(t)}\right)^{\frac{1}{n}}, \quad \text{as } x \to L(t), \tag{5.103}$$

and therefore

$$\frac{\partial h}{\partial x} \sim -\frac{\beta}{f_{max}}L(t)^{\frac{2-n}{n}\left(1-\frac{1}{(2-n)\alpha}\right)}n^{\frac{1-n}{n}}\left(1-\frac{x}{L(t)}\right)^{\frac{1-n}{n}}, \text{as } x \to L(t). \tag{5.104}$$

It follows that

$$\frac{\partial h}{\partial x}(t,L(t)) = \begin{cases} -\infty, & n > 1 \\ -\frac{\beta}{f_{max}}L(t)^{\frac{\alpha-1}{\alpha}}, & n = 1, \\ 0, & 0 < n < 1. \end{cases} \tag{5.105}$$

The gradient of the half-width leads to singularity at the fracture tip when the fracture becomes less tortuous $n > 1$. Its spatial gradient is non-zero for $n = 1$ and zero for $0 < n < 1$ which describes a tortuous fracture.

5.5 Working conditions at the fracture entry

In this section, we investigate the values taken by the parameter value α when different working conditions are imposed at the fracture, which will be obtained from (5.88) to (5.94).

5.5.1 Uncategorized working conditions

In chapter 4, section 4.4, we obtained two working conditions as a result of Sjöberg's double reduction theorem. The working condition

$$\alpha = \frac{1}{2(n+1)}, \tag{5.106}$$

was obtained as a result of a Lie point symmetry of the partial differential equation being associated with a conserved vector. In the following section, it is found that an analytical solution exists when

$$\alpha = \frac{1}{n+1}. \tag{5.107}$$

It remains to be investigated whether these two working conditions have any physical significance.

5.5.2 Constant pressure at the entry

When fluid is injected at constant pressure at the entry, the operating condition is referred to as a constant pressure working condition. From (2.40) and (5.88), the pressure at the fracture entry is

$$p(t,0) = \left(\frac{1-\frac{\sigma_R}{\Lambda h_{max}}}{1-\frac{\sigma_{zz}^{\infty}}{\Lambda h_{max}}}\right)\frac{\beta}{f_{max}}\left(1+\frac{1}{\alpha}\left(\frac{\beta}{f_{max}}\right)^n K_n t\right)^{\frac{2}{n}\left(\alpha-\frac{1}{2}\right)} f(0) + \left(\frac{\sigma_R-\sigma_{zz}^{\infty}}{\Lambda h_{max}-\sigma_{zz}^{\infty}}\right). \tag{5.108}$$

It is also clear that when the pressure at the entry is constant, the half-width, (5.88), of the fracture is also constant. The pressure at the entry is constant if $\alpha = \frac{1}{2}$.

5.5.3 The speed of propagation of the fracture

Taking the derivative of the length, (5.90), with respect to time gives the speed of propagation

$$\frac{dL}{dt} = K_n\left(\frac{\beta}{f_{max}}\right)^n\left(1+\frac{1}{\alpha}\left(\frac{\beta}{f_{max}}\right)^n K_n t\right)^{\alpha-1}. \tag{5.109}$$

The speed of propagation is constant when $\alpha = 1$.

5.5.4 Constant volume

The total volume within the fracture is given by (5.93). The constant volume working condition arises if $\alpha = \frac{1}{n+2}$. When the volume of a hydraulic fracture remains constant the length of the fracture can increase and the fracture can propagate. This is well established for $\gamma = 0$ [20]. However, in a model with leak-off ($\gamma > 0$), constant volume exists only when the rate of fluid injection is equal to the rate of fluid leak-off at the fluid-rock interface. The implication of the latter is a fracture that does not propagate. This working condition was obtained as an analytical solution derived from the association of a Lie point symmetry with a conserved vector of the PDE.

5.5.5 Constant rate of fluid injection at the fracture entry

We consider the total flux of fluid in the fracture $Q(t,0)$, given by equation (5.91) The rate at which fluid is being pumped into the fracture is constant when

$$\alpha = \frac{n+1}{n+2}. \tag{5.110}$$

5.5.6 Constant rate of leak-off at the fluid-rock interface

The rate of fluid leak-off at the fluid-rock interface is given by (5.89). Leak-off velocity is a constant independent of time when

$$\alpha = \frac{n+1}{2}. \tag{5.111}$$

The various working conditions are summarised in Table 5.1.

Working condition at the fracture entry	α
Analytical soln 1	$\frac{1}{2(n+1)}$
Analytical soln 2	$\frac{1}{n+1}$
Constant pressure	$\frac{1}{2}$
Constant speed of propagation	1
Constant rate of fluid injection at the entry	$\frac{n+1}{n+2}$
Constant rate of fluid leak-off	$\frac{n+1}{2}$
Constant volume in the fracture	$\frac{1}{n+2}$

Table 5.1: A summary of the physical significance of the working conditions at the fracture entry and the corresponding value of the parameter α.

In Section 5.6, we will investigate the analytical solutions to the boundary value problem (5.84)-(5.87) for selected working conditions.

5.6 Exact analytical solutions

The exact analytical solution of the PDE (2.60) by first analysing the analytical solution, $f(u)$, of the ODE (5.84), will be investigated. This solution, $f(u)$, is obtained by solving the boundary value problem, (5.84)-(5.87) for a specific working condition. Substituting the solution $f(u)$ into the equations for the half-width and length of the fracture gives the various properties of the fracture. Two analytical solutions are obtained.

5.6.1 Exact solution when $\alpha = \frac{1}{2(n+1)}$ and $\gamma = 1$

When $\alpha = \frac{1}{2(n+1)}$ and $\gamma = 1$ the boundary value problem (5.84)-(5.87) reduces to

$$\frac{d}{du}\left(f^n \frac{df}{du}\right) + \frac{d}{du}(uf) = 0, \tag{5.112}$$

$$f(1) = 0, \tag{5.113}$$

$$f^n(0)\frac{df}{du}(0) = 0. \tag{5.114}$$

Integrating (5.112) once gives

$$f^n \frac{df}{du} + uf = D, \tag{5.115}$$

where D is a constant. Imposing the boundary conditions (5.114) on (5.115) gives $D = 0$. It follows that (5.115) is a variable separable equation,

$$f^n \frac{df}{du} + uf = 0, \tag{5.116}$$

which when integrated gives

$$\frac{f^n}{n} = E - \frac{u^2}{2}, \tag{5.117}$$

where E is a constant. Imposing the boundary condition (5.113) on (5.117) gives $E = 1/2$. which gives the solution to the boundary value problem, (5.112)- (5.114):

$$f(u) = \left[\frac{n}{2}(1-u^2)\right]^{\frac{1}{n}}. \tag{5.118}$$

The length $L(t)$, (5.90), and the half-width $h(t,x)$, (5.88), of the fracture for the analytical solution $f(u)$ defined by (5.118) respectively are

$$h(t,x) = \beta\left[1 + \frac{4(n+1)}{n}\beta^n K_n t\right]^{-\frac{1}{n+1}}\left(1 - \left(\frac{x}{L(t)}\right)^2\right)^{\frac{1}{n}}, \tag{5.119}$$

$$L(t) = \left[1 + \frac{4(n+1)}{n}\beta^n K_n t\right]^{\frac{1}{2(n+1)}}. \tag{5.120}$$

Differentiating (5.119) with respect to x as $x \to L(t)$ gives that the spatial gradient of the half-width is

$$\frac{\partial h}{\partial x} = -\frac{2\beta x}{nL^2(t)}\left[1 + \frac{4(n+1)}{n}\beta^n K_n t\right]^{-\frac{1}{n+1}}\left(1 - \frac{x^2}{L^2(t)}\right)^{\frac{1-n}{n}}. \tag{5.121}$$

Evaluating (5.121) as $x \to L(t)$:

$$\frac{\partial h}{\partial x}(t, L(t)) = \begin{cases} -\infty, & n > 1 \\ -\frac{2\beta}{L^{\frac{3}{2}}(t)}, & n = 1, \\ 0, & 0 < n < 1, \end{cases} \tag{5.122}$$

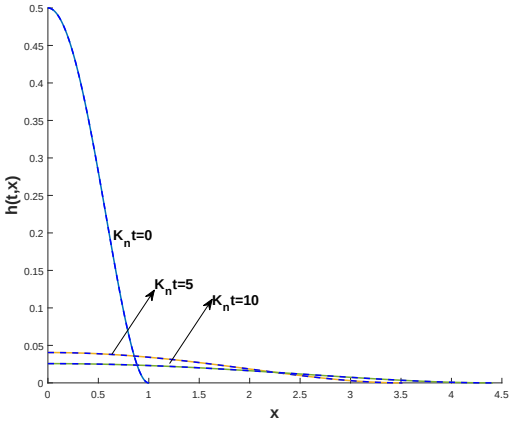
which describes the behaviour of the spatial gradient of the half-width of the fracture. From (5.114) the fluid flux at the fracture entry vanishes, and therefore,

$$S(t) = A(1 + Bt)^m = 0. \tag{5.123}$$

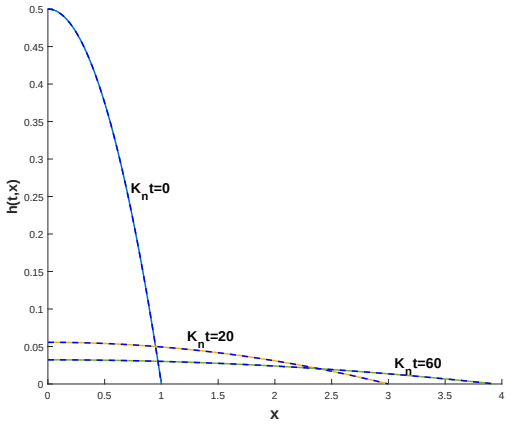
5.6.2 Exact solution when $\alpha = \frac{1}{n+1}$ and $\gamma = 1$

We investigate another analytical solutions of the form

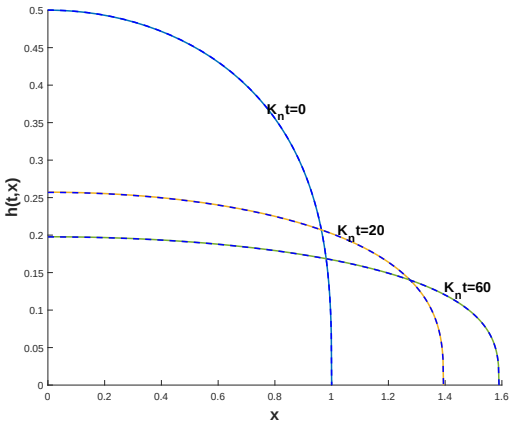
$$f(u) = r(1-u)^p, \tag{5.124}$$



(a) n=0.5

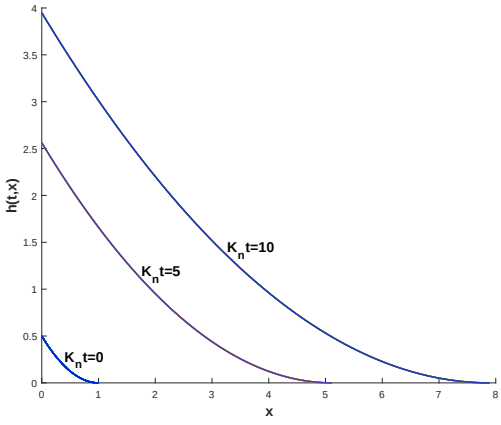


(b) n=1

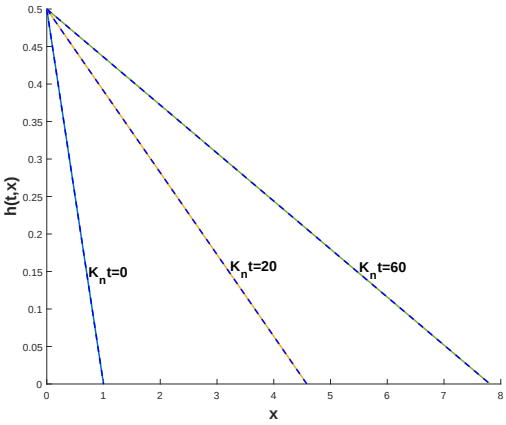


(c) n=3

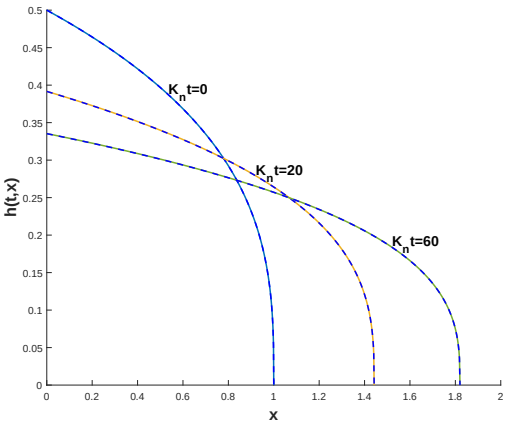
Figure 5.1: The half-width, (5.119), of a partially open fracture with $\beta = 0.5$, $\gamma = 1$ and $\alpha = \frac{1}{2(n+1)}$ plotted against x for increasing values of $K_n t$ and for a) $n = 0.5$, b) $n = 1$ and c) $n = 3$. Analytical solution (—) and numerical solution (- - -)



(a) n=0.5



(b) n=1



(c) n=3

Figure 5.2: The half-width, (5.130), of a partially open fracture with $\beta = 0.5$, $\gamma = 1$ and $\alpha = \frac{1}{(n+1)}$ plotted against x for increasing values of $K_n t$ and for a) $n = 0.5$, b) $n = 1$ and c) $n = 3$. Analytical solution (—) and numerical solution (- - -)

where r and p are constants to be determined [3, 20, 36]. Substituting (5.124) into the ordinary differential equation (5.76) results in

$$r^{n+1}p\Big[(n+1)p-1\Big](1-u)^{p(n+1)-2}-rp(1-u)^{p-1}$$
$$+r\left[p+1+\frac{1}{n}\left(\frac{1}{\alpha}-[n(1+\gamma)+2]\right)\right](1-u)^{p}=0. \tag{5.125}$$

The first two terms in (5.125) will vanish provided they have the same coefficients and exponent. That is

$$r^{n+1}p\Big[(n+1)p-1\Big](1-u)^{p(n+1)-2}-rp(1-u)^{p-1}=0. \tag{5.126}$$

This gives that

$$p=\frac{1}{n}\qquad\text{and}\quad r=n^{\frac{1}{n}}. \tag{5.127}$$

The solution (5.124) becomes

$$f(u)=n^{\frac{1}{n}}(1-u)^{\frac{1}{n}}, \tag{5.128}$$

provided the third term in (5.125) vanishes. This occurs when

$$\alpha=\frac{1}{\gamma n+1}. \tag{5.129}$$

We consider the analytical solution for $\alpha=\dfrac{1}{n+1}$ when $\gamma=1$. The half-width and the length of the model fracture respectively are

$$h(t,x)=\beta\left(1+\frac{(n+1)}{n}\beta^{n}K_{n}t\right)^{-\frac{1}{n}}\left(1-\frac{x}{L(t)}\right)^{\frac{1}{n}}, \tag{5.130}$$

$$L(t)=\left[1+\frac{(n+1)}{n}\beta^{n}K_{n}t\right]^{\frac{1}{(n+1)}}. \tag{5.131}$$

Differentiating (5.130) as $x\to L(t)$ gives the spatial gradient of the half-width

$$\frac{\partial h}{\partial x}=-\frac{\beta}{nL(t)}\left[1+\frac{(n+1)}{n}\beta^{n}K_{n}t\right]^{-\frac{1}{n}}\left(1-\frac{x}{L(t)}\right)^{\frac{1-n}{n}}, \tag{5.132}$$

and

$$\frac{\partial h}{\partial x}(t,L(t))=\begin{cases}-\infty, & n>1\\ -\frac{\beta}{L^{2}(t)}, & n=1,\\ 0, & 0<n<1.\end{cases} \tag{5.133}$$

The fluid flux at the fracture entry which generates the flow is

$$S(t)=Q(t,0)=A(1+Bt)^{m} \tag{5.134}$$

where

$$A = 2K_n\beta^{n+1}n^{\frac{1-2n}{n}}, \tag{5.135}$$

$$B = \frac{(n+1)}{n}\beta^n K_n, \tag{5.136}$$

$$m = -\frac{(n^2+n-1)}{n(n+1)}. \tag{5.137}$$

The analytical solutions for the half-width $h(t,x)$, (5.119) and (5.130), of a partially open fracture ($\beta = 0.5$) with parameter value $\gamma = 1$ is plotted against x for increasing values of the scaled time $K_n t$ in Figure 5.1 and Figure 5.2 respectively.

In Figure 5.1, the working condition $\alpha = \frac{1}{2(n+1)}$ is considered. The analytical solution results in a fracture that propagates with an increasing length and a decreasing half-width for a) $n = 0.5$, b) $n = 1$ and c) $n = 3$.

In Figure 5.2, the working condition $\alpha = \frac{1}{(n+1)}$ is considered. When $n = 0.5$, both the half-width of the fracture and the length of the fracture increase as time evolves. However, when $n = 1$, the half-width of the fracture remains constant at the fracture entry, $h(0,0) = \beta$, while the length increases with the scaled time, $K_n t$. Finally, we see that when $n = 3$, the half-width of the fracture decreases while the length of the fracture increases for increasing values of the scaled time $K_n t$.

It follows from (5.122) and (5.133) that for both analytical solutions when $n = 3$ then there is a singularity at the fracture tip. However when $0 < n < 3$, the singularity at the fracture tip is removed. These results agree with the result that tortuosity removes singularity at the fracture tip obtained by Kgatle and Mason [11].

From (5.105), (5.122) and (5.133), it is clear that the analytical solutions agree with the asymptotic solution in the epsilon (ϵ) neighbourhood of the fracture tip where ϵ is very small. We expect the asymptotic solution to also agree with the numerical solution in the ϵ-neighbourhood of the fracture tip.

5.7 Numerical solutions

In this section , we present and discuss a method of numerically solving the boundary value problem obtained in Section 5.3. Analytical solutions to the boundary value problem (5.84) to (5.87) with the two working conditions at the fracture entry which were obtained in section (5.6) will be used to test the numerical scheme used. The numerical solutions to the boundary value problem (5.84) to (5.87) with the remaining working conditions specified in section (5.5) will be investigated. Numerical solutions to the boundary value problem (5.84) to (5.87) which are obtained will be used to further investigate the half-width and the leak-off depth of the model fracture. A popular approach in literature has been to transform the boundary value problem into a pair of initial value problems [20, 37, 38]. This method was used to solve the Blasius boundary value problem. However, it can be verified that it is sufficient to transform the boundary value problem to one initial value problem using a scaling transformation in order to solve the problem. Solving the initial value problem is found be an easier approach equivalent to solving the boundary value problem.

5.7.1 A boundary value problem transformed into an initial value problem

Consider the boundary value problem, (5.84)-(5.87):

$$\frac{d}{du}\left(f^n\frac{df}{du}\right)+\frac{d}{du}\left(uf\right)+\frac{1}{n}\left(\frac{1}{\alpha}-\left[n(1+\gamma)+2\right]\right)f=0, \tag{5.138}$$

$$f(1)=0, \tag{5.139}$$

$$f^n(0)\frac{df}{du}(0)=-\frac{A}{2}\left(K_n\left(\frac{c_1}{c_4}\right)^{n+1}\right)^{\frac{1}{n}}, \tag{5.140}$$

where the consistency condition (5.87) gives

$$A=-2\left(\frac{1}{K_n}\left(\frac{c_4}{c_1}\right)^{n+1}\right)^{\frac{1}{n}}\left[\frac{1}{n}\left(\frac{1}{\alpha}-\left[n(1+\gamma)+2\right]\right)\int_0^1 f\,du+f^n(1)\frac{df}{du}(1)\right]. \tag{5.141}$$

At the fracture tip, the flux of fluid must vanish by the asymptotic solution,

$$f^n(1)\frac{df}{du}(1)=0. \tag{5.142}$$

The boundary value problem (5.138) to (5.140) is nonlinear and therefore not an easy problem to solve. We therefore consider a method previously used in solving nonlinear boundary value problems such as the Blasius boundary value problem. Particularly, we consider a method of transforming a boundary value problem into an initial value problem which is then solved using the backwards shooting method [20, 38]. It has been shown that solving the IVP is equivalent to solving the original the BVP.

Equation (5.138) is invariant under the scaling transformation

$$\bar{u}=\lambda^a u, \qquad \bar{f}=\lambda^b f \tag{5.143}$$

provided

$$b=\frac{2}{n}a. \tag{5.144}$$

Letting $a=1$, reduces (5.143) to

$$\bar{u}=\lambda u, \qquad \bar{f}=\lambda^{\frac{2}{n}} f. \tag{5.145}$$

Substituting the scaling transformation (5.145) into the ordinary differential equation (5.138) gives

$$\frac{d}{d\bar{u}}\left(\bar{f}^n\frac{d\bar{f}}{d\bar{u}}\right)+\frac{d}{d\bar{u}}\left(\bar{u}\bar{f}\right)+\frac{1}{n}\left(\frac{1}{\alpha}-\left[n(1+\gamma)+2\right]\right)\bar{f}=0, \tag{5.146}$$

where

$$0\le\bar{u}\le\lambda \quad \text{and} \quad \bar{f}(\lambda)=0. \tag{5.147}$$

We let

$$\bar{f}(0) = 1. \tag{5.148}$$

The scaling transformation (5.145) transforms equation (5.140) to

$$\frac{d\bar{f}}{d\bar{u}}(0) = \frac{1}{n}\left(\frac{1}{\alpha} - [n(1+\gamma)+2]\right)\int_0^{\lambda} \bar{f}(\bar{u})d\bar{u}. \tag{5.149}$$

Equation (5.148) gives that

$$f(0) = \lambda^{-\frac{2}{n}}. \tag{5.150}$$

The problem is to solve the initial value problem
Initial value problem I

$$\frac{d}{d\bar{u}}\left(\bar{f}^n\frac{d\bar{f}}{d\bar{u}}\right) + \frac{d}{d\bar{u}}\left(\bar{u}\bar{f}\right) + \frac{1}{n}\left(\frac{1}{\alpha} - \left[n(1+\gamma)+2\right]\right)\bar{f} = 0, \tag{5.151}$$

$$\bar{f}(0) = 1, \tag{5.152}$$

$$\frac{d\bar{f}}{d\bar{u}}(0) = \frac{1}{n}\left(\frac{1}{\alpha} - [n(1+\gamma)+2]\right)\int_0^{\lambda} \bar{f}(\bar{u})d\bar{u}, \tag{5.153}$$

where

$$\bar{f}(\lambda) = 0, \qquad 0 \le \bar{u} \le \lambda \tag{5.154}$$

The problem (5.151) to (5.153) is solved using the shooting method. If the problem is solved by shooting from $\lambda = 0$ to $\lambda = u$, it is not guaranteed that the root obtained (i.e. λ) will be correct as the scheme may overshoot or undershoot. We therefore consider solving the problem by shooting from the fracture tip $\bar{f}(\lambda)$ to the fracture entry $\bar{f}(0) = 1$.

An asymptotic solution for $\bar{f}(\bar{u})$ as $\bar{u} \to \lambda$ and its derivative $\frac{d\bar{f}}{d\bar{u}}(\bar{u})$ as $\bar{u} \to \lambda$ is used to derive an approximate value for $\bar{f}(\lambda)$ and $\frac{d\bar{f}}{d\bar{u}}(\lambda)$, with the value of lambda initially guessed and changed iteratively, by a bisection method, to give the correct value of lambda and therefore the solution $\bar{f}(\bar{u})$. The scaling transformation (5.145) is then used to obtain $f(u)$.

The asymptotic solution is obtained by applying the scaling transformation (5.145) to the asymptotic solution of $f(u)$ given by equation (5.99) to give

$$\bar{f}(\bar{u}) \sim \lambda^{\frac{1}{n}} n^{\frac{1}{n}} (\lambda - \bar{u})^{\frac{1}{n}}, \quad \text{as} \quad \bar{u} \to \lambda, \tag{5.155}$$

and therefore

$$\frac{d\bar{f}}{d\bar{u}}(\bar{u}) \sim -\lambda^{\frac{1}{n}} n^{\frac{1-n}{n}} (\lambda - \bar{u})^{\frac{1-n}{n}}, \quad \text{as} \quad \bar{u} \to \lambda. \tag{5.156}$$

The Initial Value Problem is solved using the built-in computer solver ode45 which uses the Runge-Kutta method of order 4 and 5 respectively on MATLAB while shooting backwards. The procedure can be outlined as follows:
Starting with an initial guess for λ which satisfies $\bar{f}(\lambda - \delta) = 0$, where $\bar{f}$ is the asymptotic

solution (5.155) and $\delta \ll 1$. The initial value of λ is used to solve the asymptotic solution and its derivative to obtain initial conditions. A backwards shooting method from $\bar{u} = \lambda - \delta$ to $\bar{u} = 0$ is used to obtain a solution $\bar{f}(\bar{u})$. A check is performed to see if the solution satisfies the condition $\bar{f}(0) = 1$ at an error tolerance of 10^{-3}. If this condition is satisfied we have a solution of $\bar{f}(\bar{u})$. If not, we then iteratively adjust and improve the value of λ using bisection method and shoot until the solution satisfies $\bar{f}(0) = 1$. The value of λ and the solution $\bar{f}(u)$ that satisfies the condition $\bar{f}(0)$=1 are then substituted into the scaling transformation (5.143) to obtain the numerical solution of $f(u)$.

In summary, the initial value problem (5.138) to (5.87) can be re-expressed as

$$\begin{aligned}
&\frac{d}{d\bar{u}}\left(\bar{f}^n \frac{d\bar{f}}{d\bar{u}}\right) + \frac{d}{d\bar{u}}\left(\bar{u}\bar{f}\right) + \frac{1}{n}\left(\frac{1}{\alpha} - \left[n(1+\gamma)+2\right]\right)\bar{f} = 0,\\
&\bar{f}(\lambda - \delta) \sim 0,\\
&\frac{d\bar{f}}{d\bar{u}}(\lambda - \delta) \sim (\lambda - \delta)^{\frac{1}{n}} n^{\frac{1-n}{n}} ((\lambda - \delta) - \bar{u})^{\frac{1-n}{n}},
\end{aligned}$$

where

$$f(0) = 1$$

is the target. The condition

$$f^n(0)\frac{df}{du}(0) = -\frac{A}{2}\left(K_n\left(\frac{c_1}{c_4}\right)^{n+1}\right)^{\frac{1}{n}},$$

with

$$A = -2\left(\frac{1}{K_n}\left(\frac{c_4}{c_1}\right)^{n+1}\right)^{\frac{1}{n}}\left[\frac{1}{n}\left(\frac{1}{\alpha} - \left[n(1+\gamma)+2\right]\right)\int_0^1 f\,du\right], \tag{5.157}$$

is identically satisfied. The functions $\bar{f}(\lambda)$ and $\frac{d\bar{f}}{d\bar{u}}(\lambda)$ are given by the asymptotic solution. Once the value of λ and the solution of $\bar{f}(\bar{u})$ is obtained, the solution $f(u)$ is determined using the transformation (5.145).

Accuracy of the numerical solution, $f(u)$, is verified using the analytical solutions corresponding to the working conditions, $\alpha = \frac{1}{2(n+1)}$ and $\alpha = \frac{1}{n+1}$ when $\gamma = 1$ and $\beta = 0.5$. The initial value problem is solved numerically using the analytical solutions of the two working conditions. The results obtained are compared to the results obtained from solving the boundary value problem analytically. The numerical solutions corresponding to the working conditions $\alpha = \frac{1}{2(n+1)}$ and $\alpha = \frac{1}{n+1}$ are plotted on the same set of axis with the analytical solution of the half-width corresponding to the same working conditions for $n = 0.5$, 1 and 3. In Figure 5.1 and 5.2, the half-width of a partially open fracture ($\beta = 0.5$) is plotted against x for increasing values of the scaled time $K_n t$ and with $\gamma = 1$ and for $n = 0.5$, 1 and 3. It is found that the analytical solution represented by solid lines (—) and the numerical solution represented by dashed lines (- - -) overlap thus verifying the accuracy of the obtained numerical solution. This reiterates that solving the initial value problem is equivalent to solving the boundary value problem directly.

In the next subsection we will investigate the numerical solutions corresponding to the constant pressure, constant speed of propagation, constant rate of fluid injection and the constant rate of leak-off working conditions. The properties of the fracture will be illustrated graphically.

5.7.2 Graphical results

Firstly, we established that the half-width of the fracture is given by

$$h(t,u) = \frac{\beta}{f_{max}}\left(1+\frac{1}{\alpha}\left(\frac{\beta}{f_{max}}\right)^n K_n t\right)^{\frac{2}{n}\left(\alpha-\frac{1}{2}\right)} f(u). \tag{5.158}$$

We find that $u_{max} = 0$ so that $f_{max} = f(0)$, and the half-width becomes

$$h(t,x) = \frac{\beta}{f(0)}\left(1+\frac{1}{\alpha}\left(\frac{\beta}{f(0)}\right)^n K_n t\right)^{\frac{2}{n}\left(\alpha-\frac{1}{2}\right)} f(u). \tag{5.159}$$

The leak-off depth measured as the distance from the half-width to the fluid-rock interface can be obtained by integrating the leak-off velocity (5.89)

$$v_\ell(t,x) = \gamma K_n\left(\frac{\beta}{f(0)}\right)^{(n+1)}\left(1+\frac{1}{\alpha}\left(\frac{\beta}{f(0)}\right)^n K_n t\right)^{\frac{2}{n}\left(\alpha-\frac{(n+1)}{2}\right)} f(u), \tag{5.160}$$

with respect to a similarity variable τ and evaluating the result from 0 to t. Based on the exponent of $v_\ell(t,x)$ two cases of the leak-off depth can be obtained i.e. when $\alpha = 1/2$ and $\alpha \neq 1/2$.

The length of the fracture is given by

$$L(t) = \left(1+\frac{1}{\alpha}\left(\frac{\beta}{f(0)}\right)^n K_n t\right)^{\alpha}. \tag{5.161}$$

Lastly, the volume of the fracture and the width-averaged fluid velocity were obtained to be

$$V(t) = V_0\left(1+\frac{1}{\alpha}\left(\frac{\beta}{f(0)}\right)^n K_n t\right)^{\frac{n+2}{n}\left(\alpha-\frac{1}{n+2}\right)}, \tag{5.162}$$

where

$$V_0 = 2\left(\frac{\beta}{f(0)}\right)\int_0^1 f(u)du \tag{5.163}$$

and

$$\bar{v}_x(t,u) = -K_n\left(\frac{\beta}{f(0)}\right)^n\left(1+\frac{1}{\alpha}\left(\frac{\beta}{f(0)}\right)^n K_n t\right)^{\alpha-1} f^{n-1}(u)\frac{df}{du}. \tag{5.164}$$

The fluid flux at the fracture entry is

$$S(t) = A(1+Bt)^m \tag{5.165}$$

where

$$A = -2K_n\left(\frac{\beta}{f(0)}\right)^{n+1} f^n(0)\frac{df}{du}(0), \tag{5.166}$$

$$B = \frac{1}{\alpha}\left(\frac{\beta}{f(0)}\right)^n K_n, \tag{5.167}$$

$$m = \frac{n+2}{n}\left(\alpha-\frac{n+1}{n+2}\right). \tag{5.168}$$

Following (5.160), the leak-off depth is derived to be

$$b(t,x) = \begin{cases} \alpha\gamma\left(\dfrac{\beta}{f(0)}\right)\ln\left(1+\dfrac{1}{\alpha}\left(\dfrac{\beta}{f(0)}\right)^{n}K_n t\right)f(u), & \alpha = 1/2, \quad (5.169) \\ \dfrac{\alpha\gamma n}{2\left(\alpha-\frac{1}{2}\right)}\left(\dfrac{\beta}{f(0)}\right)\left(1+\dfrac{1}{\alpha}\left(\dfrac{\beta}{f(0)}\right)^{n}K_n t\right)^{\frac{2}{n}\left(\alpha-\frac{1}{2}\right)} f(u), & \alpha \neq 1/2. \quad (5.170) \end{cases}$$

We will now investigate the numerical solutions for the various working condition. We first consider the constant pressure condition.

5.7.3 Constant pressure $\left(\alpha = \frac{1}{2}\right)$

When $\alpha = 1/2$ a constant pressure working condition is applied at the fracture entry. Following (5.169), the leak-off depth is

$$b(t,x) = \frac{\gamma}{2}\left(\frac{\beta}{f(0)}\right)\ln\left(1+\frac{1}{\alpha}\left(\frac{\beta}{f(0)}\right)^{n}K_n t\right)f(u). \quad (5.171)$$

From equation (5.159), the half-width of the fracture at the entry becomes

$$h(t,0) = \beta, \quad (5.172)$$

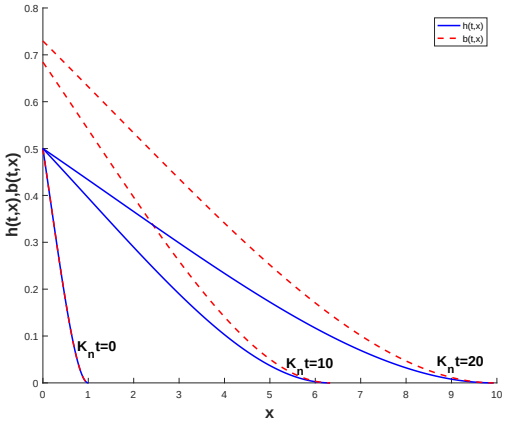
for all scaled time $K_n t$. This means that for all time, a partially open fracture will have the same constant half-width β at the fracture entry.

The half-width of the fracture, $h(t,x)$, given by (5.172), is plotted on the same set of axis as the corresponding leak-off depth, $b(t,x)$, given by (5.171), measured from the half-width.

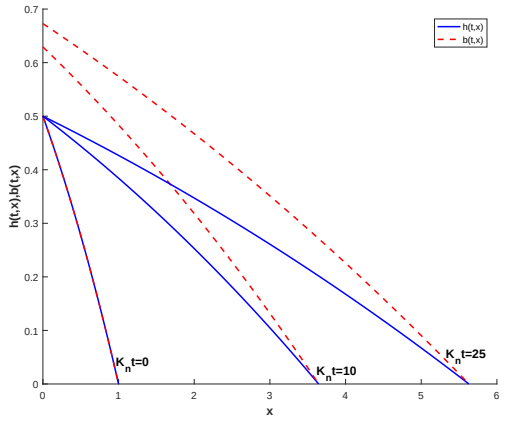
Figure 5.3 shows how the half-width and the leak-off depth evolve over time. The half-width and the leak-off depth of a partially open and pre-existing fracture model with $\beta = 0.5$ and and leak-off coefficient $\gamma = 0.2$ are plotted against x for $\alpha = 1/2$ and for $n = 0.5$, 1 and 3. As the scaled time $K_n t$ increases, the half-width of the fracture at the entry remains constant and the length of the fracture is increasing. This means that although the half-width of the fracture at the entry remains constant for all time, the fracture is propagating in the positive x-direction for all three values of n. Initially, at $K_n t = 0$, there is no fluid leak-off. However, as the scaled time $K_n t$ increases leak-off begins to occur. The amount of leak-off increases with time. This working condition tells us that if the requirement is a "long" fracture, the desirable working condition required at the fracture entry is that of constant pressure during fluid injection.

The maximum amount of leak-off , $b(t,x)$, occurs at the fracture entry as the half-width, $h(t,x)$, is at its highest. The amount of leak-off increases steadily with time and decreases along the fracture length until it vanishes at the fracture tip. We expect that leak-off also reduces the extent of propagation of a fracture at any given time as the amount of fluid that would be required to advance propagation is lost to the surrounding areas due to permeability of the encasing rock mass.

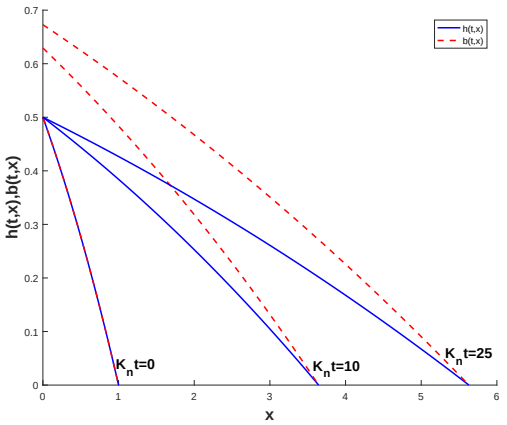
We will now investigate the constant speed of propagation, $\alpha = 1$, constant rate of fluid injection, $\alpha = \frac{n+1}{n+2}$, and the constant rate of leak-off, $\alpha = \frac{n+1}{2}$, working conditions as given in Table 5.1. The constant volume working condition will not be investigated. This working condition occurs when there is no flux at the entry and no leak-off i.e. $\gamma = 0$, however



(a) n=0.5

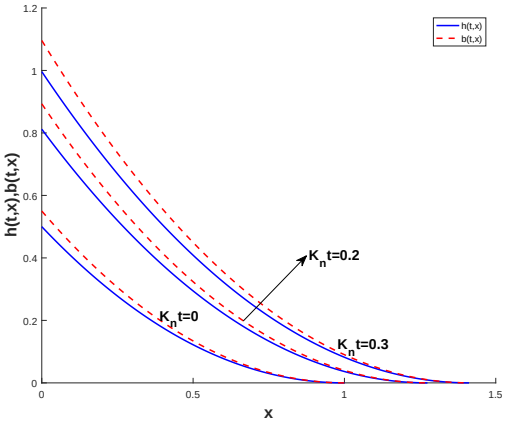


(b) n=1

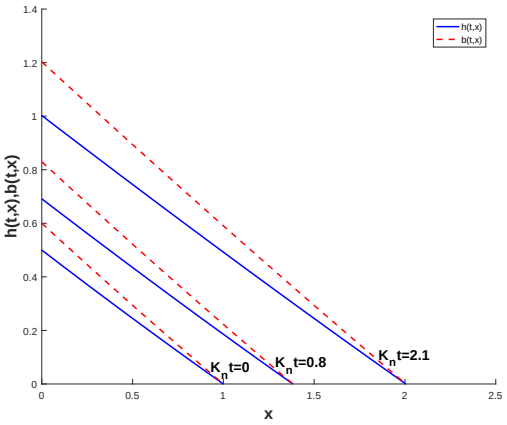


(c) n=3

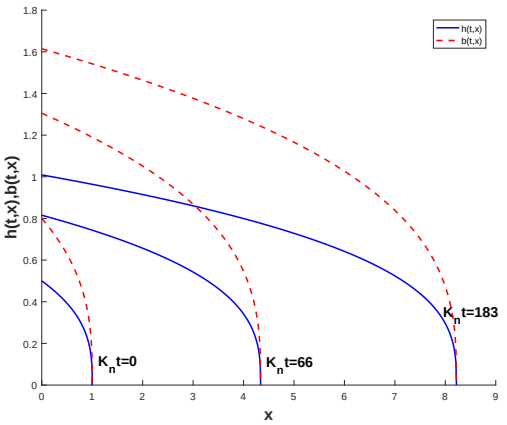
Figure 5.3: The numerical solution of the half-width, (5.172) and the leak-off depth, (5.171), of a partially open fracture ($\beta = 0.5$) and $\gamma = 0.2$ plotted against x for increasing values of the scaled time $K_n t$ for $\alpha = 1/2$ and for a) $n = 0.5$, b) $n = 1$ and c) $n = 3$.



(a) n=0.5



(b) n=1



(c) n=3

Figure 5.4: The numerical solution of the half-width, (5.158) and the leak-off depth, (5.173), of a partially open fracture ($\beta = 0.5$) and $\gamma = 0.2$ plotted against x for increasing values of the scaled time $K_n t$ for $\alpha = 1$ and for a) $n = 0.5$, b) $n = 1$ and c) $n = 3$.

resulting in a propagating fracture [11]. When $\gamma > 0$, a constant volume solution means that the flux of fluid into the fracture equals the rate of leak-off at the fluid-rock interface resulting in a non-propagating fracture. In this work, we only consider propagating fractures with $\gamma > 0$. Here the leak-off depth is given by (5.170)

$$b(t,x) = \frac{\alpha\gamma n}{2\left(\alpha-\frac{1}{2}\right)}\left(\frac{\beta}{f(0)}\right)\left(1+\frac{1}{\alpha}\left(\frac{\beta}{f(0)}\right)^{n} K_n t\right)^{\frac{2}{n}\left(\alpha-\frac{1}{2}\right)} f(u). \tag{5.173}$$

and the half-width is expected to change with time, so we use (5.159) as given.

5.7.4 Constant speed of propagation ($\alpha = 1$)

The solution for a fracture propagating with constant speed is illustrated in Figure 5.4. The half-width and leak-off depth of a partially open fracture with parameter values $\beta = 0.5$ and $\gamma = 0.2$ are plotted against x for $n = 0.5$, 1 and 3. The half-width and the length of the fracture are both steadily increasing as the scaled time, $K_n t$, increases. In this case, there is initially leak-off at $K_n t = 0$ and the amount of leak-off continues to increase with the scaled time $K_n t$. The maximum amount of leak-off occurs at the fracture entry where the half-width is also at its maximum.

5.7.5 Constant rate of fluid injection at the fracture entry $\left(\alpha = \frac{n+1}{n+2}\right)$

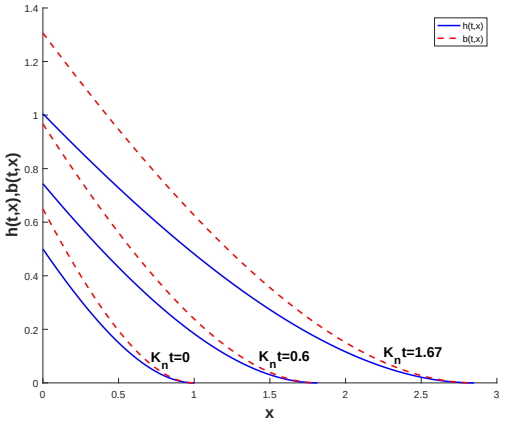
In Figure 5.5, the half-width and leak-off depth of a partially open fracture with parameter values $\beta = 0.5$ and $\gamma = 0.2$ are plotted against x for $n = 0.5$, 1 and 3. The length and half-width of the fracture are both growing, however the length appears to propagate at a much faster rate when compared to the half-width. The amount of leak-off also increases more steadily from $K_n t = 0$ to larger time scales. The working condition for constant speed of injection at the fracture entry increases the rate at which the length of the fracture propagates.

5.7.6 Constant rate of fluid leak-off at the fluid-rock interface $\left(\alpha = \frac{n+1}{2}\right)$

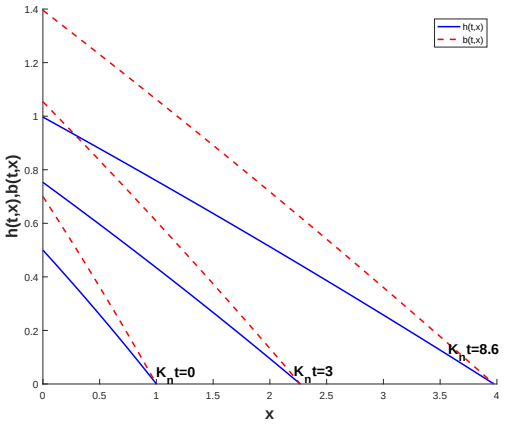
The working condition for a constant rate of fluid leak-off at the fluid-rock interface can be obtained from the leak-off velocity equation. This means that the rate at which fluid is leaving the fracture at the fluid-rock interface is constant everywhere along the fracture. In Figure 5.6, the leak-off depth increases as the scaled time $K_n t$ increases. As expected, we obtain that both the half-width of the fracture and the length of the fracture increases with the scaled time $K_n t$ thus representing a fracture that propagates. The maximum leak-off occurs at the fracture entry.

5.7.7 Length of the fracture

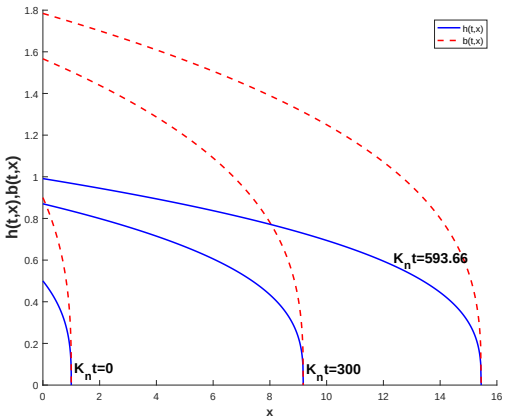
In this section we investigate the length of the fracture, (5.161), for different working conditions. The length of the partially open fracture, given by equation (5.161) with parameter values $\beta = 0.5$ are plotted against the scaled time $K_n t$ for different values of n. From Figure 5.7, for the numerical working conditions (iii)-(vii) we obtain that when $n = 0.5$, the constant speed of propagation working condition results in a longer fracture over time



(a) n=0.5

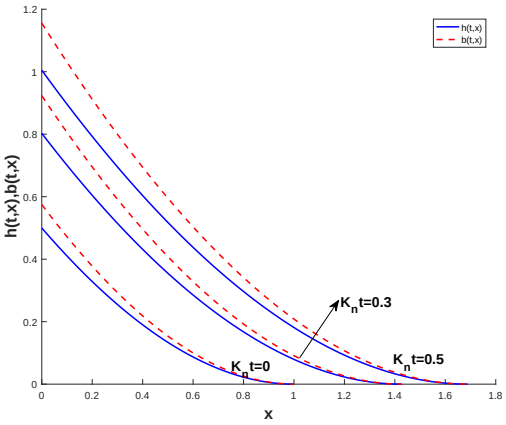


(b) n=1

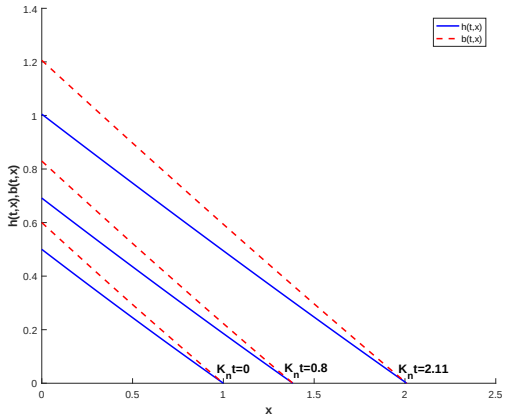


(c) n=3

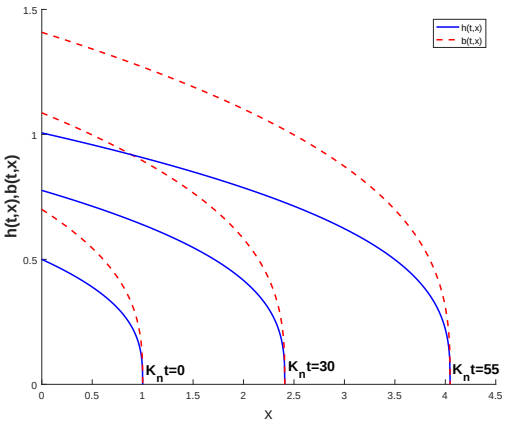
Figure 5.5: The numerical solution of the half-width, (5.158) and the leak-off depth, (5.173), of a partially open fracture ($\beta = 0.5$) and $\gamma = 0.2$ plotted against x for increasing values of the scaled time $K_n t$ for $\alpha = (n+1)/(n+2)$ and for a) $n = 0.5$, b) $n = 1$ and c) $n = 3$.



(a) n=0.5



(b) n=1



(c) n=3

Figure 5.6: The numerical solution of the half-width, (5.158) and the leak-off depth, (5.173), of a partially open fracture ($\beta = 0.5$) and $\gamma = 0.2$ plotted against x for increasing values of the scaled time $K_n t$ for $\alpha = (n+1)/2$ and for a) $n = 0.5$, b) $n = 1$ and c) $n = 3$.

and when $n = 1$ the constant pressure working condition is responsible for yielding a longer fracture. The constant rate of leak-off results in the longest fracture as the fracture becomes less tortuous at $n = 3$. The results agree with results for a tortuous fracture with no leak-off [11]. Thus giving the conclusion that tortuous fractures lead to longer fractures.

5.8 Width-averaged fluid velocity

In this section, we investigate the width-averaged fluid velocity, $\bar{v}_x(t,x)$, along the fracture, $0 \le x \le L(t)$. From equation (5.92), the width-averaged fluid velocity is given by

$$\bar{v}_x(t,u) = -K_n\left(\frac{\beta}{f_{max}}\right)^n\left(1+\frac{1}{\alpha}\left(\frac{\beta}{f_{max}}\right)^n K_n t\right)^{\alpha-1} f^{n-1}(u)\frac{df}{du}, \tag{5.174}$$

and the length of the fracture from (5.90) is

$$L(t) = \left(1+\frac{1}{\alpha}\left(\frac{\beta}{f_{max}}\right)^n K_n t\right)^{\alpha}. \tag{5.175}$$

We consider the fluid velocity ratio obtained from dividing the width-averaged fluid velocity (5.174), by the speed at which the fracture propagates, obtained by differentiating (5.175) with respect to time:

$$\frac{dL}{dt} = K_n\left(\frac{\beta}{f_{max}}\right)^n\left(1+\frac{1}{\alpha}\left(\frac{\beta}{f_{max}}\right)^n K_n t\right)^{\alpha-1}. \tag{5.176}$$

Therefore the velocity ratio is

$$\frac{\bar{v}_x}{(dL/dt)} = -f^{n-1}(u)\frac{df}{du}, \qquad 0 \le u \le 1. \tag{5.177}$$

The velocity ratio was investigated by Fareo [36] for a power law fluid driven fracture in permeable rock and Kgatle [20] for a tortuous model fracture with no leak-off. We can derive analytical expressions for the velocity ratio, (5.177), corresponding to the two analytical solutions of $f(u)$ obtained in section (5.6) for the working conditions $\alpha = 1/2(n+1)$ and $\alpha = 1/(n+1)$.

For the working condition $\alpha = 1/2(n+1)$, the exact analytical solution of $f(u)$ is given by (5.118), the derivative corresponding to (5.118) is

$$\frac{df}{du} = -\left(\frac{n}{2}\right)^{\frac{1-n}{n}}\left(1-u^2\right)^{\frac{1-n}{n}} u. \tag{5.178}$$

Substituting (5.118) and (5.178) into (5.177) gives that the velocity ratio corresponding to this working condition $\alpha = \frac{1}{2(n+1)}$,

$$\frac{\bar{v}_x}{(dL/dt)} = u, \qquad 0 \le u \le 1. \tag{5.179}$$

The velocity ratio vanishes at the entry and it increases linearly along the fracture.

For the working condition $\alpha = 1/(n+1)$, the corresponding analytical solution of $f(u)$ is given by (5.128), and the corresponding derivative is

$$\frac{df}{du} = -n^{\frac{1-n}{n}}(1-u)^{\frac{1-n}{n}}. \tag{5.180}$$

Substituting (5.128) and (5.180) into (5.177) gives that the velocity ration corresponding to the working condition $\alpha = \frac{1}{(n+1)}$ is

$$\frac{\bar{v}_x}{(dL/dt)} = 1, \qquad 0 \le u \le 1. \tag{5.181}$$

The velocity ratio is constant as the width-averaged fluid velocity equals the speed of propagation along the fracture. For the remaining working conditions which can be numerically investigated, the velocity ratio (5.177) is used to analyse the width-averaged fluid velocity in the model fracture.

Figure 5.8 shows the velocity ratio curves along the fracture length for all working conditions. For the analytical working conditions $\alpha = 1/2(n+1)$ and $\alpha = 1/(n+1)$ the velocity ratios (5.179) and (5.181) the velocity ratio curves are straight lines. The numerical solutions for the remaining working conditions yield approximately linear velocity ratio curves.

These result leads to the investigation of an approximate analytical solution in section 5.9.

5.9 Approximate analytical solutions

From the velocity ratios obtained in section 5.8 given by equations (5.179) and (5.181) we see that the velocity ratio curves resulting from the analytical solutions are straight lines. The curves for the numerical solutions for the remaining working conditions are approximately linear as shown in Figure 5.8. As a result we make the approximation that the velocity ratio curves are exactly straight lines for all the working conditions. This method was introduced by Fareo [36] to investigate an approximate analytical solution for modeling a pre-existing power-law driven fracture in permeable rock. Kgatle [20] also applied this method as the velocity ratio curves obtained for a tortuous linear hydraulic fracture in impermeable rock were approximately linear .

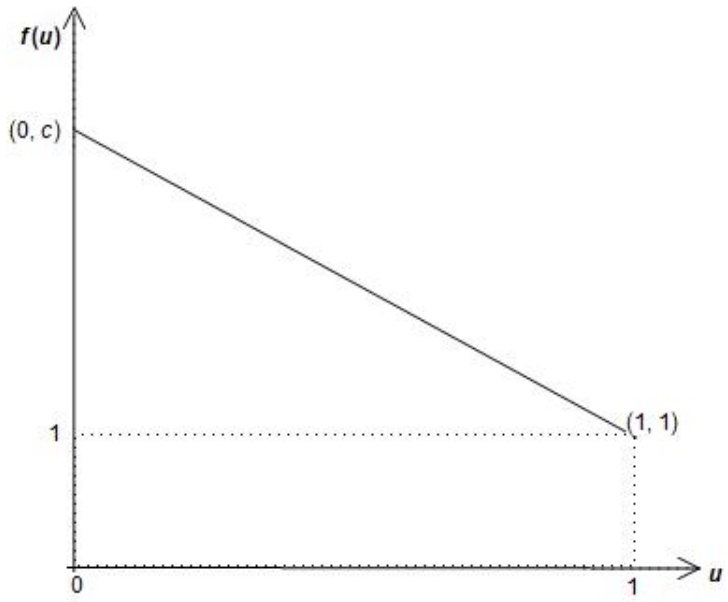
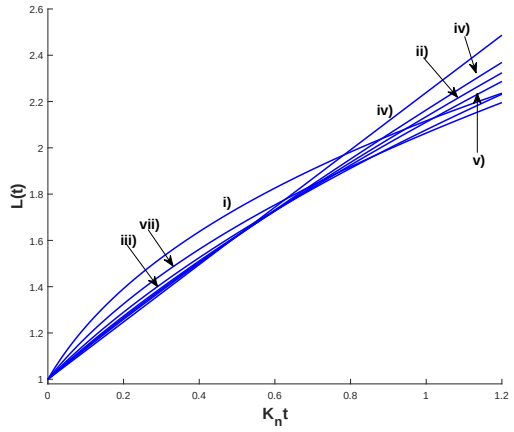
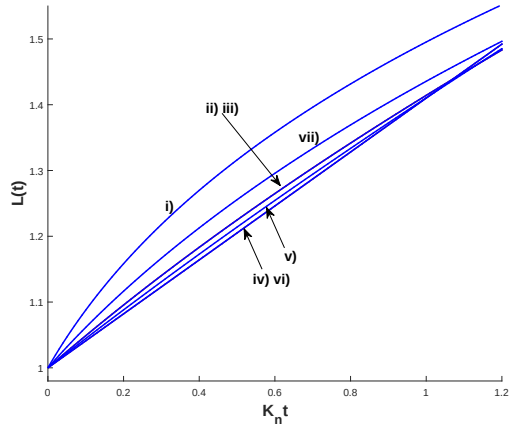


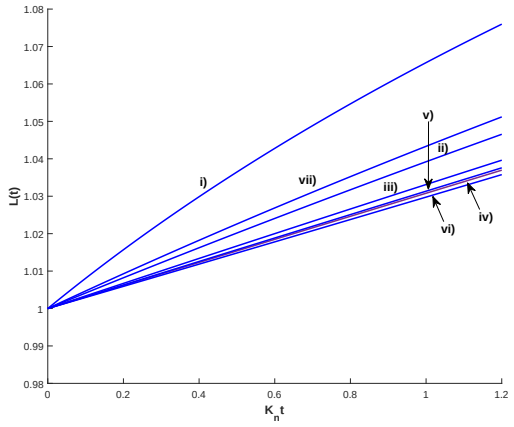
Figure 5.9: The straight line joining the points $(0,c)$ and $(1,1)$ which approximates the fluid velocity ratio curves



(a) n=0.5

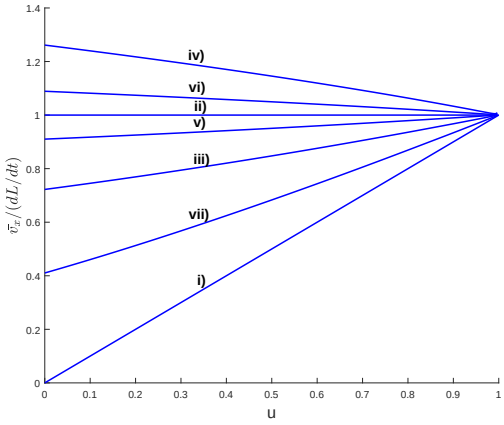


(b) n=1

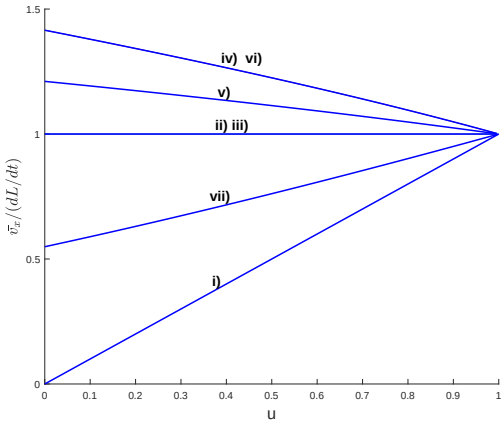


(c) n=3

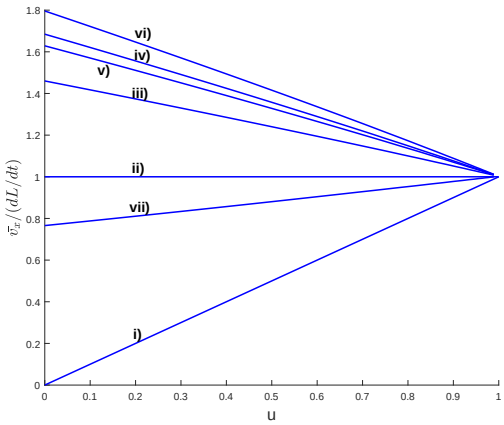
Figure 5.7: The length, (5.161), of a partially open fracture ($\beta = 0.5$) and $\gamma = 0.2$ is plotted against the scaled time $K_n t$ for the working conditions i) $\alpha = \frac{1}{2(n+1)}$, ii) $\alpha = \frac{1}{n+1}$, iii) $\alpha = \frac{1}{2}$, iv) $\alpha = 1$, v) $\alpha = \frac{n+1}{n+2}$, vi) $\alpha = \frac{n+1}{2}$ and vii) $\alpha = \frac{1}{n+2}$ and for a) $n = 0.5$, b) $n = 1$ and c) $n = 3$.



(a) n=0.5



(b) n=1



(c) n=3

Figure 5.8: The velocity ratios, $\frac{\bar{v}_x}{(dL/dt)}$, of a partially open fracture ($\beta = 0.5$) and with $\gamma = 0.2$ plotted against u with parameter values for the working conditions i) $\alpha = \frac{1}{2(n+1)}$, ii) $\alpha = \frac{1}{n+1}$, iii) $\alpha = \frac{1}{2}$, iv) $\alpha = 1$, v) $\alpha = \frac{n+1}{n+2}$, vi) $\alpha = \frac{n+1}{2}$ and vii) $\alpha = \frac{1}{n+2}$ and for a) $n = 0.5$, b) $n = 1$ and c) $n = 3$.

We approximate the curves joining the points $(0,c)$ and $(1,1)$ by a straight line curve of the form

$$\frac{\bar{v}_x}{(dL/dt)} = mu + c, \tag{5.182}$$

where c is the $\frac{\bar{v}_x}{(dL/dt)}$ intercept and the gradient m is $(1-c)$:

$$\frac{\bar{v}_x}{(dL/dt)} = (1-c)u + c. \tag{5.183}$$

Using (5.174), it follows that

$$-f^{n-1}\frac{df}{du} = (1-c)u + c \tag{5.184}$$

Integrating (5.184) subject to the boundary condition $f(1) = 0$ yields the approximate analytical solution

$$f(u) = \left[n\left(\frac{1+c}{2}\right)\left[1+\left(\frac{1-c}{1+c}\right)u\right](1-u)\right]^{\frac{1}{n}}. \tag{5.185}$$

The constant c can be obtained by reading it off the $\frac{\bar{v}_x}{(dL/dt)}$ intercept. However, an analytical expression for c which is independent of the numerical solution can be obtained.

To obtain the value of c, we substitute the approximate analytical solution $f(u)$, (5.185), into the consistency condition (5.87). The RHS of (5.87) gives

$$f^n(0)\frac{df}{du}(0) = -c\left(\frac{n(1+c)}{2}\right)^{\frac{1}{n}}. \tag{5.186}$$

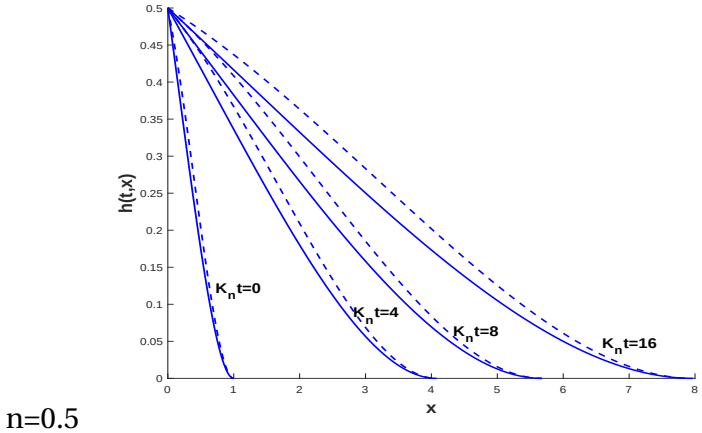
Substituting $f(u)$, (5.185), into the LHS of (5.87) and simplifying the results by making a binomial expansion of $f(u)$ in powers of $\frac{1-c}{1+c}$ and considering zero order terms gives

$$\frac{1}{n}\left(\frac{1}{\alpha} - [n(\gamma+1)+2]\right)\int_0^1 f(u)du = \left(\frac{1}{n+1}\right)\left(\frac{n(1+c)}{2}\right)^{\frac{1}{n}}\left(\frac{1}{\alpha} - [n(\gamma+1)+2]\right). \tag{5.187}$$

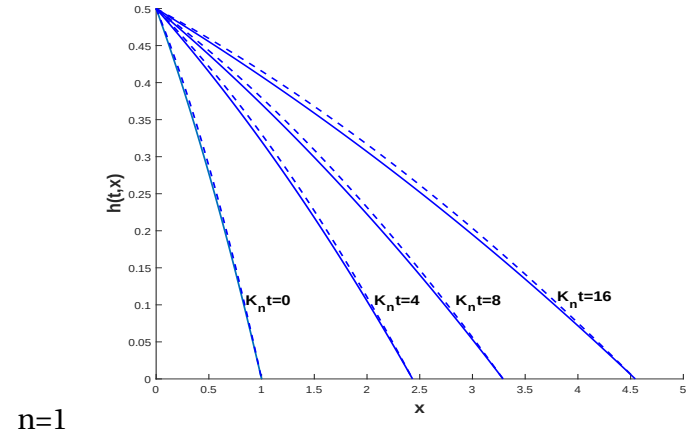
Equating the LHS and the RHS of (5.87) with the aid of equations (5.186) and (5.187) gives the analytical expression for the $\frac{\bar{v}_x}{(dL/dt)}$ intercept

$$c = -\frac{1}{n+1}\left(\frac{1}{\alpha} - [n(1+\gamma)+2]\right). \tag{5.188}$$

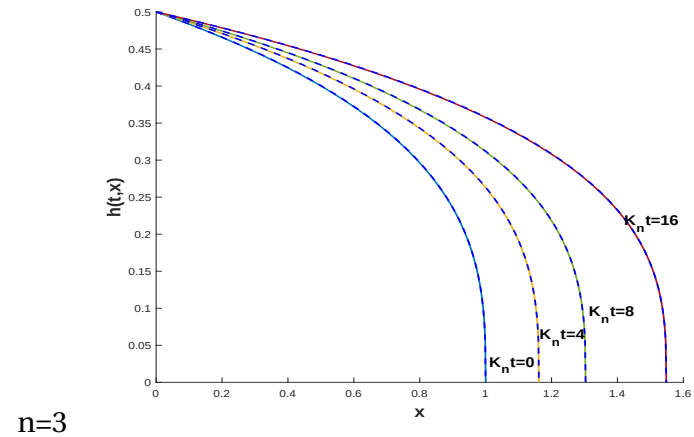
Figure 5.10 gives a comparison of the approximate analytical solution derived from the width-averaged fluid velocity represented by the solid line (—) and the numerical solution represented by the dashed line (−−) for the half-width of a partially open fracture ($\beta = 0.5$) for the constant pressure working condition $\alpha = 1/2$. The solution is a bad approximation for very tortuous fractures i.e. $n = 0.5$ but as the fracture becomes less tortuous the approximate analytical solution is found to be in agreement with the numerical solution making the solution $f(u)$ given by equation (5.185) a good enough choice to use to obtain solutions of the problem.



n=0.5



n=1



n=3

Figure 5.10: A comparison of the approximate analytical solution and the numerical solution of the half-width of the fracture for a partially open fracture ($\beta = 0.5$) and $\gamma = 0.2$ for the constant pressure working condition $\alpha = 1/2$ and for a) $n = 0.5$, b) $n = 1$, and c) $n = 3$. Analytical solution (—) and numerical solution (- - -)

5.10 Comparisons between leak-off and no leak-off

In this section, a comparison of the results obtained for a linear hydraulic fracture with tortuosity propagating in impermeable [11] and permeable rock is done. We consider working conditions that are common to both cases, namely constant pressure, constant speed of propagation and constant rate of fluid injection at the fracture entry. The total volume of the fracture and the length of the fracture will be compared for a model with leak-off and a model without leak-off.

The volume of the fracture is given by equation (5.93) and (5.94)

$$V(t) = V_0\left(1 + \frac{1}{\alpha}\left(\frac{\beta}{f_{max}}\right)^n K_n t\right)^{\frac{n+2}{n}\left(\alpha - \frac{1}{n+2}\right)}, \tag{5.189}$$

where

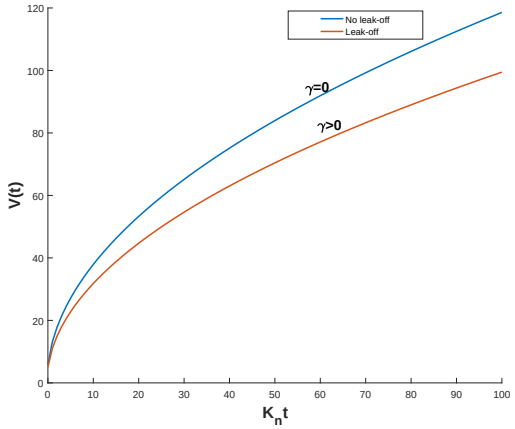
$$V_0 = 2\left(\frac{\beta}{f_{max}}\right)\int_0^1 f(u)\,du, \tag{5.190}$$

and the length of the fracture is given by (5.161):

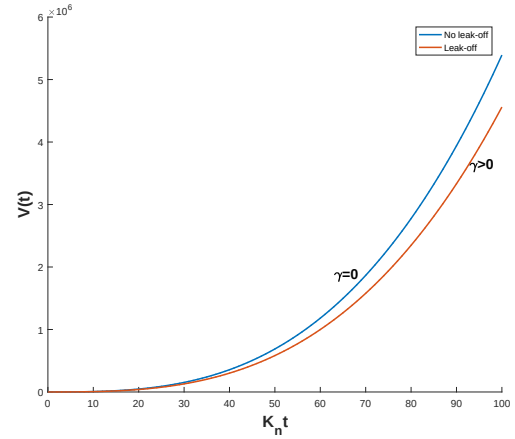
$$L(t) = \left(1 + \frac{1}{\alpha}\left(\frac{\beta}{f_{max}}\right)^n K_n t\right)^{\alpha}. \tag{5.191}$$

In Figure 5.11, the volume of a partially open fracture (5.189)-(5.190) is plotted against increasing values of the scaled time $K_n t$ for a fracture without leak-off ($\gamma = 0$) and a fracture with leak-off ($\gamma > 0$) for $n = 0.5$. We obtain that the volume increases as the scaled time $K_n t$ increases. When the working condition is $\alpha = 1/2$ and $n = 0.5$, the exponent in (5.189) is a between 0 and 1, making the volume a power function. As the scaled time increases, the volume increases but tends to curve towards the x-axis as shown by Figure 5.11a. When $\alpha = 1$, the volume of the fracture increases as the scaled time increases. However, it tends to increase exponentially. Finally, when $\alpha = \frac{n+1}{n+2}$, the volume of the fracture increases linearly as the scaled time increases as shown in Figure 5.11c. These results show that volume of the fracture is more when there is no leak-off when compared to the case of fluid leak-off at the fluid-rock interface for the three working conditions. This is due to the fact that at the fluid-rock interface, some of the injected fluid (which would otherwise be available to advance a fracture in an impermeable fracture) is lost to the surrounding rock mass encasing the fracture in a permeable medium.

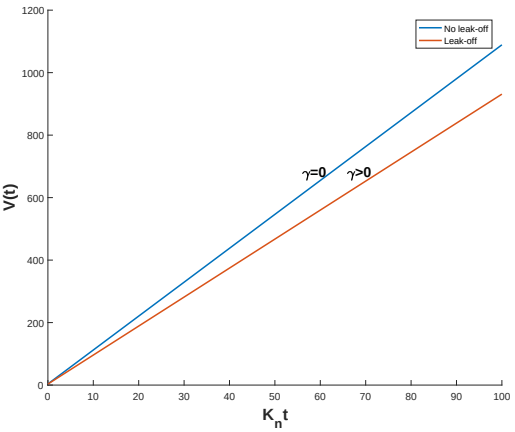
Figure 5.12, shows the length of a partially open fracture, (5.191), plotted against the scaled time $K_n t$ for a fracture propagating in impermeable rock without leak-off ($\gamma = 0$) and a fracture propagating in permeable rock with fluid leak-off ($\gamma > 0$) for the working conditions a) constant pressure, b) constant speed of propagation and c) the constant rate of fluid injection at the fracture entry and for the $n = 0.5$. In Figure 5.12a, the working condition considered is $\alpha = 1/2$. The length of the fracture is increasing as the scaled time $K_n t$ increases. Since the length is raised to the power α, it becomes a power function and the exponent is $1/2$. When $\alpha = 1$, the length of the fracture is plotted in Figure 5.12b. As a result of this working condition, the length is increasing linearly as the scaled time increases. When $\alpha = \frac{n+1}{n+2}$ and $n = 0.5$, the value of the exponent in (5.191) is 0.6 making it identical to Figure 5.12a. We can easily see that the length of the fracture is less when



(a) $\alpha = 1/2$

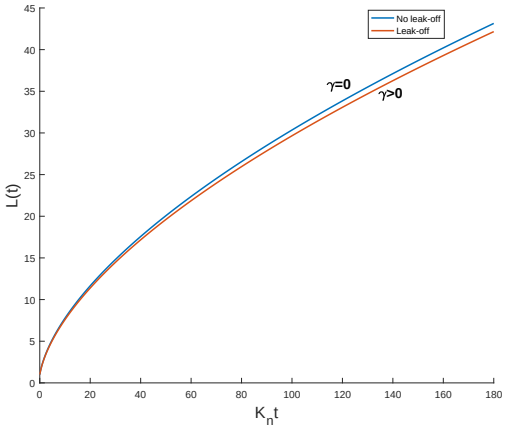


(b) $\alpha = 1$

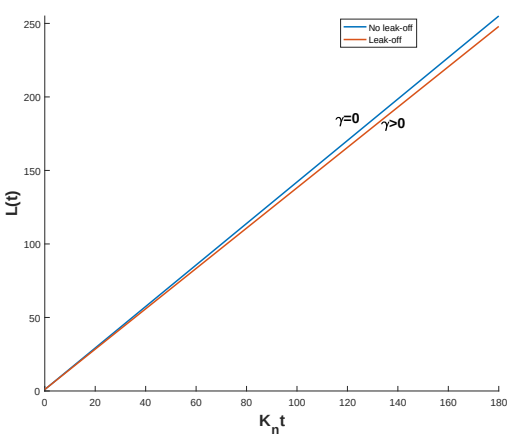


(c) $\alpha = (n+1)/(n+2)$

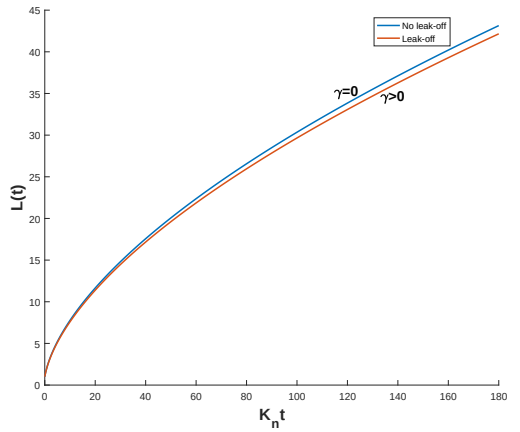
Figure 5.11: The volume, (5.189), without leak-off ($\gamma = 0$) and with leak-off ($\gamma > 0$) of a partially open fracture ($\beta = 0.5$) is plotted against $K_n t$ and $n = 0.5$ for the working conditions a) $\alpha = 1/2$, b) $\alpha = 1$ and c) $\alpha = (n+1)/(n+2)$.



(a) $\alpha = 1/2$



(b) $\alpha = 1$



(c) $\alpha = (n+1)/(n+2)$

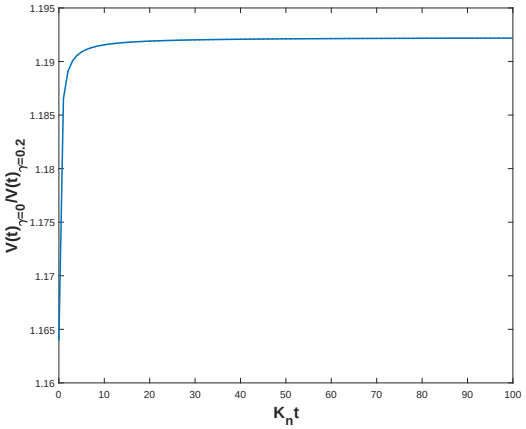
Figure 5.12: The length, (5.161), without leak-off ($\gamma = 0$) and with leak-off ($\gamma > 0$) of a partially open fracture ($\beta = 0.5$) is plotted against $K_n t$ for $n = 0.5$ for the working conditions a) $\alpha = 1/2$, b) $\alpha = 1$ and c) $\alpha = (n+1)/(n+2)$.

there is fluid leak-off, however the difference is not great. Therefore although fluid leak-off results in a fracture with a shorter length, the fracture will continue to propagate for all the specified working conditions.

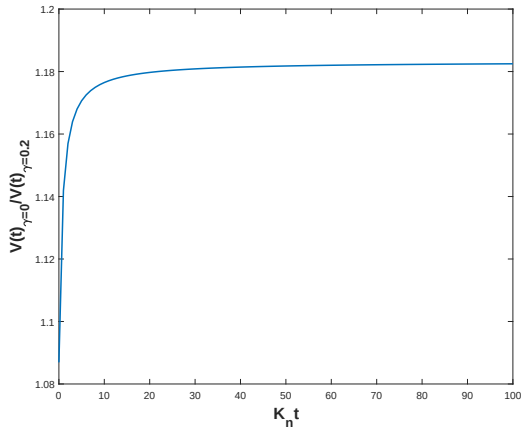
The volume ratio is equal to

$$\frac{V_{\gamma=0}}{V_{\gamma>0}},$$

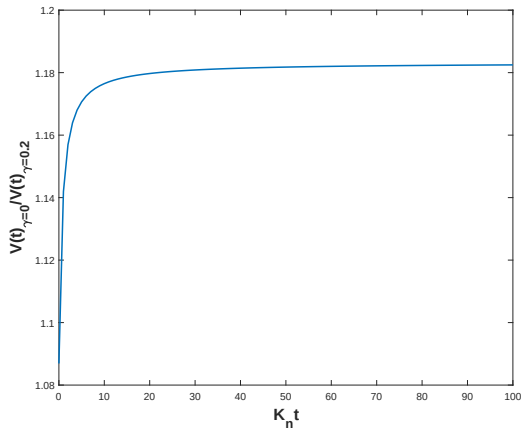
where $V_{\gamma=0}$ is the volume of a fracture with no leak-off, $V_{\gamma>0}$ is the volume of a fracture with leak-off and γ is the leak-off coefficient. In Figure 5.13, a rapid change of the volume occurs within the first ten units of the scaled time $K_n t$ for a tortuous fracture. In Figure 5.14, the ratio of volumes shows that the change of volume occurs gradually over time for fractures with little to no tortuosity.



(a) $\alpha = 1/2$

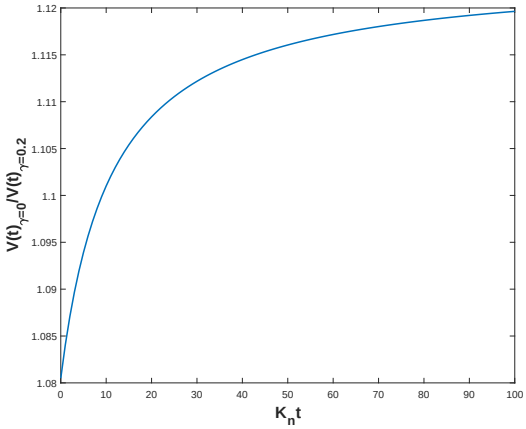


(b) $\alpha = 1$

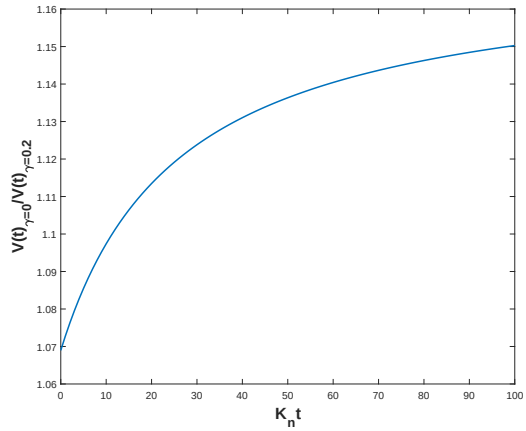


(c) $\alpha = (n+1)/(n+2)$

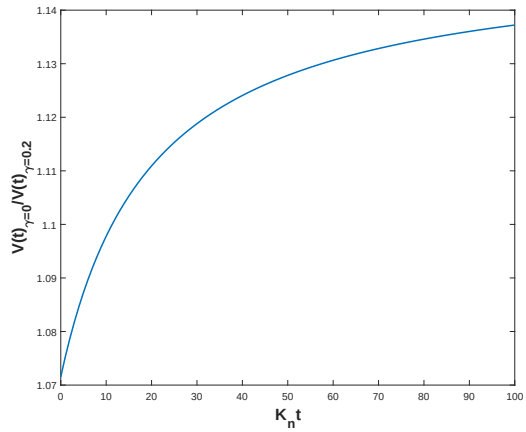
Figure 5.13: The ratio of volumes, (**??**), of a partially open fracture ($\beta = 0.5$) with leak-off ($\gamma > 0$) and without leak-off ($\gamma = 0$) is plotted against the scaled time $K_n t$ for for $n = 0.5$ using the working conditions a) $\alpha = 1/2$, b) $\alpha = 1$, and c) $\alpha = \frac{n+1}{n+2}$.



(a) $\alpha = 1/2$



(b) $\alpha = 1$



(c) $\alpha = (n+1)/(n+2)$

Figure 5.14: The ratio of volumes, (**??**), of a partially open fracture ($\beta = 0.5$) with leak-off ($\gamma > 0$) and without leak-off ($\gamma = 0$) is plotted against the scaled time $K_n t$ for for $n = 3$ using the working conditions a) $\alpha = 1/2$, b) $\alpha = 1$, and c) $\alpha = \frac{n+1}{n+2}$.

Chapter 6

Case II: Group invariant solution for $c_2 = c_4 = 0$ - Traveling Wave Solution

6.1 Introduction

In this chapter, we consider the governing nonlinear equation (2.60) when the parameter values c_2 and c_4 in the Lie point symmetry of (2.60) obtained in Appendix (A) vanish (i.e. $c_2 = c_4 = 0$). The resulting group invariant solution of the problem is a traveling wave solution which will be analysed to gain insight on the various properties of a linear hydraulic fracture propagating in permeable rock.

6.2 Group invariant solution

We derive the group invariant solution corresponding to the Lie point symmetry generator of the non-linear diffusion equation (2.60) when the constants c_2 and c_4 are zero.

The Lie point symmetry generator the derivation of which is outlined in Appendix (A) is

$$X = (c_1 + c_2 t)\frac{\partial}{\partial t} + (c_3 + c_4 x)\frac{\partial}{\partial x} + \frac{1}{n}(2c_4 - c_2)h\frac{\partial}{\partial h} \tag{6.1}$$

where c_1, c_2, c_3, c_4 are constants, provided the leak-off velocity, $v_\ell(t,x)$, satisfies the first order linear partial differential equation

$$(c_1 + c_2 t)\frac{\partial v_\ell}{\partial t} + (c_3 + c_4 x)\frac{\partial v_\ell}{\partial x} = \frac{1}{n}(2c_4 - (n+1)c_2)v_\ell. \tag{6.2}$$

We consider $c_2 = 0$ and $c_4 = 0$. Therefore Equations (6.1) and (6.2) respectively become

$$X = c_1\frac{\partial}{\partial t} + c_3\frac{\partial}{\partial x}, \tag{6.3}$$

and

$$c_1\frac{\partial v_\ell}{\partial t} + c_3\frac{\partial v_\ell}{\partial x} = 0. \tag{6.4}$$

The group invariant solution of the fracture half-width, $h(t,x)$ of the PDE (2.60), is obtained by solving the characteristic equation

$$X\Big(h(t,x)-\Phi(t,x)\Big)\Big|_{h=\Phi}=0, \tag{6.5}$$

where $h(t,x)=\Phi(t,x)$. This results in the first order partial differential equation

$$c_1\frac{\partial\Phi}{\partial t}+c_3\frac{\partial\Phi}{\partial x}=0. \tag{6.6}$$

The characteristic curves corresponding to the differential equation are

$$\frac{dt}{c_1}=\frac{dx}{c_3}=\frac{d\Phi}{0}. \tag{6.7}$$

The first differential equation gives

$$I_1=x-\frac{c_3}{c_1}t, \tag{6.8}$$

where I_1 is a constant. The last term in (6.7) gives

$$I_2=\Phi(t,x), \tag{6.9}$$

where I_2 is a constant. The general solution for the PDE (6.6) is $I_2=F(I_1)$, where F is an arbitrary function. With the aid of (6.8) and (6.9) the group invariant solution of the half-width of the model fracture is

$$h(t,x)=F(\xi), \tag{6.10}$$

where

$$\xi=x-\frac{c_3}{c_1}t. \tag{6.11}$$

is the similarity variable.

Now, the group invariant solution of the leak-off velocity, $v_\ell(t,x)$, at the fluid rock interface can be derived by setting c_2 and c_4 to zero in equation (6.2):

$$c_1\frac{\partial v_\ell}{\partial t}+c_3\frac{\partial v_\ell}{\partial x}=0, \tag{6.12}$$

and solving the first order PDE. The characteristic curves corresponding to the differential equation (6.12) are

$$\frac{dt}{c_1}=\frac{dx}{c_3}=\frac{dv_\ell}{0}. \tag{6.13}$$

The first differential equation and the last term give

$$I_3=x-\frac{c_3}{c_1}t, \tag{6.14}$$

and

$$I_4 = v_\ell(t,x), \tag{6.15}$$

where I_3 and I_4 are constants. The general solution of the PDE (6.12) is $I_4 = G(I_3)$ where G is an arbitrary function. It follows from (6.14) and (6.15) that the group invariant solution of the leak-off velocity is

$$v_\ell(t,x) = G(\xi), \tag{6.16}$$

where the similarity variable, ξ, is given by (6.11).

Substituting the group invariant solution of the half-width (6.10) and leak-off velocity (6.16) into the non-linear diffusion equation (2.60) transforms the PDE to an ODE

$$K_n \frac{d}{d\xi}\left(F^n(\xi)\frac{dF}{d\xi}\right) + \frac{c_3}{c_1}\frac{dF}{d\xi} - G(\xi) = 0. \tag{6.17}$$

We now consider the boundary conditions for the nonlinear diffusion equation (2.60). At the fracture tip $h(t, L(t)) = 0$, results in

$$F(Y(t)) = 0, \tag{6.18}$$

where

$$Y(t) = L(t) - \frac{c_3}{c_1}t. \tag{6.19}$$

Differentiating (6.18) with respect to t gives

$$\frac{dF}{dY}\frac{dY}{dt} = 0. \tag{6.20}$$

Since $\frac{dF}{dY} \neq 0$ it follows that $\frac{dY}{dt} = 0$ and $Y(t) = k$, where k is a constant. We choose the characteristic length of the fracture to be the initial length of the fracture such that in dimensionless variables the initial length of the fracture is $L(0) = 1$. It follows that the length of the fracture is

$$L(t) = 1 + \frac{c_3}{c_1}t. \tag{6.21}$$

Therefore the boundary condition at the fracture tip given by (6.18) is reduced to

$$F(1) = 0. \tag{6.22}$$

It was found in Chapter 5 that for fluid leak-off $f_{max} = F(0)$. It is found in this chapter that $x_{max} = 0$ and $h^*(0,0) = \beta$ therefore

$$F(0) = \beta. \tag{6.23}$$

The following properties, expressed in terms of the group invariant solution of both half-width and the leak-off velocity, are obtained: The volume flux of fluid in the fracture

$$Q(t,x) = -2K_n F^n(\xi)\frac{dF}{d\xi}. \tag{6.24}$$

At the fracture entry, $x = 0$ and for $t = 0$ the volume flux of fluid becomes

$$Q(0,0) = -2K_n F^n(0)\frac{dF}{d\xi}(0) = A, \tag{6.25}$$

where A is a constant. Equation (6.25) can be re-expressed as

$$F^n(0)\frac{dF}{d\xi}(0) = -\frac{A}{2K_n}. \tag{6.26}$$

The value of A would be obtained from the consistency condition (2.53). The flux of fluid flowing out of the fracture,

$$q(t) = 2\int_{-\frac{c_3}{c_1}t}^{1} G(\xi)d\xi, \tag{6.27}$$

the volume of the fracture,

$$V(t) = 2\int_{-\frac{c_3}{c_1}t}^{1} F(\xi)d\xi, \tag{6.28}$$

and the width-averaged fluid velocity,

$$\bar{v}_x(t,x) = -K_n F^{n-1}(\xi)\frac{dF}{d\xi}. \tag{6.29}$$

6.3 Leak-off velocity proportional to the half-width of the fracture

We assume that there exists a proportional relationship between the leak-off arbitrary function, $G(\xi)$, and the half-width arbitrary function, $F(\xi)$, such that

$$G(\xi) = \gamma F(\xi) \tag{6.30}$$

where γ is the leak-off coefficient. In this work we consider the case $\gamma > 0$. This transformation is applied on the related properties and the results are summarized below: The problem is to solve

$$K_n\frac{d}{d\xi}\left(F^n(\xi)\frac{dF}{d\xi}\right) + \frac{c_3}{c_1}\frac{dF}{d\xi} - \gamma F(\xi) = 0, \tag{6.31}$$

subject to

$$F(1) = 0, \tag{6.32}$$

$$F(0) = \beta \tag{6.33}$$

and

$$h(t,x) = F(\xi), \tag{6.34}$$

$$v_\ell(t,x) = \gamma F(\xi), \tag{6.35}$$

$$L(t) = 1 + \frac{c_3}{c_1} t, \tag{6.36}$$

$$Q(t,x) = -2K_n F^n(\xi) \frac{dF}{d\xi}, \tag{6.37}$$

$$q(t) = 2\int_{-\frac{c_3}{c_1}t}^{1} \gamma F(\xi) d\xi, \tag{6.38}$$

$$V(t) = 2\int_{-\frac{c_3}{c_1}t}^{1} F(\xi) d\xi, \tag{6.39}$$

$$\bar{v}_x = -K_n F^{n-1} \frac{dF}{d\xi}. \tag{6.40}$$

The consistency condition is

$$-2K_n F^n\left(-\frac{c_3}{c_1}t\right)\frac{dF}{d\xi}\left(-\frac{c_3}{c_1}t\right) = 2\frac{d}{dt}\int_{-\frac{c_3}{c_1}t}^{1} F(\xi)d\xi + 2\gamma\int_{-\frac{c_3}{c_1}t}^{1} F(\xi)d\xi - 2K_n F^n(1)\frac{dF}{d\xi}(1), \tag{6.41}$$

which can be obtained with the aid of (6.11) and (6.36) by substituting (6.37) and (6.38) into equation (2.53).The flux at the entry at time t is not of the form

$$S(t) = A(1+Bt)^m \tag{6.42}$$

as in Chapter (5). It is given by (6.37) after the problem has been solved.

We will now proceed to investigate an asymptotic solution of the ODE.

6.4 Asymptotic Solution

In this section we seek to investigate the asymptotic behavior of the ODE (6.31). We can approximate the behavior of $F(\xi)$ as $\xi \to 1$ by an asymptotic solution. We investigate a solution of the form

$$F(\xi) \sim a(1-\xi)^s, \quad \text{as} \qquad \xi \to 1 \tag{6.43}$$

where a and s are constants that need to be determined. Substituting (6.43) into the ODE (6.31) gives

$$a^{n+1}K_n\Big(s^2(n+1)-s\Big)\Big(1-\xi\Big)^{s(n+1)-2} - as\left(\frac{c_3}{c_1}\right)\Big(1-\xi\Big)^{s-1} - \gamma a\Big(1-\xi\Big)^s = 0, \qquad \text{as} \quad \xi \to 1. \tag{6.44}$$

By balancing the exponents of the first and second terms we find that

$$s = \frac{1}{n}. \tag{6.45}$$

Balancing coefficients of the first and second terms gives

$$a = \left(\frac{c_3 n}{c_1 K_n}\right)^{\frac{1}{n}}. \tag{6.46}$$

The third term vanishes as $\xi \to 1$. Therefore the asymptotic solution is

$$F(\xi) \sim \left(\frac{c_3 n}{c_1 K_n}\right)^{\frac{1}{n}} \left(1-\xi\right)^{\frac{1}{n}}, \quad \text{as} \quad \xi \to 1. \tag{6.47}$$

The derivative corresponding to this asymptotic solution is

$$\frac{dF}{d\xi} \sim -\left(\frac{c_3 n}{c_1 K_n}\right)^{\frac{1}{n}} \left(1-\xi\right)^{\frac{1-n}{n}}, \quad \text{as} \quad \xi \to 1, \tag{6.48}$$

and therefore

$$F^n(\xi)\frac{dF}{d\xi}(\xi) \sim -\frac{1}{n}\left(\frac{c_3 n}{c_1 K_n}\right)^{\frac{n+1}{n}} (1-\xi)^{\frac{1}{n}} \quad \text{as} \quad \xi \to 1. \tag{6.49}$$

The fluid flux is therefore zero at the fracture tip, $\xi = 1$,

$$F^n(1)\frac{dF}{d\xi}(1) = 0. \tag{6.50}$$

6.5 Numerical solutions

We investigate the existence of a numerical solution for a traveling wave solution. Again we use a backwards shooting method to shoot for a solution from the fracture tip to the fracture entry as fully outlined in Section 5.7. In this case, we make a guess for the ratio $\frac{c_3}{c_1}$ and apply the bisection method to iterate until we obtain a value of α that satisfies the half-width of the fracture at the entry

$$h(0,0) = \beta. \tag{6.51}$$

The boundary value problem to solve is

$$K_n \frac{d}{d\xi}\left(F^n(\xi)\frac{dF}{d\xi}\right) + \frac{c_3}{c_1}\frac{dF}{d\xi} - \gamma F(\xi) = 0, \tag{6.52}$$

subject to the boundary conditions

$$F(1) = 0, \tag{6.53}$$
$$F(0) = \beta. \tag{6.54}$$

It is not necessary to transform the problem into an initial value problem using a scaling transformation as it can solved directly. The value of the diffusion constant K_n is obtained from experimental results [4]. It has been obtained that when $n = 3$, $a_n = 1$ which gives that the diffusion constant given by equation (2.61) is $K_n = 1/3$. We will however use this value of $K_n = 1/3$ to obtain numerical results for all values of n.

The traveling wave solution is solved in two parts since the problem is a moving boundary problem in the domain $\xi \in \left(-\frac{c_3}{c_1}t, 1\right)$.

Part I: Obtaining the ratio $\frac{c_3}{c_1}$ at $t = 0$
An initial guess of the ratio $\frac{c_3}{c_1}$ is made and substituted into the problem. The solution is solved from the fracture tip to the fracture entry. The asymptotic solution (6.47) and its derivative (6.48) evaluated in the epsilon neighbourhood of the fracture tip are used as initial conditions. We then use the backwards shooting method to shoot from the close proximity of the tip, $1-\delta$, where $\delta \ll 1$, to the fracture entry using the initial value of $\frac{c_3}{c_1}$. We then check if obtained solution satisfies the initial condition $F(0) = \beta$ for time $t = 0$. If this condition is not satisfied, we use the bisection algorithm to iterate the value of the ratio $\frac{c_3}{c_1}$ until such a ratio $\frac{c_3}{c_1}$ that satisfies the condition (6.54) is obtained. The solution $F(\xi)$ that satisfies the condition (6.54) is the numerical solution of the problem at $t = 0$.

Part II: A solution for $t > 0$
The domain which was used to solve Case I was independent of time. Since this is a traveling wave solution the domain is time dependent and for $t > 0$ the problem needs to be re-solved.

For subsequent times, $t > 0$, we re-solve the problem using the value of $\frac{c_3}{c_1}$ obtained from part I. The initial value problem is solved once by the shooting method to get a solution $F(\xi)$ that is valid for all time greater than zero.

6.6 Results

Using the shooting method we obtain the ratio $\frac{c_3}{c_1}$ corresponding to each value of n. The following values of the ratio $\frac{c_3}{c_1}$ are obtained for each corresponding value of n:

Value of n	ratio $\frac{c_3}{c_1}$
$n = 0.5$	0.5446
$n = 1$	0.2022
$n = 3$	0.0526

Table 6.1: Parameter values $\frac{c_3}{c_1}$ for various values of n and $\beta = 0.75$ in the traveling wave solution.

In Figure 6.1, the half-width of the fracture is plotted against x for a partially open fracture with the parameter values $\beta = 0.75$, $\gamma = 0.2$, $K_n = 1/3$ and for a) $n = 0.5$, b) $n = 1$ and c) $n = 3$ and the corresponding values of the ratio $\frac{c_3}{c_1}$ given in Table 6.1. The half-width of the fracture and the length of the fracture are both increasing as time t increases. However, the half-width of the fracture increases faster than the length. For increasing times, the shape of the half-width of the fracture of a traveling wave solution is preserved as the fracture propagates.

6.6.1 The length of the fracture

In Figure 6.2, the length of the fracture given by (6.36)

$$L(t) = 1 + \frac{c_3}{c_1} t$$

is plotted against time for parameter values $\beta = 0.75$, $\gamma = 0.2$, $K_n = 1/3$ and for the working conditions corresponding to the n value. The fracture is longer for $n = 0.5$ and this length decreases as as n increases. We see that as the fracture becomes less tortuous, i.e $n > 1$, the fracture propagates much slower for increasing time t.

6.7 Width-averaged fluid velocity

Following the analysis done in Section 5.8, we investigate the width-averaged fluid velocity, $\bar{v}_x(t,x)$, along the fracture corresponding to a traveling wave solution. We consider the velocity ratio defined as the ratio of the width-averaged fluid velocity and the speed of propagation of the fracture dL/dt.

The width-average fluid velocity given by (6.40) is

$$\bar{v}_x = -K_n F^{n-1} \frac{dF}{d\xi}, \tag{6.55}$$

and differentiating the length (6.36) with respect to time gives a constant value

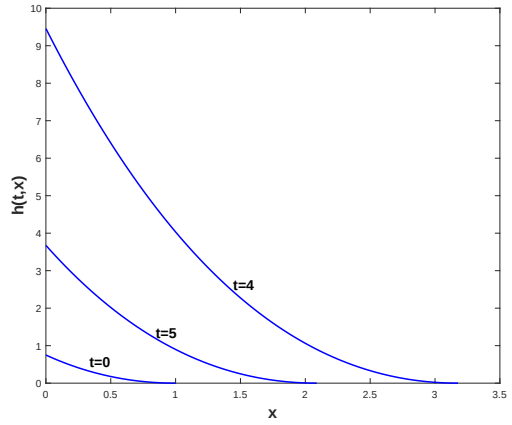
$$\frac{dL}{dt} = \frac{c_3}{c_1}. \tag{6.56}$$

This implies that the speed of propagation of the fracture is constant. Therefore the working condition for the traveling wave solution is constant speed. From (6.55) and (6.56) the fluid velocity ratio is

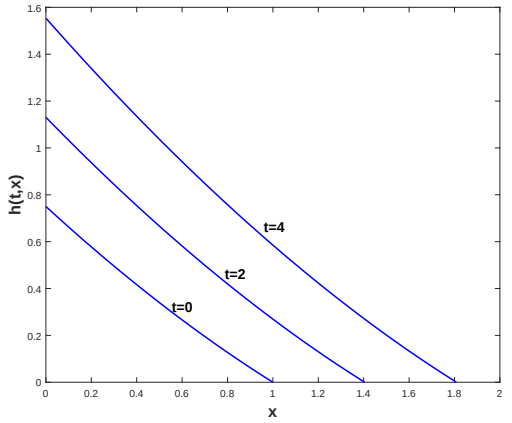
$$\frac{\bar{v}_x}{(dL/dt)} = -\left(\frac{c_1 K_n}{c_3}\right) F^{n-1} \frac{dF}{d\xi}. \tag{6.57}$$

In Figure 6.3, the velocity ratio is plotted against ξ for the parameter values $\beta = 0.75$, $\gamma = 0.2$, $K_n = 1/3$ and for a) $n = 0.5$, b) $n = 1$ and c) $n = 3$ using the corresponding values of the ratio $\frac{c_3}{c_1}$ as listed in Table 6.1 for time $t = 0$. We obtain that the velocity ratio plots are approximately straight lines for time $t = 0$.

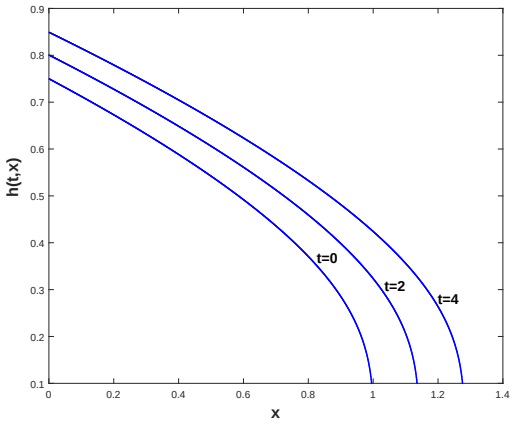
Since the velocity ratio plots are approximately straight lines, it is clear that a linear approximation of the velocity ratio curves may lead to the derivation of the approximate analytical solution. It is expected that the approximate analytical solution will give good approximations that are close to the numerical solution as the velocity ratio curves are approximately linear. The approximate analytical solution can be a useful approximation for the half-width of the fracture when the analytical solution is not attainable and when the numerical solutions are difficult to produce and a readily available solution is required.



(a) n=0.5

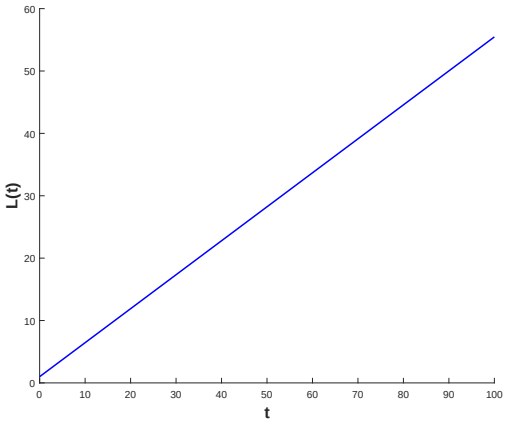


(b) n=1

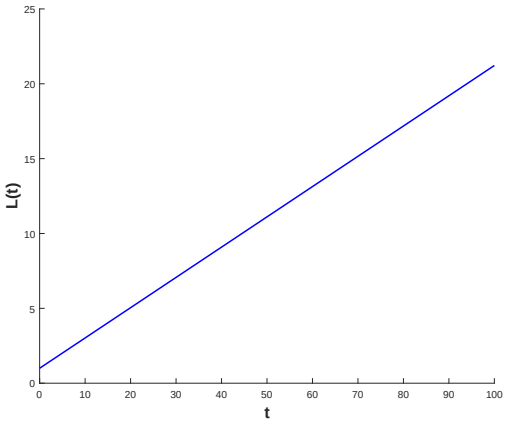


(c) n=3

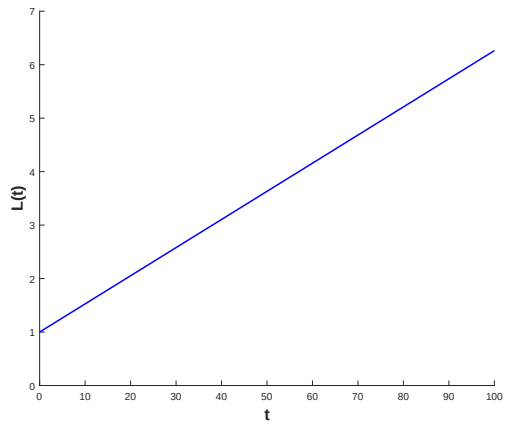
Figure 6.1: The half-width, 6.34 , is plotted against x for different values of time t for $\beta = 0.75$, $\gamma = 0.2$ and $K_n = 1/3$ for values of $\frac{c_3}{c_1}$ given in Table 6.1 for a) $n = 0.5$, b) $n = 1$ and c) $n = 3$.



(a) n=0.5

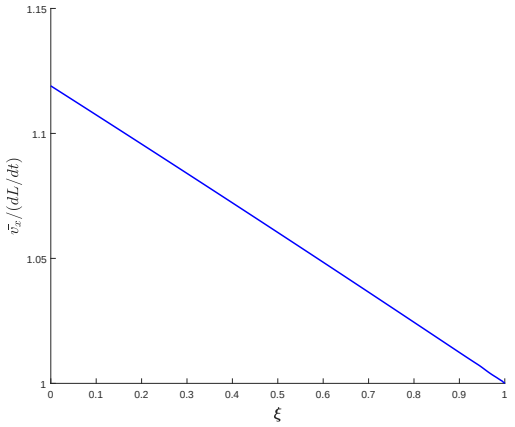


(b) n=1

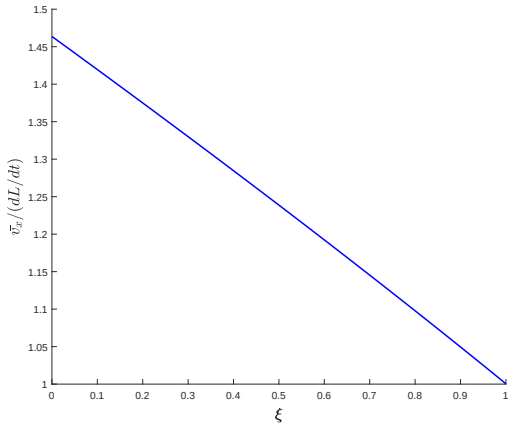


(c) n=3

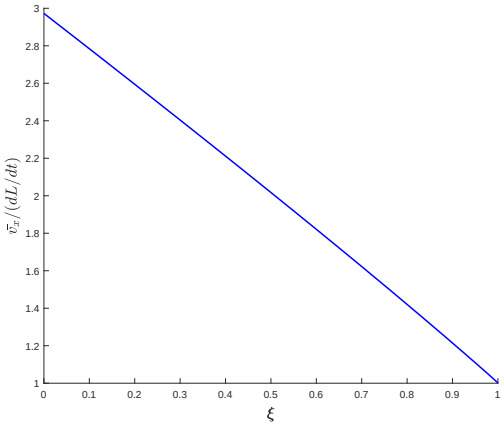
Figure 6.2: The length, 6.36 , is plotted against time t, for $\beta = 0.75$, $\gamma = 0.2$ and $K_n = 1/3$ for values of $\frac{c_3}{c_1}$ given in Table 6.1 for a) n=0.5, b) n=1 and c) n=3



(a) n=0.5



(b) n=1



(c) n=3

Figure 6.3: The fluid velocity ratio for a traveling wave solution is plotted against ξ at time $t = 0$ with parameter values $\beta = 0.75$, $\gamma = 0.2$ and $K_n = 1/3$, for values of the ratio $\frac{c_3}{c_1}$ given in Table 6.1 and for a) $n = 0.5$, b) $n = 1$ and c) $n = 3$.

Chapter 7

Case III: Group invariant solution for $c_2 = 0$, $c_4 \neq 0$ - Exponential solution

7.1 Introduction

In this Chapter, we investigate a group invariant solution that exists when the constant $c_2 = 0$ in the Lie point symmetry generator obtained in Appendix A. In Section 7.2, the group invariant solution corresponding to the Lie point symmetry is derived where we later let $c_3 = 0$. A proportional relationship between the half-width of the fracture and the leak-off velocity is considered in Section 7.3. In Section 7.4, an asymptotic solution is derived which will be used to investigate numerical solutions in Section 7.5.

7.2 Group Invariant solution

In Appendix A, the Lie point symmetry generator of the PDE (5.1) was derived to be

$$X = (c_1 + c_2 t)\frac{\partial}{\partial t} + (c_3 + c_4 x)\frac{\partial}{\partial x} + \frac{1}{n}(2c_4 - c_2)h\frac{\partial}{\partial h}, \tag{7.1}$$

where c_1, c_2, c_3 and c_4 are constants, provided the leak-off velocity, $v_\ell(t,x)$, satisfies the first order linear partial differential equation

$$(c_1 + c_2 t)\frac{\partial v_\ell}{\partial t} + (c_3 + c_4 x)\frac{\partial v_\ell}{\partial x} = \frac{1}{n}(2c_4 - (n+1)c_2)v_\ell. \tag{7.2}$$

Consider the case where $c_2 = 0$, the Lie point symmetry generator (7.1) and equation (7.2) become

$$X = c_1\frac{\partial}{\partial t} + (c_3 + c_4 x)\frac{\partial}{\partial x} + \frac{2}{n}c_4 h\frac{\partial}{\partial h}, \tag{7.3}$$

and

$$c_1\frac{\partial v_\ell}{\partial t} + (c_3 + c_4 x)\frac{\partial v_\ell}{\partial x} = \frac{2}{n}c_4 v_\ell. \tag{7.4}$$

We now derive the group invariant solution of the fracture half-width, $h(t,x) = \phi(t,x)$, of the PDE (2.60), by solving the characteristic equation

$$X\big(h(t,x) - \phi(t,x)\big)\Big|_{h=\phi} = 0. \tag{7.5}$$

Applying the generator (7.3) to equation (7.5) gives the first order nonlinear diffusion equation

$$c_1\frac{\partial\phi}{\partial t}+(c_3+c_4x)\frac{\partial\phi}{\partial x}=\frac{2c_4}{n}\phi. \tag{7.6}$$

The characteristic curves corresponding to the first order partial differential equation (7.6) are

$$\frac{dt}{c_1}=\frac{dx}{c_4\left(\frac{c_3}{c_4}+x\right)}=\frac{n}{2c_4}\frac{d\phi}{\phi}. \tag{7.7}$$

Equating the first two expressions in (7.7) and solving the result gives

$$k_1=\frac{\left(\frac{c_3}{c_4}+x\right)}{\exp\left(\frac{c_4}{c_1}t\right)}, \tag{7.8}$$

where k_1 is a constant. Similarly the first and last expressions in (7.7) give

$$k_2=\frac{\phi}{\exp\left(\frac{2c_4}{nc_1}t\right)}, \tag{7.9}$$

where k_2 is a constant. The group invariant solution is of the form $k_2=F(k_1)$. Since $h(t,x)=\phi(t,x)$, it follows that the group invariant solution of the half-width of the model fracture, $h(t,x)$, is

$$h(t,x)=\exp\left(\frac{2c_4}{nc_1}t\right)F(\xi), \tag{7.10}$$

where

$$\xi=\frac{\frac{c_3}{c_4}+x}{\exp\left(\frac{c_4}{c_1}t\right)}, \tag{7.11}$$

is the similarity variable. The group invariant solution of the half-width (7.10) is valid provided equation (7.4) is satisfied.

Consider now the leak-off velocity $v_\ell(t,x)$. Since equation (7.4) is the same as (7.6) the solution of (7.4) is

$$v_\ell(t,x)=\exp\left(\frac{2c_4}{nc_1}t\right)G(\xi), \tag{7.12}$$

where the similarity variable, ξ, is given by equation (7.11).

Now that the general form of the group invariant solution for the half-width of the fracture (7.10) and the leak-off velocity (7.12) are obtained, it is necessary to express the nonlinear diffusion equation (2.60), the boundary conditions and all related properties of the fracture in terms of the group invariant solution (7.10) and (7.12).

The partial derivatives of the similarity variable, (7.11),

$$\frac{\partial \xi}{\partial x} = \frac{1}{\exp^{\frac{c_4}{c_1}t}}, \qquad \frac{\partial \xi}{\partial t} = -\frac{c_4}{c_1}\xi, \tag{7.13}$$

will be used to express the problem in terms of the group invariant solutions. Substituting (7.10) and (7.12) with the aid of (7.13) into the nonlinear second order partial differential equation (2.60) results in the ODE

$$K_n \frac{d}{d\xi}\left(F^n \frac{dF}{d\xi}\right) + \frac{c_4}{c_1}\frac{d}{d\xi}(\xi F) - \frac{c_4}{c_1}\left(\frac{2}{n}+1\right)F - G = 0. \tag{7.14}$$

We choose $c_3 = 0$ in the similarity variable (7.11) such that when x tends to zero, ξ also tends to zero. Expressing the boundary condition at the fracture tip in terms of the group invariant solution gives the following results:
At $x = L(t)$,

$$h(t, L(t)) = 0, \tag{7.15}$$

which results in

$$F(E(t)) = 0, \tag{7.16}$$

where

$$E(t) = \frac{L(t)}{\exp\left(\frac{c_4}{c_1}t\right)}. \tag{7.17}$$

Differentiating (7.17) with respect to t gives

$$\frac{dF(E)}{dt} = \frac{dF}{dE}\frac{dE}{dt} = 0. \tag{7.18}$$

It is clear that $\frac{dF}{dE} \neq 0$ since F depends on $E(t)$ and therefore $\frac{dE}{dt} = 0$ which implies that

$$E(t) = k, \tag{7.19}$$

where k is a constant. We choose the characteristic length of the fracture to be the initial length of the fracture such that in dimensionless variables,

$$L(0) = 1. \tag{7.20}$$

Applying (7.20) to (7.17) gives the length of the fracture:

$$L(t) = \exp\left(\frac{c_4}{c_1}t\right). \tag{7.21}$$

It follows that the boundary condition at the fracture tip (7.16) is

$$F(1) = 0. \tag{7.22}$$

We consider fluid leak-off at the interface and fluid injection at the fracture entry. We find that the maximum half-width is at the fracture entry. Thus $\xi_{max} = 0$ and

$$h(0,0) = \beta, \tag{7.23}$$

which is the maximum value that the half-width of the fracture can attain. This results in $F_{max} = F(0)$ which gives that

$$F(0) = \beta \tag{7.24}$$

is a condition that needs to be satisfied by the solution of the ODE (7.14).

The flux of fluid into the fracture is derived from (2.65),

$$Q(t,x) = -2K_n h^n \frac{\partial h}{\partial x}, \tag{7.25}$$

which, using (7.10) and (7.11), becomes

$$Q(t,x) = -2K_n \exp\left(\left(1+\frac{2}{n}\right)\frac{c_4}{c_1}t\right) F^n \frac{dF}{d\xi}. \tag{7.26}$$

At the fracture entry, $x = 0$, we have that the volume flux of fluid is

$$Q(t,0) = -2K_n \exp\left(\left(1+\frac{2}{n}\right)\frac{c_4}{c_1}t\right) F^n(0) \frac{dF}{d\xi}(0). \tag{7.27}$$

The fluid flux at the fracture entry, $S(t)$, is therefore of the form

$$S(t) = Q(t,0) = A\exp(Bt), \tag{7.28}$$

where

$$A = -2K_n F^n(0) \frac{dF}{d\xi}(0), \tag{7.29}$$

$$B = \left(\frac{n+2}{n}\right)\frac{c_4}{c_1}. \tag{7.30}$$

Equation (7.29) may be re-expressed as, using (7.24),

$$\frac{dF}{d\xi}(0) = -\frac{A}{2K_n\beta^n}, \quad \frac{c_4}{c_1} = \frac{n}{(2+n)}B. \tag{7.31}$$

The constants A, B and β are prescribed as far as the group invariant solution and numerical solution allow.

The volume flux of fluid leaving the fracture at the fluid-rock interface is

$$q(t) = 2\int_0^{L(t)} v_\ell(t,x)\,dx. \tag{7.32}$$

Using the group invariant solution of the leak-off velocity, (7.12), and the derivatives of the similarity variable, (7.13), we find that

$$q(t) = 2\exp\left[\left(1+\frac{2}{n}\right)\frac{c_4}{c_1}t\right]\int_0^1 G(\xi)\,d\xi. \tag{7.33}$$

In order to express the consistency condition in terms of the group invariant solution, we need to derive expressions for the volume and total flux of fluid in the fracture. The volume of the fracture can be derived from

$$V(t) = 2\int_0^{L(t)} h(t,x)\,dx, \tag{7.34}$$

and using the group invariant solution of the half-width, (7.10), equation (7.34) becomes

$$V(t) = 2\exp\left[\left(1+\frac{2}{n}\right)\frac{c_4}{c_1}t\right]\int_0^1 F(\xi)\,d\xi. \tag{7.35}$$

Finally, using (7.27), (7.33) and (7.35), we can obtain the consistency condition given by

$$\frac{dV}{dt} = Q(t,0) - q(t) - Q(t,L(t)) \tag{7.36}$$

which needs to be satisfied. In terms of the group invariant solution, equation (7.36) becomes

$$K_n F^n(0)\frac{dF}{d\xi}(0) = -\left[\frac{c_4}{c_1}\left(\frac{2}{n}+1\right)\int_0^1 F(\xi)\,d\xi + \int_0^1 G(\xi)\,d\xi\right] + K_n F^n(1)\frac{dF}{d\xi}(1). \tag{7.37}$$

Therefore, using (7.37), equation (7.29) becomes

$$A = 2\left[\frac{c_4}{c_1}\left(\frac{2}{n}+1\right)\int_0^1 F(\xi)\,d\xi + \int_0^1 G(\xi)\,d\xi\right] - K_n F^n(1)\frac{dF}{d\xi}(1). \tag{7.38}$$

It can be verified that the consistency condition (7.37) can be obtained by integrating the ordinary differential equation (7.14) with respect to ξ from $\xi = 0$ to $\xi = 1$ and using the boundary condition (7.22). Finally, we express the width-averaged fluid velocity

$$\bar{v}_x = -K_n h^{n-1}\frac{\partial h}{\partial x}, \tag{7.39}$$

in terms of the group invariant solution to obtain

$$\bar{v_x} = -K_n \exp\left(\frac{c_4}{c_1}t\right)F^{n-1}(\xi)\frac{dF}{d\xi}. \tag{7.40}$$

7.3 Leak-off velocity proportional to the half-width of the fracture

Having assumed that the half-width of the fracture is proportional to the leak-off velocity, we can describe the relation between $F(\xi)$ and $G(\xi)$ as

$$G(\xi) = \gamma F(\xi). \tag{7.41}$$

Substituting (7.41) into the problem gives

$$K_n\frac{d}{d\xi}\left(F^n\frac{dF}{d\xi}\right) + \frac{c_4}{c_1}\frac{d}{d\xi}(\xi F) - \left(\frac{c_4}{c_1}\left(\frac{2}{n}+1\right)+\gamma\right)F = 0, \tag{7.42}$$

subject to

$$F(1) = 0, \tag{7.43}$$

$$F(0) = \beta, \tag{7.44}$$

$$F^n(0)\frac{dF}{d\xi}(0) = -\frac{A}{2K_n}, \tag{7.45}$$

$$B = \left(1 + \frac{2}{n}\right)\frac{c_4}{c_1} \tag{7.46}$$

and A is given by the identically satisfied consitency condition as

$$A = 2\left(\frac{c_4}{c_1}\left(\frac{2}{n} + 1\right) + \gamma\right)\int_0^1 F(\xi)d\xi - K_n F^n(1)\frac{dF}{d\xi}(1) \tag{7.47}$$

and

$$h(t,x) = \exp\left(\frac{2c_4}{nc_1}t\right)F(\xi), \tag{7.48}$$

$$v_\ell(t,x) = \gamma\exp\left(\frac{2c_4}{nc_1}t\right)F(\xi), \tag{7.49}$$

$$L(t) = \exp\left(\frac{c_4}{c_1}t\right), \tag{7.50}$$

$$Q(t,x) = -2K_n\exp\left[\left(1 + \frac{2}{n}\right)\frac{c_4}{c_1}t\right]F^n\frac{dF}{d\xi}, \tag{7.51}$$

$$q(t,x) = 2\gamma\exp\left[\left(1 + \frac{2}{n}\right)\frac{c_4}{c_1}t\right]\int_0^1 F(\xi)d\xi, \tag{7.52}$$

$$V(t) = 2\exp\left[\left(1 + \frac{2}{n}\right)\frac{c_4}{c_1}t\right]\int_0^1 F(\xi)d\xi, \tag{7.53}$$

$$\bar{v_x} = -K_n\exp\left(\frac{c_4}{c_1}t\right)F^{n-1}(\xi)\frac{dF}{d\xi}. \tag{7.54}$$

It can be verified that the consistency condition (7.47) can be obtained by integrating (7.42) with respect to ξ from $\xi = 0$ to $\xi = 1$ and using the boundary condition (7.43).

7.4 Asymptotic Solution

We approximate the behaviour of $F(\xi)$ as $\xi \to 1$ by looking for an asymptotic solution of (7.14) with (7.41) of the form

$$F(\xi) \sim C(1-\xi)^s, \quad \text{as} \quad \xi \to 1, \tag{7.55}$$

where C and s are constants to be determined. The boundary condition $F(1) = 0$ is satisfied by (7.55). Substituting (7.55) into the ODE (7.42) gives

$$K_n C^{n+1} s\Big(s(n+1) - 1\Big)(1-\xi)^{s(n+1)-2} - \frac{c_4}{c_1}Cs(1-\xi)^{s-1}$$
$$-C\left(\left(\frac{2}{n} - s\right)\frac{c_4}{c_1} + \gamma\right)(1-\xi)^s \sim 0, \quad \text{as} \quad \xi \to 1. \tag{7.56}$$

The first two terms in (7.56) vanish provided that their exponents are equal,

$$s(n+1)-2=s-1 \tag{7.57}$$

which implies that

$$s=\frac{1}{n}. \tag{7.58}$$

Equating coefficients of the first two terms gives

$$C=\left(\frac{c_4 n}{K_n c_1}\right)^{\frac{1}{n}}. \tag{7.59}$$

Substituting (7.58) and (7.59) into (7.56) gives

$$C\left(\left(\frac{2}{n}+s\right)\frac{c_4}{c_1}+\gamma\right)(1-\xi)^{\frac{1}{n}}\to 0, \quad \text{as} \quad \xi\to 1. \tag{7.60}$$

It is clear that the expression in (7.60) vanishes as $\xi\to 1$. Therefore, the asymptotic solution (7.55) of the ordinary differential equation (7.42) is

$$F(\xi)\sim\left(\frac{c_4 n}{K_n c_1}\right)^{\frac{1}{n}}(1-\xi)^{\frac{1}{n}} \quad \text{as} \quad \xi\to 1, \tag{7.61}$$

and

$$\frac{dF}{d\xi}(\xi)\sim-\frac{1}{n}\left(\frac{c_4 n}{K_n c_1}\right)^{\frac{1}{n}}(1-\xi)^{\frac{1-n}{n}} \quad \text{as} \quad \xi\to 1. \tag{7.62}$$

This solution $F(\xi)$ holds for all values of the parameters α, $\gamma>1$, K_n and $n>0$. The half-width of the fracture (7.48) using the asymptotic solution (7.61) is given by

$$h(t,x)\sim\exp\left(\frac{2c_4}{nc_1}t\right)\left(\frac{nc_4}{K_n c_1}\right)^{\frac{1}{n}}(1-\xi)^{\frac{1}{n}} \quad \text{as} \quad \xi\to 1. \tag{7.63}$$

Also using (7.61) and (7.62),

$$F^n(\xi)\frac{dF}{d\xi}\sim-\left(\frac{c_4 n}{c_1 K_n}\right)^{\frac{n+1}{n}}(1-\xi)^{\frac{1}{n}}\to 0 \quad \text{as} \quad \xi\to 1. \tag{7.64}$$

Thus the fluid flux, (7.51), vanishes at the fracture tip

$$F^n(1)\frac{dF}{d\xi}(1)=0. \tag{7.65}$$

7.5 Numerical Solutions

The numerical solution of $F(\xi)$ is investigated using the backwards shooting method from the fracture tip to the fracture entry. We obtained that the maximum half-width of the fracture occurs at the entry and as such

$$F(0)=h(0,0)=\beta, \tag{7.66}$$

is a condition that the numerical solution needs to satisfy.

The boundary value problem to solve is

$$K_n \frac{d}{d\xi}\left(F^n \frac{dF}{d\xi}\right) + \frac{c_4}{c_1}\frac{d}{d\xi}(\xi F) - \left(\frac{c_4}{c_1}\left(\frac{2}{n}+1\right)+\gamma\right)F = 0, \tag{7.67}$$

subject to

$$F(1) = 0, \tag{7.68}$$
$$F(0) = \beta, \tag{7.69}$$

where

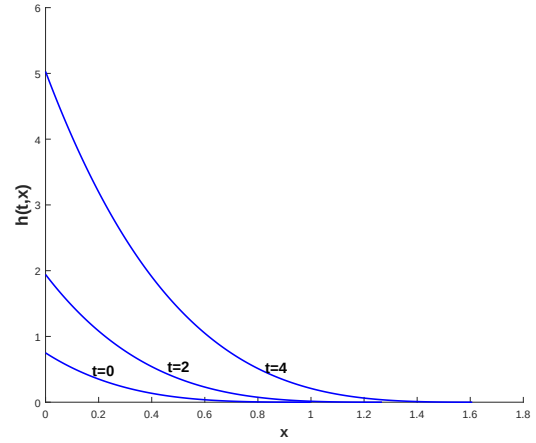
$$F^n(0)\frac{dF}{d\xi}(0) = -\frac{A}{2K_n}, \quad \frac{c_4}{c_1} = \frac{n}{(2+n)}B \tag{7.70}$$

and A is given by the identically satisfied consitency condition

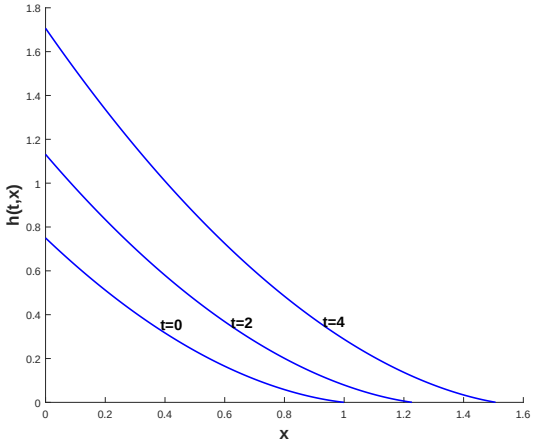
$$F^n(0)\frac{dF}{d\xi}(0) = -\frac{1}{K_n}\left(\frac{c_4}{c_1}\left(\frac{2}{n}+1\right)+\gamma\right)\int_0^1 F(\xi)d\xi. \tag{7.71}$$

The boundary value problem need not be transformed into an initial value problem as it can be solved directly using the backwards shooting method. The problem is solved by first making an initial guess for the ratio $\frac{c_4}{c_1}$ and substituted into the problem. The solution is solved from the fracture tip to the fracture entry. The asymptotic solution (7.61) and its derivative evaluated in the epsilon neighbourhood of the fracture tip are used as initial conditions. A backwards shooting from $F(1-\delta) = 0$ and $F(0)$ using $\frac{c_4}{c_1}$ is used to shoot for the solution $F(\xi)$. The solution is checked to see if it satisfies the condition $F(0) = \beta$ at the fracture entry. If this condition is satisfied we have obtained a solution of $F(\xi)$. If not, we use the bisection method to iteratively adjust the value of $\frac{c_4}{c_1}$ and continuously shoot until the initial condition is satisfied. The solution of $F(\xi)$ is used to obtain properties of the fracture for increasing time t.

In Figure 7.1, the half-width of the fracture, (7.48), is plotted against x for parameter values $\beta = 0.75$, $\gamma = 0.2$ for a) $K_n = 1/3$, $n = 0.5$ and b) $K_n = 2/3$, $n = 1$. Both the half-width of the fracture and the length of the fracture are increasing as time t increases. The half-width increases much faster than the length. It can be verified that the exponential solution results in open fractures, $\beta > 1$, for $n = 3$ and $K_n = 1/3$. The analysis of open fractures is not being considered in this work. For all values of the diffusion constant K_n, the solution of the half-width for $n = 0.5$ results in partially open fractures. However, only values of $K_n > 1/3$ result in partially open fractures for $n = 1$. We can make assumptions about the type of fracture that arises from the exponential solution given the relationship between K_n and n. If the value of K_n decreases as n decreases, i.e. as the fracture becomes more tortuous, then exponential solution can only describe open fractures. If K_n increases as n decreases, then its possible to have partially open fractures from the exponential solution.



(a) n=0.5



(b) n=1

Figure 7.1: The half-width of the fracture, 7.10, is plotted against x with parameter values $\beta = 0.75$, $\gamma = 0.2$ and for a) $K_n = 1/3$ and $n = 0.5$ and b) $K_n = 2/3$ and $n = 1$.

Chapter 8

CONCLUSIONS

The main aim of the research was to investigate the propagation of a linear hydraulic fracture with tortuosity and fluid leak-off at the fluid rock interface. A pre-existing tortuous partially open fracture was replaced by a two-dimensional symmetric model fracture with a modified Reynolds' flow law to account for the effect of asperities at the fluid-rock interface on the fluid flow. The lubrication approximation was also used to model the problem since the length of the fracture is much less in magnitude than the half-width of the fracture. The Perkins-Kern and Nordgren (PKN) approximation, relating the half-width of the fracture with the normal stress at the fracture walls, together with the linear crack law were used to close the model. The boundary conditions at the fracture tip and the fracture entry were obtained.

The methods of obtaining solutions discussed in Chapter 3 were used in Chapter 4 to derive the conservation laws of the nonlinear diffusion equation. Two conserved vectors of the first and second kind were obtained from the direct method. The multipliers method was also used to investigate if other conserved vectors otherwise missed by the direct method could be obtained. Association of a Lie point symmetry with a conserved vector, obtained using a definition by Kara nd Mahomed, gave two working conditions, $\alpha = \frac{1}{2(n+1)}$ and $\alpha = \frac{1}{(n+2)}$. The working condition $\alpha = \frac{1}{(n+2)}$ was not used as it s a constant volume solution. By Sjöberg's double reduction theorem, these working conditions were used to obtain exact analytical solutions of the problem.

In Chapter 5, the general case of the group invariant solution obtained by setting the constant c_3 from the Lie point symmetry generator equal to zero was investigated. The various fracture properties were expressed in terms of the group invariant solution of the half-width of the fracture and the leak-off velocity. We assumed a proportional relationship between the half-width of the fracture and the leak-off velocity. By analysing the properties of the fracture expressed in terms of the group invariant solution, four working conditions at the fracture entry were obtained. The constant pressure working condition, $\alpha = 1/2$, obtained when fluid is injected at the fracture entry at a constant pressure, the constant speed of propagation working condition, $\alpha = 1$, constant rate of fluid injection at the fracture entry, $\alpha = \frac{n+1}{n+2}$, and the constant rate of leak-off at the fluid-rock interface, $\alpha = \frac{n+1}{2}$, working condition. The boundary value problem was transformed into an initial value problem using a scaling transformation in-order to solve the problem numerically. The problem was solved using the built-in solver ode45 on MATLAB. The solution was shot from the fracture tip to the fracture entry subject to satisfying the boundary conditions. It was found that for the constant pressure working condition, $\alpha = 1/2$, the half-width of the partially open fracture remains constant as the the fracture propagates in the

positive x-direction for increasing time. Initially at $K_n t = 0$ there is no leak-off. For all other working conditions we obtained that the fracture propagates in the positive x direction with leak-off occurring even at $K_n t = 0$. The analysis of the width-averaged fluid velocity lead to the derivation of an approximate analytical solution which agreed well with the numerical solution for all values of n. The agreement between the approximate analytical solution and the numerical solution improves even further as the fracture becomes less tortuous ($n > 1$). Approximate analytical solutions are useful when analytical solutions are unattainable, when numerical solutions are difficult to compute and when a readily available solution is required. It has been found that the fracture propagates for all working conditions. Both quantities of the length and the volume of a partially open tortuous fracture in impermeable rock was found to be greater in magnitude than those of a partially open tortuous fracture in permeable rock for various working conditions and for $0 < n < 3$. This is because the fluid that was available for further propagation in an impermeable tortuous fracture is now lost to the surrounding rock in a permeable tortuous fracture. The volume ratio of a tortuous fracture in impermeable rock rapidly exceeds the volume of a tortuous fracture in permeable rock for small values of the scaled time $K_n t$.

The traveling wave solution of the model was obtained in Chapter 6. This solution, obtained as a result of setting the constants c_2 and c_4 to zero in the Lie point symmetry generator of the partial differential equation, had to be solved in a domain that is time dependent. An important factor about this type of solution is how it is solved, it is solved in two parts. Firstly, for $t = 0$, the problem is solved to obtain the value of the ratio $\frac{c_3}{c_1}$ which gives the initial profile of the fracture. Secondly, the value of the ratio $\frac{c_3}{c_1}$ is used to solve the problem for all subsequent times. The solution is then used to obtain the properties of the fracture. It is found that as time increases, the fracture propagates at a constant speed given by $\frac{c_3}{c_1}$ and the shape of the half-width of the fracture is preserved for all time for a given value of n. The velocity ratio plots of the traveling wave solution for $t = 0$ were approximately linear. It is expected that approximating the velocity ratio curves to be exactly linear will lead to an approximate analytical solution that agrees well with the numerical results.

Setting the constants c_2 and c_3 to zero resulted in a group invariant solution of the half-width and the leak-off velocity that has an exponential function. The value of K_n is found to have a big influence on the type of fracture that propagates (open or partially open fractures) when the group invariant solution is given by an exponential function. We could only obtain partially open fractures for $n = 0.5$ and $n = 1$. It is thus important to understand the relationship between K_n and n. The value of K_n is determined through experiments and the readily available value is $K_n = 1/3$ which corresponds to $n = 3$. For a fracture with little to no asperities ($n = 3$), it was found that for $K_n = 1/3$ only open fracture are obtained. For $1 < n < 3$, open or partially fractures can only be obtained for $K_n < 1/3$. This suggests an inverse relationship between K_n and n for a fracture with little to no asperities.

The analysis of a tortuous linear hydraulic fracture propagating in permeable rock can be expanded further by considering another model to describe fluid leak-off at the fluid-rock interface. Darcy's law for porous media can be used to describe fluid leak-off at the fluid-rock interface. This will result in a coupled system consisting of the nonlinear diffusion equation for the half-width of the fracture and Darcy's law to describe the leak-off velocity.

Appendices

Appendix A

Lie point symmetries

Derivation of the Lie point symmetries of the nonlinear diffusion equation for a linear hydraulic fracture with tortuosity and fluid leak-off at the fluid rock interface

In this section we outline the detailed derivation of the Lie point symmetries of the nonlinear diffusion equation

$$\frac{\partial h}{\partial t} = K_n \frac{\partial}{\partial x}\left(h^n \frac{\partial h}{\partial x}\right) - v_\ell(t,x), \tag{A.1}$$

which can be written as

$$F = h_t - K_n n h^{n-1} h_x^2 - K_n h^n h_{xx} + v_\ell(t,x), \tag{A.2}$$

where K_n is the diffusion constant and the subscripts denote partial differentiation. The nonlinear diffusion equation describes the propagation of the fracture half-width during hydraulic fracturing, the rock encasing the fracture is permeable. Since the rock is permeable, there is fluid leak-off onto the surrounding rock. This fluid leaks at the rate $v_\ell(t,x)$; this is the leak-off velocity.

The Lie point symmetry generator

$$X = \xi^1(t,x,h)\frac{\partial}{\partial t} + \xi^2(t,x,h)\frac{\partial}{\partial x} + \eta(t,x,h)\frac{\partial}{\partial h} \tag{A.3}$$

of Equation (A.1) satisfies the invariance condition

$$X^{[2]} F\Big|_{F=0} = 0. \tag{A.4}$$

The Lie point symmetries can be derived by solving the determining equation (A.4) for $\xi^1(t,x,h)$, $\xi^2(t,x,h)$ and $\eta(t,x,h)$. $X^{[2]}$ is the second prolongation of X, it is given by

$$X^{[2]} = X + \zeta_1 \frac{\partial}{\partial h_t} + \zeta_2 \frac{\partial}{\partial h_x} + \zeta_{11} \frac{\partial}{\partial h_{tt}} + \zeta_{12} \frac{\partial}{\partial h_{xt}} + \zeta_{22} \frac{\partial}{\partial h_{xx}}, \tag{A.5}$$

and ζ_i and ζ_{ij} are defined by

$$\zeta_i = D_i(\eta) - h_k D_i(\xi^k), \qquad i = 1,2, \tag{A.6}$$

$$\zeta_{ij} = D_j(\zeta_i) - h_{ik} D_j(\xi^k), \qquad i = 1,2. \tag{A.7}$$

there is a summation over the repeated index k which runs from 1 to 2. D_i and D_j which represent the total derivatives with respect to the independent variables t and x are given by

$$D_1 = D_t = \frac{\partial}{\partial t} + h_t \frac{\partial}{\partial h} + h_{tt} \frac{\partial}{\partial h_t} + h_{xt} \frac{\partial}{\partial h_x} + \cdots \tag{A.8}$$

$$D_2 = D_x = \frac{\partial}{\partial x} + h_x \frac{\partial}{\partial h} + h_{tx} \frac{\partial}{\partial h_t} + h_{xx} \frac{\partial}{\partial h_x} + \cdots \tag{A.9}$$

From expanding the determining equation A.5, we obtain

$$\xi^1 \frac{\partial v_\ell}{\partial t} + \xi^2 \frac{\partial v_\ell}{\partial x} + \eta\Big(- K_n n(n-1) h^{n-2} h_x^2 - K_n n h^{n-1} h_{xx} \Big) + \zeta_1 + \zeta_2(-2K_n n h^{n-1} h_x) + \zeta_{22}(-K_n h^n)\Big|_{F=0} = 0. \tag{A.10}$$

Substituting the expressions for ζ_1, ζ_2 and ζ_{22} into the determining Equation (A.5) we obtain

$$\Big[(2K_n n h^{n-1} \xi_x^2 - K_n n(n-1) h^{n-2} \eta + 2K_n h^n \xi_{xh}^2 - K_n h^n \eta_{hh} - 2K_n n h^{n-1} \eta_h) h_x^2 +$$

$$(2K_n n h^{n-1} \xi_h^2 + K_n h^n \xi_{hh}^2) h_x^3 + (-\xi_t^2 - 2K_n n h^{n-1} \eta_x - 2K_n h^n \eta_{xh} + K_n h^n \xi_{xx}^2) h_x$$

$$+ (2K_n h^n \xi_x^2 - K_n n h^{n-1} \eta - K_n h^n \eta_h) h_{xx} + (2K_n h^n \xi_{xh}^1 + 2K_n n h^{n-1} \xi_x^1 - \xi_h^2) h_x h_t$$

$$+ (K_n h^n \xi_{hh}^1 + 2K_n n h^{n-1} \xi_h^1) h_x^2 h_t + (\eta_h - \xi_t^1 + K_n h^n \xi_{xx}^1) h_t + 2K_n h^n \xi_x^1 h_{xt} -$$

$$\xi_h^1 h_t^2 + K_n h^n \xi_h^1 h_t h_{xx} + 3K_n h^n \xi_h^2 h_x h_{xx} + 2K_n h^n \xi_h^1 h_x h_{xt} + \xi^1 \frac{\partial v_\ell}{\partial t} + \xi^2 \frac{\partial v_\ell}{\partial x} +$$

$$\eta_t - K_n h^n \eta_{xx} \Big]\Big|_{F=0} = 0 \tag{A.11}$$

Now from equation (A.2)

$$h_{xx} = \frac{h_t - K_n n h^{n-1} h_x^2 + v_l}{K_n h^n}, \tag{A.12}$$

which we use to replace h_{xx} in Equation (A.11). After the substitution we obtain

$$\begin{aligned}
&\Big(-\xi_t^2 - 2K_n n h^{n-1}\eta_x - 2K_n h^n \eta_{xh} + K_n h^n \xi_{xx}^2 + 3\xi_h^2 v_\ell\Big) h_x \\
&+ \Big(2K_n h^n \xi_{xh}^1 + 2K_n n h^{n-1}\xi_x^1 + 2\xi_h^2\Big) h_x h_t \\
&+ \Big(K_n n h^{h-2}\eta + 2K_n h^n \xi_{xh}^2 - K_n h^n \eta_{hh} - K_n n h^{n-1}\eta_h\Big) h_x^2 \\
&+ \Big(-K_n n h^{n-1}\xi_h^2 + K_n h^n \xi_{hh}^2\Big) h_x^3 + \Big(K_n h^n \xi_{hh}^1 + K_n n h^{n-1}\xi_h^1\Big) h_x^2 h_t \\
&+ \Big(K_n h^n \xi_{xx}^1 - \xi_t^1 + 2\xi_x^2 - \frac{n}{h}\eta + \xi_h^1 v_l\Big) h_t + 2K_n h^n \xi_h^1 h_x h_{xt} \\
&+ 2K_n h^n \xi_x^1 h_{xt} + \xi^1 \frac{\partial v_\ell}{\partial t} + \xi^2 \frac{\partial v_\ell}{\partial x} + \eta_t - K_n h^n \eta_{xx} \\
&+ \Big(2\xi_x^2 - \frac{n}{h}\eta - \eta_h\Big) v_\ell = 0. \qquad \text{(A.13)}
\end{aligned}$$

The functions to be determined are independent of derivatives of h, Equation (A.13) is separated according to partial derivatives of h. One the equates the coefficients of the partial derivatives of h to zero.

Firstly, separating Equation (A.13) with respect to $h_x h_{tx}, h_{tx}$ and $h_x h_t$ gives

$$h_x h_{tx}: \qquad \xi_h^1 = 0, \qquad \text{(A.14)}$$

which implies that

$$\xi^1 = \xi^1(t, x); \qquad \text{(A.15)}$$

$$h_{tx}: \qquad \xi_x^1 = 0, \qquad \text{(A.16)}$$

which implies that

$$\xi^1 = \xi^1(t). \qquad \text{(A.17)}$$

$$h_x h_t: \qquad 2K_n h^n \xi_{xh}^1 + 2K_n n h^{n-1}\xi_x^1 + 2\xi_h^2 = 0, \qquad \text{(A.18)}$$

from Equation (A.17), this reduces to

$$\xi_h^2 = 0, \qquad \text{(A.19)}$$

which implies that

$$\xi^2 = \xi^2(t, x). \qquad \text{(A.20)}$$

Separating Equation (A.13) by h_x^3 and $h_x^2 h_t$ does not bring any new results. We now separate Equation (A.13) by h_x and h_t which gives

$$h_t: \qquad K_n h^n \xi_{xx}^1 - \xi_t^1 + 2\xi_x^2 - \frac{n}{h}\eta + \xi_h^1 v_\ell = 0, \qquad \text{(A.21)}$$

which when simplified by Equation (A.17) and (A.19) gives

$$\eta = \frac{h}{n}(2\xi_x^2 - \xi_t^1). \tag{A.22}$$

$$h_x: \qquad -\xi_t^2 - 2K_n n h^{n-1}\eta_x - 2K_n h^n \eta_{xh} + K_n h^n \xi_{xx}^2 + 3\xi_h^2 v_\ell = 0, \tag{A.23}$$

which when simplified using Equation (A.17) and (A.22) gives

$$\xi_{xx}^2\left(\frac{3n+4}{n}\right)K_n h^n + \xi_t^2 = 0, \tag{A.24}$$

which can be separated using powers of h

$$h^0: \qquad \xi_t^2 = 0, \tag{A.25}$$

which implies that

$$\xi^2 = \xi^2(x), \tag{A.26}$$

$$h^n: \qquad \xi_{xx}^2 = 0, \tag{A.27}$$

which implies that

$$\xi^2 = c_3 + c_4 x, \tag{A.28}$$

where c_3 and c_4 are constants. Separating Equation (A.13) by h_x^2

$$h_x^2: \qquad K_n n h^{h-2}\eta + 2K_n h^n \xi_{xh}^2 - K_n h^n \eta_{hh} - K_n n h^{n-1}\eta_h = 0, \tag{A.29}$$

using Equation (A.22) and (A.28), h_x^2 is satisfied. Using the result (A.28), equation (A.22) becomes

$$\eta = \frac{h}{n}(2c_4 - \xi_t^1). \tag{A.30}$$

The remainder from Equation (A.13) is

$$\xi^1\frac{\partial v_\ell}{\partial t} + \xi^2\frac{\partial v_\ell}{\partial x} + \eta_t - K_n h^n \eta_{xx} + (2\xi_x^2 - \frac{n}{h}\eta - \eta_h)v_\ell = 0, \tag{A.31}$$

which after using Equation (A.30) simplifies to

$$\xi^1\frac{\partial v_\ell}{\partial t} + \xi^2\frac{\partial v_\ell}{\partial x} - \frac{h}{n}\xi_{tt}^1 + \frac{1}{n}(-2c_4 + (n+1)\xi_t^1)v_\ell = 0. \tag{A.32}$$

Equating the coefficients of powers of h on each side of Equation (A.32) gives

$$h: \qquad \xi_{tt}^1 = 0, \tag{A.33}$$

which implies that

$$\xi^1 = c_1 + c_2 t, \tag{A.34}$$

where c_1 and c_2 are constants.

$$h^0: \qquad \xi^1 \frac{\partial v_l}{\partial t} + \xi^2 \frac{\partial v_l}{\partial x} + \frac{1}{n}((n+1)\xi^1_t - 2c_4)\, v_\ell = 0, \tag{A.35}$$

using (A.28) and (A.34) this simplifies to

$$(c_1 + c_2 t)\frac{\partial v_\ell}{\partial t} + (c_3 + c_4 x)\frac{\partial v_\ell}{\partial x} = \frac{1}{n}(2c_4 - (n+1)c_2)\, v_\ell \tag{A.36}$$

It follows from Equations (A.28), (A.30) and (A.34) that

$$\eta(h) = \frac{h}{n}(2c_4 - c_2), \quad \xi^1(t) = c_1 + c_2 t, \quad \xi^2(x) = c_3 + c_4 x \tag{A.37}$$

and therefore the Lie point symmetry generator of the linear hydraulic fracture given by the partial differential equation (A.1) is

$$X = (c_1 + c_2 t)\frac{\partial}{\partial t} + (c_3 + c_4 x)\frac{\partial}{\partial x} + \frac{1}{n}(2c_4 - c_2)h\frac{\partial}{\partial h} \tag{A.38}$$

$$= c_1 X_1 + c_2 X_2 + c_3 X_3 + c_4 X_4, \tag{A.39}$$

where

$$X_1 = \frac{\partial}{\partial t}, \tag{A.40}$$

$$X_2 = t\frac{\partial}{\partial t} - \frac{h}{n}\frac{\partial}{\partial h}, \tag{A.41}$$

$$X_3 = \frac{\partial}{\partial x}, \tag{A.42}$$

$$X_4 = x\frac{\partial}{\partial x} + \frac{2h}{n}\frac{\partial}{\partial h}. \tag{A.43}$$

Bibliography

[1] A. Granberg and K.K. Schmidt. What is hydraulic fracturing? *Propublica*, ONLINE.

[2] J.Q. Norris, D.L. Turcotte, E.M. Moores, E.E. Brodsky, and J.B. Rundle. Fracking in tight shales: What is it, what does it accomplish, and what are its consequences? *Annual Review of Earth and Planetary Sciences*, 44:1–37, 2016.

[3] A. D. Fitt, D. P. Mason, and E. A. Moss. Group invariant solution for a pre-existing fluid-driven fracture in impermeable rock. *Zeitschrift für angewandte Mathematik und Physik*, 58(6):1049–1067, 2007.

[4] A.D. Fitt, A.D. Kelly, and C.P. Please. Crack propagation models for rock fracture in a geothermal energy reservoir. *SIAM Journal on Applied Mathematics*, 55(6):1592–1608, 1995.

[5] M.J. Economidies, D.N. Mikhailov, and V.N Nikolaevskiy. On the problem of fluid leak-off during hydraulic fracturing. *Transport in porous media*, 67:487–499, 2007.

[6] A.G. Fareo and D.P. Mason. A group invariant solution for a pre-existing fluid-driven fracture in permeable rock. *Nonlinear Analysis: Real World Applications*, 12(1):767 – 779, 2011.

[7] J. Bear. *Dynamics of fluids in porous media*. American Elsevier, New York,USA, reprint edition, 1972.

[8] S. H. Emerman, D. L. Turcotte, and D. A. Spence. Transport of magma and hydrothermal solutions by laminar and turbulent fluid fracture. *Physics of the Earth and Planetary Interiors*, 41(4):249 – 259, 1986.

[9] D. A. Spence, P. W. Sharp, and D. L. Turcotte. Buoyancy-driven crack propagation: a mechanism for magma migration. *Journal of Fluid Mechanics*, 174:135–153, 1987.

[10] D. A. Spence and D. L. Turcotte. Magma-driven propagation of cracks. *Journal of Geophysical Research: Solid Earth*, 90(B1):575–580, 1985.

[11] M.R.R. Kgatle and D.P. Mason. Propagation of a linear hydraulic fracture with tortuosity. *International Journal of Non-Linear Mechanics*, 61:39 – 53, 2014.

[12] J. Qian, Z. Chen, H. Zhan, and H. Guan. Experimental study of the effect of roughness and Reynolds number on fluid flow in rough-walled single fractures: A check of local cubic law. *Hydrological Processes*, 25:614–622, 2011.

[13] A. P. Oron and B. Berkowitz. Flow in rock fractures: The local cubic law assumption re-examined. *Water Resources Research*, 34(11):2811–2825, 1998.

[14] P. A. Witherspoon, J. S. Y. Wang, K. Iwai, and J. E. Gale. Validity of cubic law for fluid flow in a deformable rock fracture. *Water Resources Research*, 16:1016–1024, 1980.

[15] T. K. Perkins and L. R. Kern. Widths of hydraulic fractures. *Journal of Petroleum Technology*, 13:937–949, 1961.

[16] R.P. Nordgren. Propagation of vertical hydraulic fracture. *Journal of Petroleum Technology*, 12:306–314, 1972.

[17] R.J. Pine and P.A. Cundall. Applications of the fluid-rock interaction programme (frip) to the modelling of hot dry geothermal energy systems. *Proceedings of International Symposium on Fundamentals of Rock Joints*, pages 293–302, 1985.

[18] A. Sjöberg. Double reduction of pdes from the association of symmetries with conservation laws with applications. *Applied Mathematics and Computation*, 184(2):608 – 616, 2007.

[19] H. Flanders. Differentiation under the integral sign. *The American Mathematical Monthly*, 80(6):615–627, 1973.

[20] M.R.R. Kgatle. *Propagation of a hydraulic fracture with tortuosity : linear and hyperbolic crack laws*. PhD Thesis, School of Computer Science and Applied Mathematics, University of the Witwatersrand, Johannesburg, South Africa, 2016.

[21] D. A. Spence and P. Sharp. Self-similar solutions for elastohydrodynamic cavity flow. *Proceedings of the Royal Society of London A: Mathematical, Physical and Engineering Sciences*, 400(1819):289–313, 1985.

[22] J. Xiang. *A PKN hydraulic fracture model study and formation permeability determination*. Thesis, Texas A M University, Texas, United States of America.

[23] J. R. King and M. Bowen. Moving boundary problems and non-uniqueness for the thin film equation. *European Journal of Applied Mathematics*, 12(3):321–356, 2001.

[24] N. N. Smirnov and V. P. Tagirova. Self-similar solutions of the problem of formation of a hydraulic fracture in a porous medium. *Fluid Dynamics*, 42(1):60–70, 2007.

[25] F. Oliveri. Lie symmetries of differential equations: Classical results and recent contributions. *Symmetry*, 2(2):658–706, 2010.

[26] N. H. Ibragimov and R. L. Anderson. *One-parameter transformation groups, in: N. H. Ibragimov (Ed.), CRC Handbook of Lie Group Analysis of Differential Equations. Symmetries, Exact Solutions and Conservation Laws*. CRC Press, Boca Raton, vol.1, pp.7-14, 1994.

[27] W. Hereman. Review of symbolic software for Lie symmetry analysis. *Mathematical and Computer Modelling*, 25(8):115 – 132, 1997.

[28] R. Naz, D.P. Mason, and F.M. Mahomed. Conservation laws and conserved quantities for laminar two-dimensional and radial jets. *Nonlinear Analysis: Real World Applications*, 10(5):2641 – 2651, 2009.

[29] A. H. Kara and F. M. Mahomed. Relationship between symmetries and conservation laws. *International Journal of Theoretical Physics*, 39(1):23–40, 2000.

[30] G.W. Bluman, A.F. Cheviakov, and S.C. Anco. Construction of conservation laws: how the direct method generalizes Noether's theorem. *Group Analysis of Differential Equations and Integrable Systems 4th Workshop Proceedings*, page 13–35, 2009.

[31] R Naz. Conservation laws for some systems of nonlinear partial differential equations via multiplier approach. *J. Appl. Math.*, 2012, Special Issue:13 pages, 2012.

[32] R. Naz, F.M. Mahomed, and D.P. Mason. Comparison of different approaches to conservation laws for some partial differential equations in fluid mechanics. *Applied Mathematics and Computation*, 205(1):212 – 230, 2008.

[33] A. H. Kara and F. M. Mahomed. A basis of conservation laws for partial differential equations. *Journal of Nonlinear Mathematical Physics*, 9(sup2):60–72, 2002.

[34] M.R.R. Kgatle and D.P. Mason. Linear hydraulic fracture with tortuosity: Conservation laws and fluid extraction. *Internatinal Journal of Non-Linear Mechanics*, 79:10–25, 2016.

[35] R. L. Burden and J. D. Faires. *Numerical Analysis*. Cengage Learning, 2010.

[36] A.G. Fareo. *Group invariant solutions for a pre-existing fracture driven by a non-Newtonian fluid in permeable and impermeable rock*. PhD Thesis, School of Computer Science and Applied Mathematics, University of the Witwatersrand, Johannesburg, South Africa, 2012.

[37] M.S. Klamkin. On the transformation of a class of boundary value problems into initial value problems for ordinary differential equations. *SAIM Review*, 4:4347, 1962.

[38] A.G. Fareo. *Group invariant solutions for a pre-existing fluid-driven fracture in permeable rock*. MSc Dissertation, School of Computer Science and Applied Mathematics, University of the Witwatersrand, 2008.

[39] A.G. Fareo and D.P. Mason. Group invariant solutions for a pre-existing fluid-driven fracture in permeable rock. *Nonlinear Analysis: Real World Application*, 12:767–779, 2011.